POLITECNICO
MILANO 1863

SCUOLA DI INGEGNERIA INDUSTRIALE
E DELL'INFORMAZIONE

Towards DC smart grid: integration of renewable energy sources, energy storages, and electric vehicle charging stations into DC railway power systems.

TESI DI LAUREA MAGISTRALE IN ENERGY ENGINEERING - INGEGNERIA ENERGETICA

Author: **Nicolò Magnani**

Student ID: 968832
Advisor: Prof. Alberto Dolara
Academic Year: 2022-2023

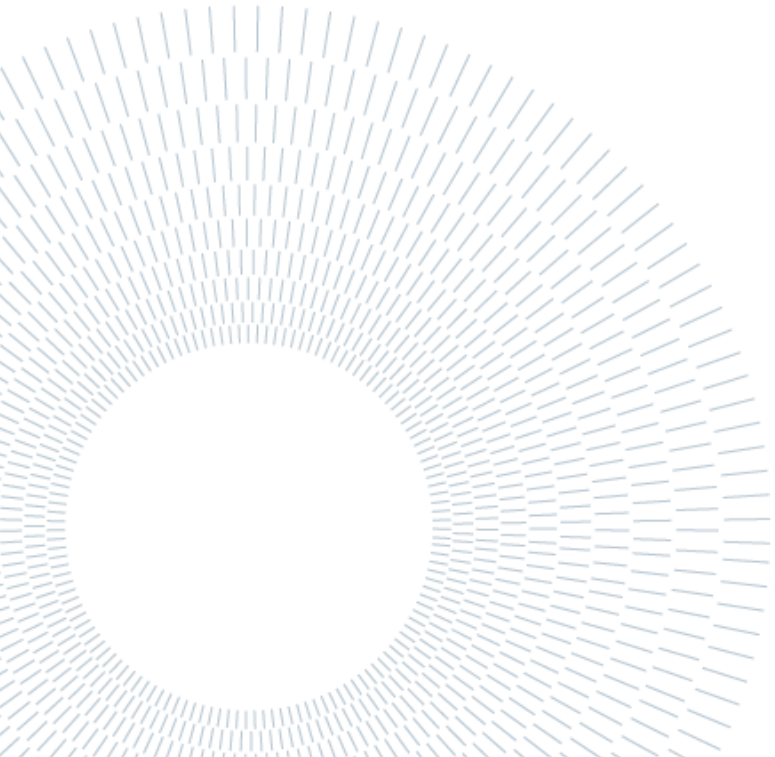

Abstract

This thesis for the Master's Degree in Energy Engineering focuses on how smart mobility, one of the key points of the new European Union Directives, and renewables can be integrated into the railway transportation system so to create a sort of "*DC Railway Smart Grid*" whereby the braking power of trains - that could be wasted - is recovered by supplying electric car batteries parked in the proximity of the railway stations. Moreover, electric storage systems and photovoltaic generators connected to the same DC railway smart grid allow to increase the penetration of renewables in an energy-intensive sector, such as transportation, and to improve the *power quality* within the railway electrical system.

The idea of recovering the braking energy of trains to recharge electric vehicles can be successful along railway lines traveled by local or suburban trains, whose service includes many stops, and used by commuters who reach the stations with their own car. In this work the Milano Cadorna – Saronno railway line has been identified to have the aforementioned features and it has been taken and a benchmark to study the proposed solutions. In particular, the section between the two electrical substations located in Novate and in Saronno of the Cadorna (Milan) – Saronno railway is simulated in the different scenarios. The thesis is organized as follows:

An *Introduction* to highlights the main objectives of this work and to provide an overview of the European railway transportation system.

A first chapter to describe the *State of the Art* of the involved technologies. It describes the railway electrical system and considers the trains that run on it. Then, it firstly focuses on the electric cars and later on the battery storage and the photovoltaic systems which may be additionally introduced in the grid.

The second chapter describes the *Methodology* of how all the systems studied were modeled using MATLAB and SIMULINK and how they are connected to the network itself.

The third chapter, *Simulations*, presents the different DC railway smart grid configurations proposed and the results obtained.

The work ends with the conclusions.

Key-words: *DC smartgrid, Railway system, Electric car charging station*

Abstract in italiano

Questa tesi di Laurea Magistrale in Ingegneria Energetica investiga come una mobilità smart, uno dei punti chiave delle nuove Direttive dell'Unione Europea, e le rinnovabili possano integrarsi al sistema ferroviario con lo scopo di sfruttare la potenza in frenata dei treni stessi, che altrimenti potrebbe perdersi, e creare una sorta di "*DC Railway Smart Grid*" alimentando parcheggi di auto elettriche, inoltre un sistema di accumulo elettrico e generazione con il fotovoltaico connessi alla stessa *DC Railway Smart Grid* permetterebbe di aumentare la penetrazione di rinnovabili in un settore energy-intensive, come quello dei trasporti, a migliorare la *power quality* all'interno dell'intero sistema ferroviario.

L'idea di recuperare l'energia frenante dei treni per ricaricare i veicoli elettrici può avere successo lungo le linee ferroviarie percorse da treni locali o extraurbani, il cui servizio prevede numerose fermate, e utilizzate dai pendolari che raggiungono le stazioni con la propria auto.

Questo lavoro riguarda specificamente il settore ferroviario tra le due cabine elettriche situate a Novate e a Saronno della ferrovia Cadorna (Milano) – Saronno ed è simulato in scenari diversi.

La tesi è strutturata come segue:

Un'introduzione per evidenziare i principali obiettivi di questo lavoro e fornire una panoramica del sistema di trasporto ferroviario europeo.

Un primo capitolo per descrivere lo *Stato dell'Arte* delle tecnologie coinvolte partendo dalla ferrovia stessa studiata per poi passare ai treni che la percorrono, si presenterà il funzionamento delle colonne di ricarica per auto elettriche per poi spiegare il sistema di accumulo introdotto e infine il sistema fotovoltaico, tutte infrastrutture che possono essere introdotte all'interno della rete.

Il secondo capitolo che andrà a spiegare la *Metodologia* di come tutti i sistemi studiati siano stati modellati tramite MATLAB e SIMULINK e di come si siano collegati alla rete stessa.

Il terzo capitolo, *Simulazioni*, per presentare le varie configurazioni della DC railway smart grid e i risultati ottenuti.

Il lavoro finisce con le conclusioni.

Parole chiave: *DC smartgrid, Sistema ferroviario, Sistemi caricamento macchine elettriche*

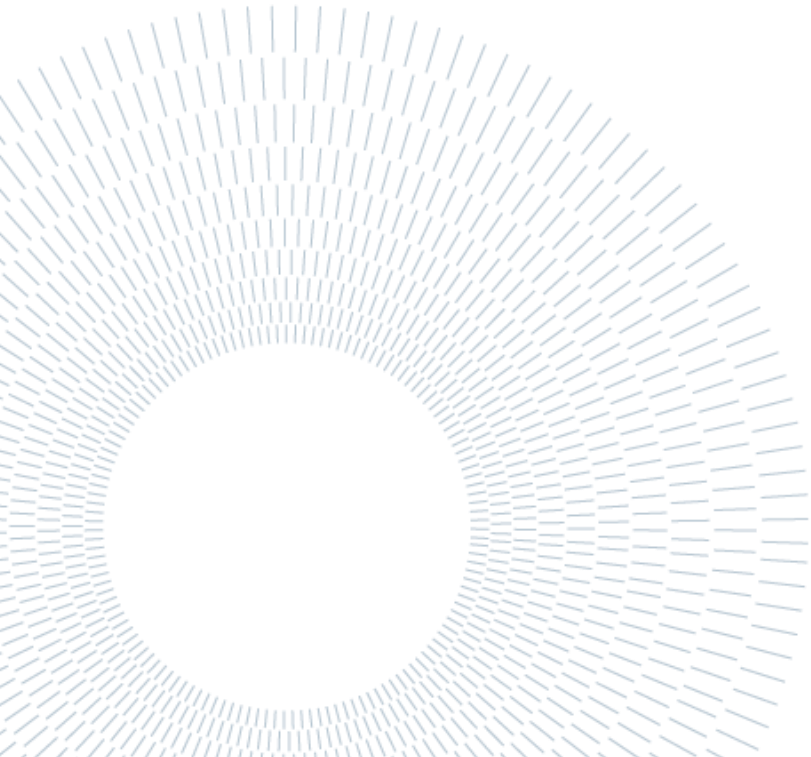

Contents

Introduction

There is a widespread growing awareness in the EU population around environmental issues which asks for a change in attitude to halt or at least limit as much as practicably possible deterioration of the environment we live in, which the European Union is trying to give answers to. Specifically for the transportation system, Europe has set itself an ambitious target: "by 2050 the EU must reduce emissions from transport by 60% compared to 1990 levels, and continue to reduce pollution from vehicles." [1]

How reach it is not yet fixed, but EU identified two main axes to map our path to it:

- increase the efficiency of transport systems, making maximum use of digital technologies, encouraging the shift to low-emission modes;
- accelerate the transition to low and/or zero emission vehicles.

For instance, in recent years in terms of mobility of goods - an essential component of the internal market of the European Union, contributing to economic growth and job creation in each country - the volume of inland freight transportation in Italy (by road, rail, inland waterways and air) has stabilized at around 450 billion tons per kilometer per year, as shown in the table below. [2]

YEAR	ROAD	RAIL	SEA	AIR	TOTAL
2003	203,3	20,4	276,6	0,3	500,5
2004	227,8	22,1	279,5	0,3	529,6
2005	242,9	22,7	288,9	0,3	554,7
2006	229,3	24,2	296,9	0,3	550,7
2007	223,6	25,3	296,9	0,3	546,2
2008	222,6	16,3	301,1	0,3	540,3
2009	207,9	17,8	301,1	0,2	527,1
2010	216,5	18,6	276,4	0,3	511,7
2011	185,6	19,7	267,1	0,3	472,7
2012	166,7	20,3	261,6	0,3	448,9

2013	168,6	19	246,7	0,3	434,6
2014	160,1	20,2	232,5	0,3	413,1
2015	161,2	20,8	254,2	0,3	436,5
2016	164	21,1	254,3	0,31	439,6
2017	165,2	21,6	257,5	0,33	444,6
2018	167,5	22	258,5	0,34	448,3

Table 0.1 : Volume of inland freight transportation

The table shows that rail transport is very underused in Italy compared to road transport despite its undoubted advantages in terms of CO2 equivalent produced and therefore as impact on the environment: there is therefore ample room for action in this sector.

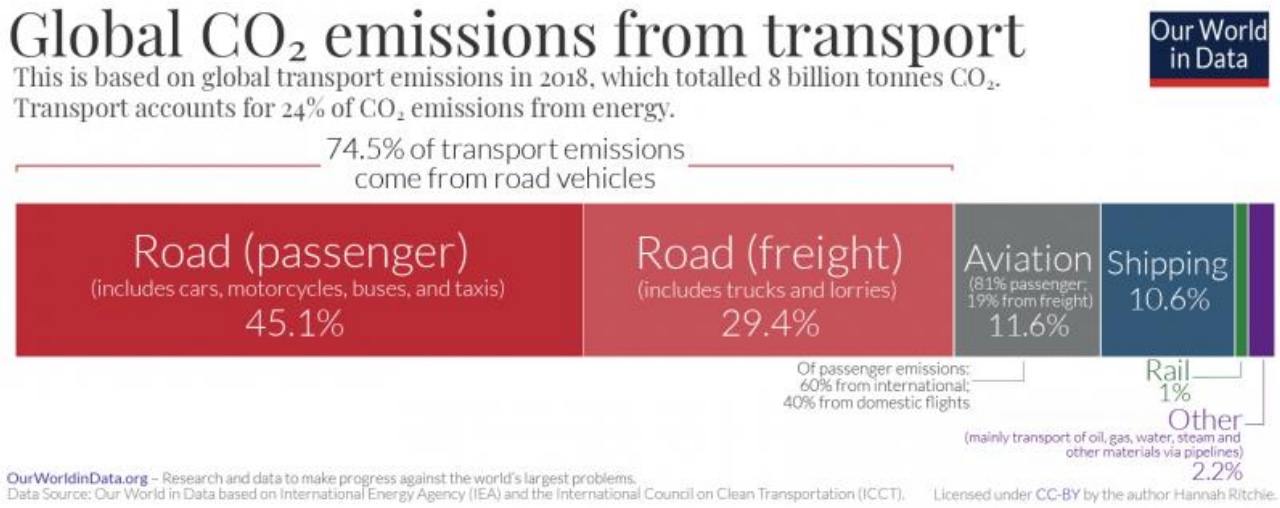

Figure 0.1 : Emissions from transport

An effort is required if the objectives set in the Paris agreements (1.5 ° C etc.) are to be respected.

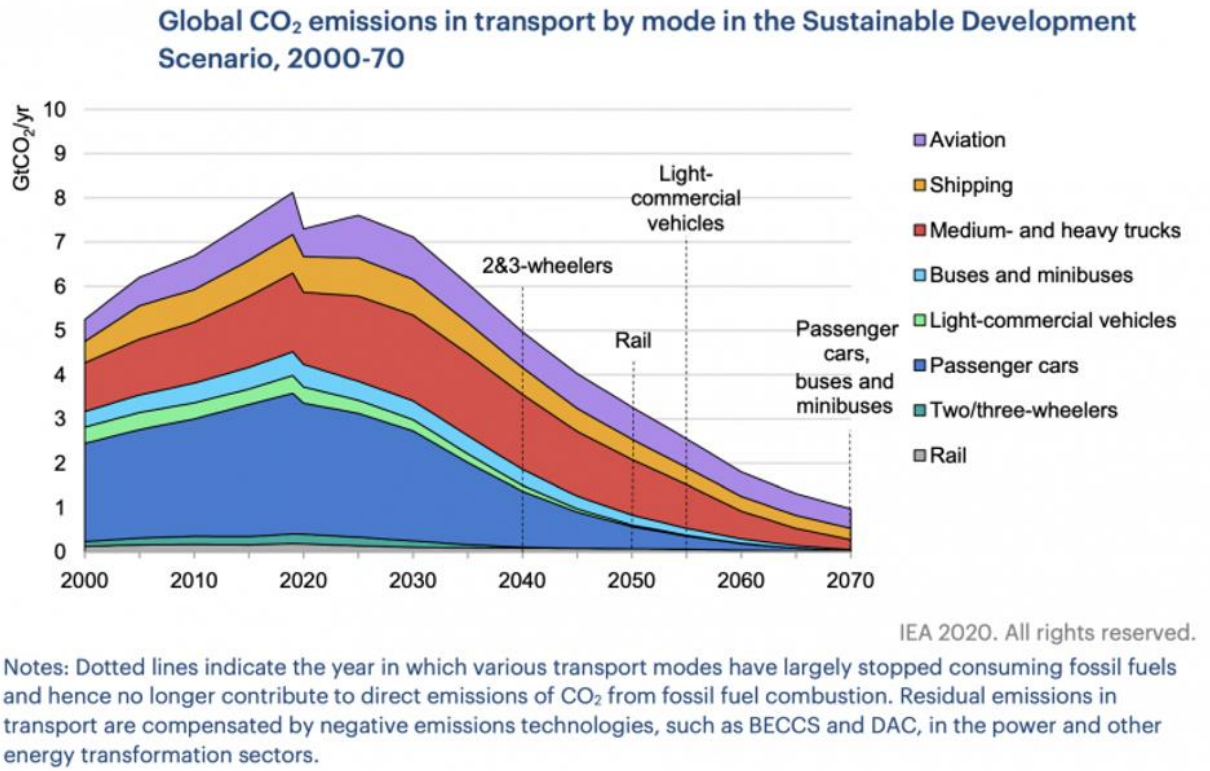

Figure 0.2 : Future emissions scenario

According to "Our world in data" [3] the rail sector must reach net zero emissions around 2050 (in compliance with the objectives imposed by the EU mentioned above).

Transport in general is not without costs to our society because of greenhouse gas and pollutant emissions.
Today overall transport emissions are around 25% of the EU's total greenhouse gas emissions, and these emissions have increased over recent years. To be the "first climate-neutral continent by 2050" requires changes in transport. The goal is to reach a 90% reduction in transport-related greenhouse gas emissions by 2050.

Smart mobility and a more efficient railway system are two of the main targets of the *EU Green Deal*.

This thesis focuses on public transport and more specifically on rail transport, a sector that can certainly be improved but which already excels in terms of quantity of CO2 / kWh or CO2 / km emitted, investigating how smart mobility and the railway system can be integrated so that, power losses of the latter are used to recharge parked electric cars.

The main target of this work is to design a *DC Smart Grid* integrating railway system and electric cars and to this end a sector of the Milano Cadorna – Saronno railway has been selected and modelled because characterized by intense train traffic with stations already organized with car parks to host a considerable number of cars of daily commuters.

Finally, it was investigated how the integration of renewable sources and stationary storage systems can interact with the railway network and improve it.

1 State of art

1.1. History of the electric railway

The very first electric drive transport supported by an infrastructure for energy supply dates 1879 with Werner von Siemens presenting a locomotive powered by 150 V direct current and 2.2kW at the *Berlin Exhibition:* a device defined as "*little more than a toy*". After only two years, Siemens & Halske put the first electric tram into service in Lichterfelde, near Berlin, on a route of about 2.5 km: the vehicle had a total power of about 7.5 kW [4].

Just a few years later, the technology of electric railway traction spread throughout Europe in the tramway sector first and then in the railway. One of the reasons for this success of the electric traction is attributed to the danger associated to the use of the steam traction in urban contexts, due to its exhaust gases, completely absent in an electric traction.

In Italy, the history of electric railway started as early as 1897, where the Minister of Transport proposed three experimental options for different routes in Northern Italy:

- Battery powered train on the Bologna - S.Felice sul Panaro and Milan - Monza lines;
- direct current traction at 650 V, first assumed for the Rome - Frascati, then for the more demanding Milan - Varese;
- high-voltage three-phase traction on the Ferrovie della Valtellina. [4]

The first of the three option was unsuccessful while the other two gave promising results. The real challenge had become to raise the voltage as much as possible (up to values of 3000 V which at the time were considered very high). The development of the three-phase traction (third option) was more difficult and initially delayed by technical issues especially related on how to modulate electric motor speed.
In the first half of the twentieth century, with the expansion of thermoelectric and hydroelectric plants in Italy, the railway lines powered by AC began to extend more and more with the most used power supply frequency of 16 2/3 Hz (corresponding to the 50Hz of the network divided by 3 given by the three-phase). From the '30s onwards, and until today, instead it was preferred to use a continuous power supply at 3000 V.

The distribution over the years in Italy of the various technologies is illustrated in the figure below [4]

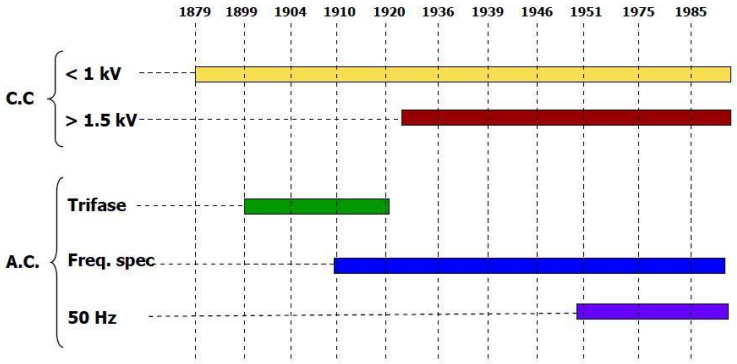

Figure 1.1 : Distribution over the years of electric railways

Railway infrastructures have been continuously improved worldwide to meet both the economic and demographic growth. [6]

The need to guarantee high voltages to supply increasingly powers while maintaining contained currents - to reduce losses and to ease the link with the catenary system - led to the development of multiple and diversified solutions in the various regions of the world.

The rapid differentiation led to an irrational heterogeneity in contrast with the need for technological standardization.[5]

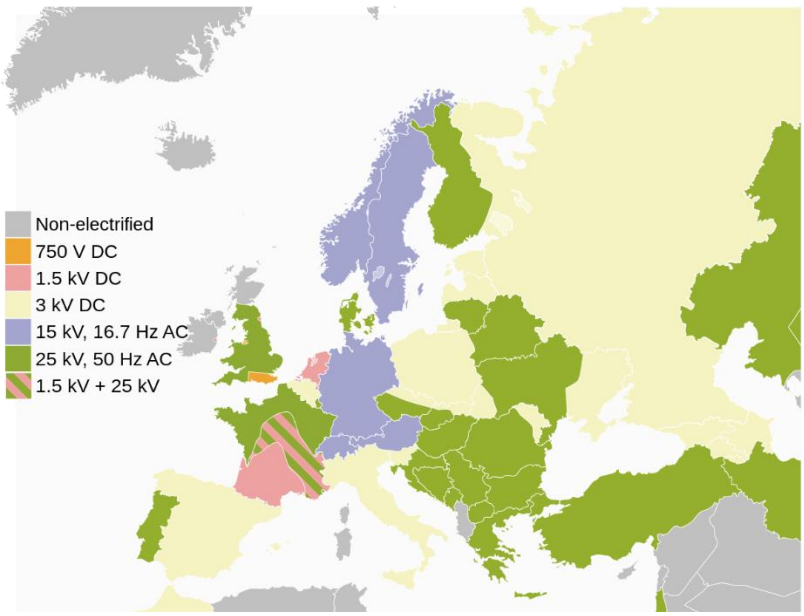

Figure 1.2 : Distribution in Europe of electric railways

Today, in Italy, in addition to the traditional 3kV DC line there is also a 2×25 kV – 50 Hz for the high speed trains. 11921 km of railway are electrified in 3 kV DC and 1296 km are in 2×25 kV - 50Hz AC.

Figure 1.3 : Distribution in Italy of electric railways

1.2. Italian railway system

Like all other electrical rail transportation systems, the Italian rail network is organized as depicted in the following figure with the following components:

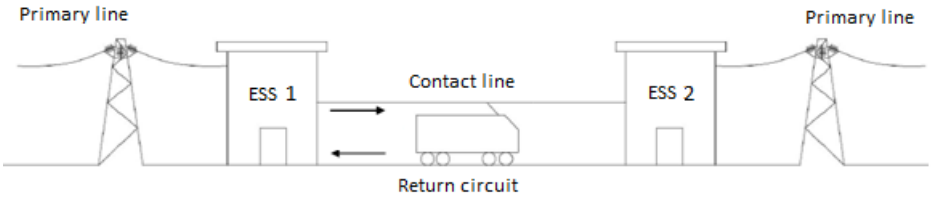

Figure 1.4 : Electric component of a railway system

The energy for the DC railway line supply is derived from the national distribution grid which provides high-voltage energy converted into 3 kV DC in electric substations (hereinafter often referred to as "ESS") along the line (the AC voltage undergoes a double transformation, first is lowered through transformers and then is rectified to DC). The electrical substations are installed with an about 20 km span with each railway line section fed by two substations. Power is supplied to moving trains with a (nearly) continuous overhead line conductor running along the track.

1.2.1. Electric substation

"Considering the high powers, in the traction electrical substations 12 pulse converters are used for their lower harmonic content and the higher conversion efficiency, even if the commutation losses are higher. Today the three-phase Graetz bridge is used. A single bridge is constituted by six diodes branch connected following the scheme of Figure 1.5. Each diode

branch is constituted by 6 diodes in order to reach the maximum line voltage. The 12-pulse reaction is obtained connecting two conversion groups in parallel supplied by a Ddy or a Yyd transformer".[7]

Because of the diode rectifiers the system is not intrinsically reversible: it is therefore not possible for the train supply system to inject energy to the AC electrical grid. The power flow is unidirectional.

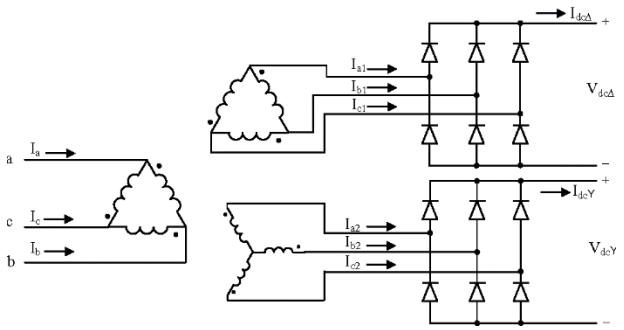

Figure 1.5 : Diodes rectifier

The two Graetz bridges conversion groups of diodes connected in parallel, have structural constraints: each rectifier group has a nominal power of $P_n = V_{max} * I_n$ = 3600 V *1500 A = 5.4 MW, which is given by the maximum voltage bearable by the network for the nominal current of the electrical substations. Furthermore, both the contact system and the ESS must always meet the so-called "Railway applications — Supply voltages of traction systems" and "Railway Applications — Fixed installations and rolling" [8], [9]

- The current that can circulate must not cause the maximum overtemperature to be exceeded;
- The maximum sustainable load from rectifiers must not be exceeded;
- The pantograph voltage values shall not exceed or be less than the maximum and the minimum.

In addition, two different and extraordinary time bands are also identified for the electrical substation.

1. "Normal exercise" where they are considered moments of the day when traffic is heaviest ("*ore di punta*"or "*Rush hour*");
2. "Abnormal operation" where only extraordinary and "anomalous" events to lines or plants are considered (malfunction, blockage of an electrical substation, etc.)

In *normal* operation, the expected traffic must be supported without exceeding the imposed limits, but in *abnormal and* short-term and extraordinary operation, it is possible to exceed these limits due to the increased stress of the system, and it is also

allowed for trains to withstand greater stresses during this period due to the lowering of the voltage.

In this work, only normal exercise is considered.

As regard to the power of the ESS, it should be noted that the standards currently used by RFI provide for the use of 3.6 MW or 5.4 MW approved conversion groups. The performance of rectifier assemblies is shown in the following table: [10]

Nominal power [kW]	Nominal current [A]	Mean square current [A]		Peak current [A]
		Normal Operations	Abnormal Operations	Maximum Duration 5min
3600	1000	1500	2000	3000
5400	1500	2250	3000	3500

Table 1.1 : ESS's currents constrain

In addition, the set limits for the mean square current are precautionary because:

- Under normal conditions, each group is able to support an overload of 50% compared to the rated load continuously without time limits while this maximum load, on which the verification is based, is unlikely to last more than 2-3 hours in everyday operations;
- Under abnormal conditions, a 100% overload can be supported for 2 hours, which is certainly less than the typical duration of the abnormal conditions. If there are long-term failures operations limitations may be imposed on the affected section.

For the calculation of the current in quadratic mean the standard EN 50388 gives a reference on the time to be used summarized in the following table:

Function	Duration	Comments
Protection	80 ms up to 300 ms for AC 25 kV 60 ms up to 300 ms for AC 15 kV 20 ms up to 100 ms for DC	Clearance of short-circuit faults depending on factors such as the intensity of the short-circuit current. Shortest duration typically relates to highest fault currents.
Back up protection	300 ms to 2 s	Clearance of fault on back-up protection.
Peak load current	1 s to 5 s	At supply points and for individual contact lines. Applicable to computer simulations, effect on feeding arrangements and assessment of back-up protection.
	1 min	RMS. average current for calculation of thermal loading on equipment.
Thermal overloading	30 s to 20 min preferred value: 10 min	RMS. average current for calculation of thermal loading on equipment.
Long-term loading	1 h, 2 h	Conventional parameter to define long-term railway load.

Table 1.2 : Reference time

To calculate the current in the square mean in normal situation this thesis adopts the value of 1h using the following equation:

$$I_{ESS,rms} = \sqrt{\frac{1}{T_2-T_1}\int_{T_1}^{T_2}\left[I_{ESS,t}\right]^2 dt} \quad (1\text{-}1)$$

Where:

- With $T_2 - T_1$ equals to one hour;

$I_{ESS,rms}$ is sampled discretely second by second, therefore the formula can be simplified as follows:

$$I_{ESS,rms} = \sqrt{\frac{\sum_t \left[I_{ESS,t}\right]^2}{T_2-T_1}} \quad (1\text{-}2)$$

The ESS, supplies the required energy catenary system at 3000 V and return circuit with which trains interact.

The electrical circuit of a single track can therefore be schematized as follows[1]:

1.2.2. Contact Line

The task of the contact line is to supplying current to the various trains in circulation.

The applicable standards [12] specify that the voltage must always be between **3600V and 2000V** [11], which correspond to a +20%/-33% range of the nominal voltage; in

[1] the various resistances will be explained in the following chapters 2.2.1

terms of current, the standards impose a limit on the overtemperature that can be tolerated by the overhead lines (messenger wire and contact wire) namely 40 °C under nominal conditions and 50 °C under abnormal conditions [9] assuming the most unfavorable conditions with regard to ambient temperature, i.e. 40 °C because of the sun heating. The maximum precautionary value is therefore 80 °C (90 °C in abnormal conditions).

The temperature is a function of the current density and the residence time. An indicative value of **5 A / mm²** is used with regard to the current density.

Section of contact system may vary as follows:

Type of catenary system		
Name	Equipment	Section
FF0	1 Contact wire and 1 Messenger wire	220 mm²
FF1	2 Contact wire and 1 Messenger wire	320 mm²
FF2	2 Contact wire and 2 Messenger wire	440 mm²
FF3	2 Contact wire and 1 Messenger wire	460 mm²
FF4	2 Contact wire and 2 Messenger wire	610 mm²

Figure 1.6 : Different kind of contacts line

All these constraints, both for ESS and return circuits, and reference values derive from the following standards

- **CEI EN 50119** With regard to the heating of the conductors, and therefore the maximum permissible current;
- **CEI EN 50163** With regard to permissible voltage drops and maximum voltage;
- **CEI EN 50388** [9] With regard to the value of the average useful voltage that must be available to the train and the maximum short-circuit currents allowed in the network, it also defines the characteristic times for the calculation of the quantities in quadratic mean.

1.2.3. Return circuit

The return circuit is composed by one or both rails of the track. Some of the functions of the return circuit are equal to that of the contact line in order to ensure smooth railway operation. It is also important to underline that part of the current in the return circuit can be dispersed into the ground as isolation between the track and the ground is not perfect. In the return circuit, to avoid dispersed current, return wires are installed so to create a sort of current preferential path preventing ground dispersion.

The rail has the following section:

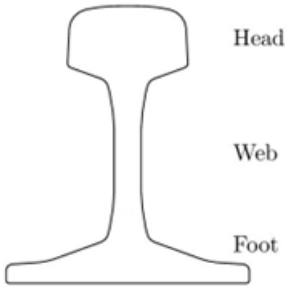

Figure 1.7 : Rail section [14]

The track [15] consists of two rails made of steel positioned at a fixed distance, known as gauge, fixed to prestressed reinforced concrete sleepers. The part of the rail in contact with the wheels of the train is called "*head*" (upper part) and rests on the "*web*", which in turn rests on the "*foot*" (lower part). In order to compensate centrifugal force in curves, the external rail can be elevated compared to the other.

The reference regulations of those aspects is the **UNI EN 13674** [15].

1.3. Electrical Vehicles

The automotive market is currently undergoing significant changes with the increasing use of electrical powertrains. Electric powertrains can be divided mainly into the following categories:

- Battery electric vehicle (BEV) - BEV is a type of electric vehicle that uses chemical energy stored in rechargeable batteries. Instead of internal combustion engines, BEVs use electric motors and electric power converters for propulsion.
- Plug-in Hybrid Electric Vehicle (PHEV) – is a hybrid electric vehicle whose battery pack can be recharged by plugging into an external electric power source, in addition to internally by its on-board internal combustion engine.

It is also important to underline that: "*Sales of EVs more than doubled in 2021 on the previous year and are continuing to rise strongly in 2022. Suffice it to say that only in the 2012 just 120 000 EVs were sold worldwide. In 2021 more than that number were sold each week.*" [16]

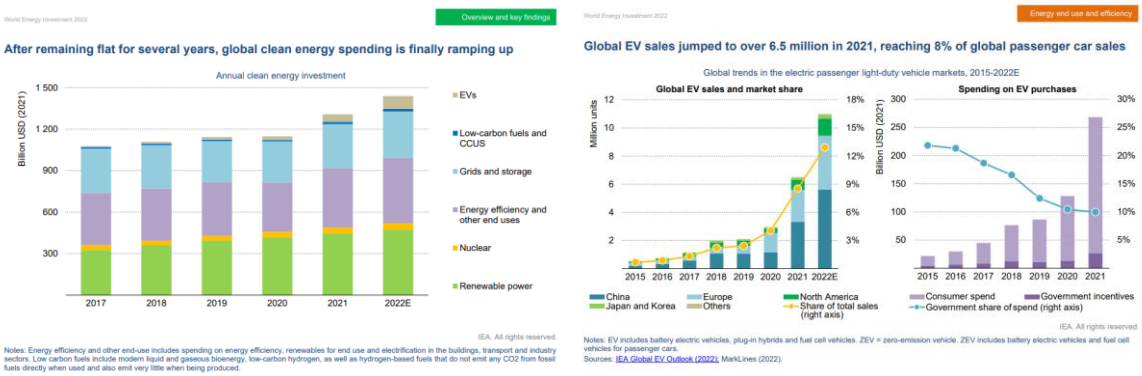

Figure 1.8 : Electric vehicles sales

There has been a significant sales growth especially in China and Europe where electric vehicles exceeded sales of diesel vehicles.

In addition, the number of charging stations has been also growing for years: in 2019, the number of available recharging points has increased by 40% compared to 2018, from 5.2 million to 7.3 million. Investments in public electric vehicle charging infrastructure increased in 2021 by more than 20% compared to 2020, approaching $10 billion in 2022. [17]

1.4. Chargers

Chargers are different from country to country and from manufacturer to another.

In Italy chargers can be classified as follows:

"The standard power charging point includes the following types (AC):

- Domestic: 3.7 kW;
- slow: equal to or less than 7.4 kW;
- accelerated: greater than 7.4 kW and up to 22 kW.

The high-power charging point includes the following types (DC):

- fast: greater than 22 kW and equal to or less than 50 kW;
- ultra-fast: greater than 50 kW."[18]

Considering the constraints on the maximum and minimum voltage associated during charging and discharging cycles, the batteries have typically the following characteristic curve (State of charge – Voltage) Figure 1.9

There are therefore charging and discharging processes that take these constraints into account without affecting efficiency.

The charging mode used is the one described in the study [19].

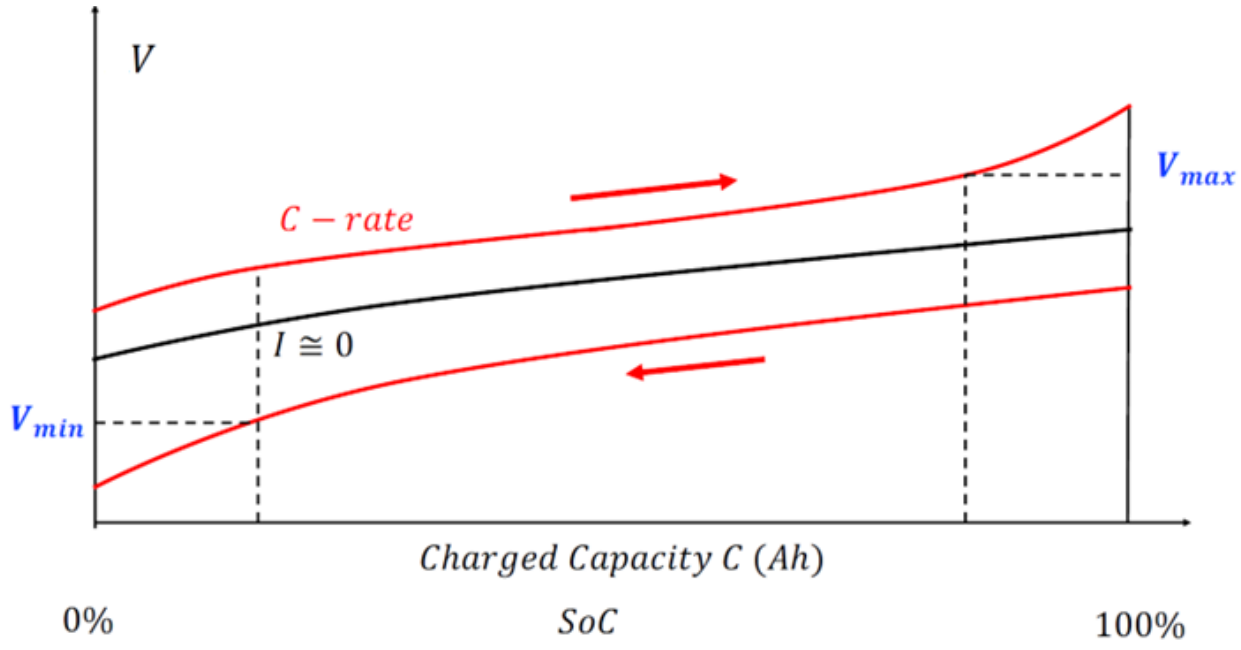

Figure 1.9 : Charge and discharge curve

Consistently the resulting charging mode curves have the following characteristics:

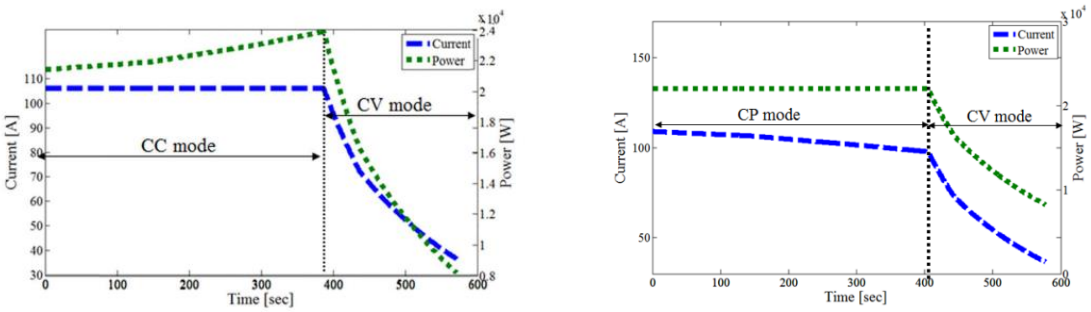

Figure 1.10 : Different discharge curve

The standard charging mode provides that in the first stretch, until the maximum voltage is reached, the current remains constant (DC), but this leads to an increase in power to values even higher than the nominal ones; this increase leads to greater overall losses. The method indicated below instead tries to keep the power constant at the nominal value (CP) in the first section, lowering the current as the SOC increases: this method is more efficient and is the one used by the charging columns from which the data for the thesis work were actually taken.

1.5. Stationary batteries

A stationary battery is an energy storage power station that uses a group of batteries to store electrical energy. Battery storage is the fastest responding dispatchable source of power on electric grids, and it is used to stabilise those grids[2].

As it will appear evident in chapter 2.4, in order to determine the power flow of the stationary batteries, a fuzzy logic controller has been introduced.

1.5.1. Fuzzy logic

The aim of the fuzzy logic in this contest is to create a sort of "Energy management system" able to control numerous parameters not leading necessarily to a unique solution.

Fuzzy logic is often associated with machine learning, although with some differences: the inventor himself, L.A.Zadeh in 1965 called it "the logic for working with words". He defined "linguistic variables" as "variables whose values are not number but words or sentences in a natural or artificial language".[20]

We are therefore confronted with a logic that is no longer binary - where everything is either 0 or 1 - but where each variable is defined in a continuous space between 0 and 1.

The term "fuzzy", in fact, indicates something that lacks precision and/or clarity. In everyday life it is difficult to find something that is completely true or false and fuzzy logic is therefore a tool that allows us to reason with great flexibility, taking into account the inaccuracy and uncertainty that permeates our world.

In practice this logic is well suited for nonlinear systems with any number of outputs and inputs in areas where the systems are not easily modeled with the more conventional tools of mathematics.

1.5.1.1. Components

The whole Fuzzy logic process is usually divided into four components:

1) Fuzzification
2) Fuzzy rules/knowledge base
3) Inference method
4) Defuzzification

1.5.1.2. Fuzzification

It is used to convert inputs into fuzzy sets.

[2] There is plenty of choice in terms of battery size and characteristics. This work has not defined a specific type or group of batteries to be modelled but it simply assumes that a storage capacity is available.

As already mentioned, the inputs may not be well quantifiable, or they can also be, but they are not well cataloged. This concept is easily explained with an example. Is a person of 1.90 m tall? One of 1.80 m? In a Boolean logic you must put a boundary between high or low, that is, for example a person of 1.79 m is short while one centimeter taller is tall.

To make it more sensible and smoother you can create a fuzzy set of this type:

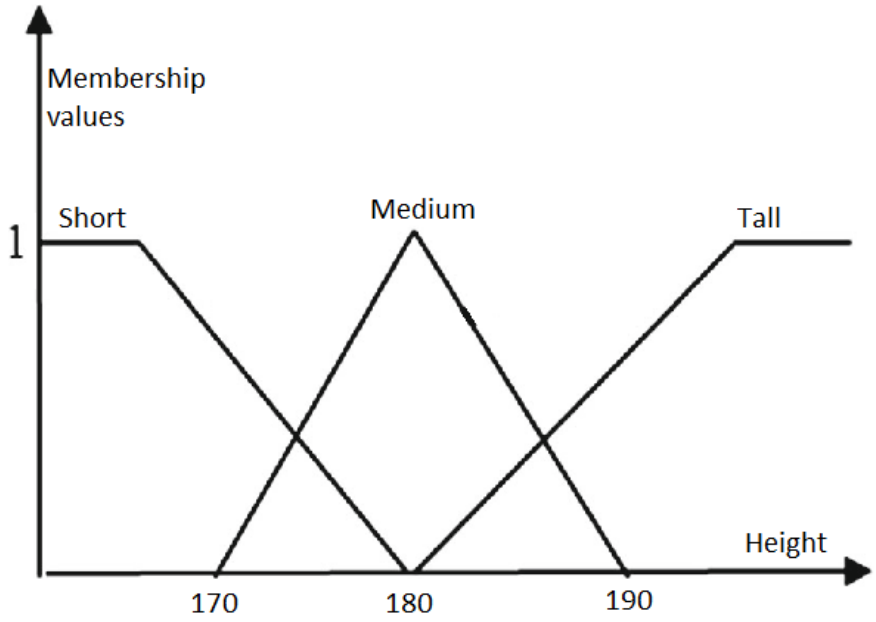

Figure 1.11 : Example of membership function

These curves are called "Membership functions" and indicate how much an input belongs to a given set. In the example, a person of 1.85 m will be 65% medium and 35% high (and 0% low). the input that is not easily cataloged therefore is however uniquely defined in this fuzzy set

It is essential to highlight how these membership functions can be built and defined; There are various methods: you can use the common sense and experience of the controller himself (who builds this control system) or you can do a poll or a survey among experts or even ordinary people.

The forms of these functions are arbitrary e.g. triangular, trapezoidal, Gaussian, one can try to imitate as best as possible how to catalog the result of the poll and/or reality itself.

1.5.1.3. Fuzzy rules

These are "if-then" rules that can be formulated starting from the opinion of experts., from data clustering or genetic algorithms etc.

The rules therefore have the form of the type "if TEMPERATURE is HOT then FAN is FAST" if we refer to the fan speed of a fan coil and the temperature of a chamber, for

example. Usually, to have more degrees of freedom in modeling fuzzy logic, we try to merge multiple inputs within the same rule in the following way:

"if TEMPERATURE is HOT and I AM is SWEAT then FAN is FAST".

It should be noted that since HOT and SWEAT are no longer Boolean variables but fuzzy sets (with continuous values between 0 and 1), the logical command AND will no longer output 0 or 1, but will behave like the MIN function; the logical operator OR is represented by the function MAX and the NOT of the variable, for example X, is equivalent to 1 – X.

Finally, the number of rules needed to describe the system well is variable. A number that is too small may not define the system in its entire operating range, while the maximum number of rules not to oversize the problem is $\prod_N x_n$ with x number of membership functions of the umpteenth input.

1.5.1.4. Inference method

For each rule it is possible to associate a precedence to obtain the output allowing to give more weight to some rules than others.

1.5.1.5. Defuzzification

The last step is defuzzification.

Once the output has been constructed as a fuzzy set (the same procedure as the inputs) you can use a defuzzification logic – the one most used in the literature is the *Centroid* – thus obtaining a precise numerical output.

Starting from an intrinsically *vague and* fuzzy *linguistic* variable to arrive at a precise numerical output was in fact the goal of fuzzy logic itself.

You can therefore define, for each possible input value, an output or a series of outputs.

From these, we finally obtain surfaces or hypersurfaces that represent all the possible solutions of fuzzy logic, in order to offer a simple method, especially at the computational level, to solve the given problem.

The following is an example of a fuzzy surface:[21]

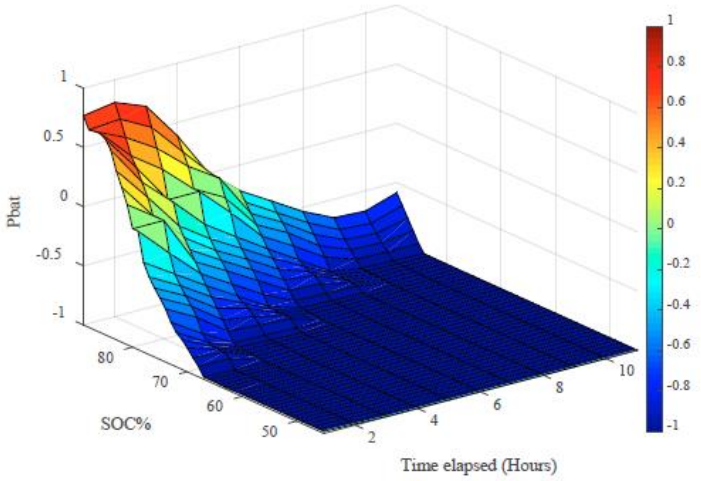

Figure 1.12 : Example of fuzzy surface

1.5.1.6. Pros and Cons of Fuzzy Logic

Pros:

- Fuzzy logic is more likely to represent real-world problems than binary logic.
- By only making surface (or hypersurface) interpolations to obtain the final output of this logic, it has a low computational burden compared to many other logics.
- It is a logic that works with imprecise and inaccurate, *vague and fuzzy* inputs.

Cons:

- It is a logic dependent on human expertise and knowledge.
- Being a logic that relies on inaccurate inputs, they must be tested and validated during the creation of the control logic.

1.6. Benchmark

The concept of DC hub associated to a railway network is rear in literature.

This thesis This work takes inspiration from various papers, in particular has been primarily inspired by two [6], [22], where the railway networks is similar to the one that will be presented here but their focus is solely on how the various components can be connected and the control systems of those components.

In literature there are also problems regarding maximization / minimization of costs or a sizing of a particular component with no ambitious to model the entire system.

There are papers that describes not only DC high voltage railway network, but for example we have the AC at 25 kV with [24], [25] and also there are studies concern the tram network or the subway [27].

The following studies sum up the bests configurations for each type of network [26].

It is also very common in literature to also add a generation within the system. This thesis also sees how the introduction of a photovoltaic system can improve it.

2 Methodology

The method utilized to develop the railway network model - inclusive of all the various components described in the previous chapter - is quite linear: a specific sector of the Italian railway network in its current configuration has been first selected and - once modelled with data available to public, on internet – it has been used as a sort of baseline for all simulations as well as to illustrate the relevant existing technical constraints and the area of potential developments.

The selected "baseline" network is a model of a portion of the existing Trenord Cadorna – Saronno line: the **Novate – Saronno** sector. This sector has been selected because limited by only two ESSs (one in Novate and one in Saronno) and its railway stations have plenty of room to accommodate electric car parks and/or photovoltaic systems.

The analysis of the simulations described in the following chapter 3 have been focused on four scenarios: two different configurations (as described here below) of the railway sector in its current status during two different hours of the day characterized by either high traffic when trains are composed of 8 elements (hereinafter referred to as "Rush hour") or low traffic on the line when trains are composed of 5 elements (hereinafter referred to as "Off-peak hour").

The various components described in the previous chapter i.e. car parks, storage systems and photovoltaic modules, are added one by one to the baseline network model and then subject to dedicated simulations.

Trains, Railway network, Car Parks, Stationary batteries and PV modules have been modelled as described in the following paragraph of this chapter 2.

2.1. Train modelling

The following model was made through MATLAB[28] and Simulink[29]

The train taken into consideration in this work is the TSR: Regional Service Train called (for the Ferrovie dello Stato, FS) ALe 711 if equipped with a cabin, otherwise if it is not ALe 710; instead Ferrovie Nord, FN, calls it EB.711 and EB.710 with the same criteria.

The train has the following characteristics: [30]

TRAIN	TSR EB711/EB710 ALe711/ALe710
Rated supply voltage	3 kV
Maximum speed	140 km/h
Continuous power	680 kW
Hourly power [ORARIA]	760 kW
Mass without load 711/710	58 t/53 t
Mass at full load 711/710	71 t/68 t
Average mass considered	62.5 t
Maximum acceleration	0.9 m/s²
Maximum deceleration	1.1 m/s²
Base speed [BASE]	40 km/h

Table 2.1 : TSR characteristic values

Figure 2.1 : TSR EB 711 [31]

The choice of train and its route was weighed against the following factors:

1. the TSR EB711/710 is the train that passes on the route considered, the **Cadorna – Saronno;**
2. The route in question is very busy and used largely by daily travelers who typically reach the various stations by car (then leaving it in the parking lots assumed to be properly equipped with charging columns);
3. The TSR has a modular configuration: each element has electric motors and it is assumed that each element of the train behaves in the same way in terms of power consumption;
4. the network in question is 3 kV, which allows, when external components are connected to it (such as EV charging parks) a higher quality power flow compared to having lower voltages and/or domestic voltages;
5. There are several trains travelling on this line at the same time throughout the day. This would allow for the possible recovery of powers otherwise unrecovered (see regenerative braking of trains at times when demand for other trains is not high enough) which would contribute to relieve the national grid of additional loads, a very sensitive issue today given the ever-growing power demand. ;

2.1.1. Mechanical characteristic

For the modeling of the problem, we started from the second principle of dynamics, in fact a moving train has an acceleration force that will be equal to:

$$F_a = F_t - F_r = m_e \cdot a \tag{2.1}$$

Where:

- F_a is the accelerating force;
- F_t is the traction force generated by the motor, given by the mechanical characteristic of the vehicle;
- F_r is the resistance force to the motion;
- m_e is the equivalent mass, including the inertial effect of the rotating masses (in this study assumed at 10% of the total mass);
- a is the acceleration.

The mechanical characteristic in the ideal world is a hyperbole in the Force-speed plane that generates through the product of its components a constant power, but at low speeds we have 3 limits that make the hyperbola a curve of this type:

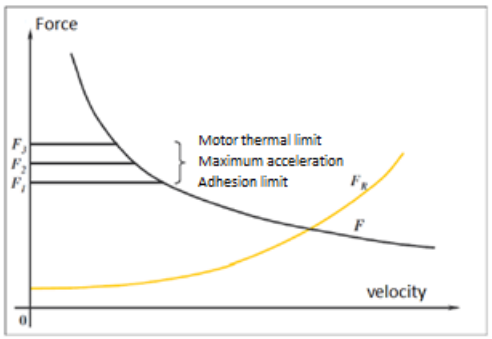

Figure 2.2 : Mechanical characteristic

These limits are:

1. acceleration cannot exceed a certain threshold for passenger comfort (and safety);
2. The forces cannot reach too high values (which happens at low speeds) to protect the engine from mechanical and thermal stresses;
3. it is necessary to respect the wheel grip limits.

This implies that the mechanical characteristic has a plateau with almost constant force up to base speed, then returns to the hyperbola stretch with a constant power profile

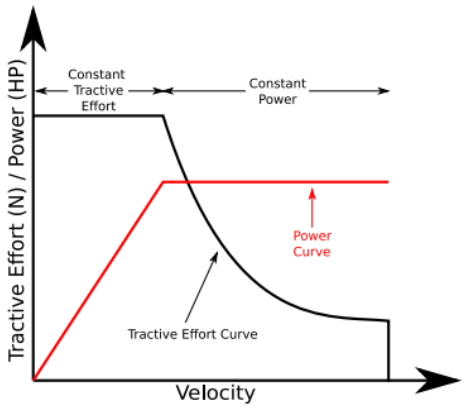

Figure 2.3 : Mechanical characteristic and power curve

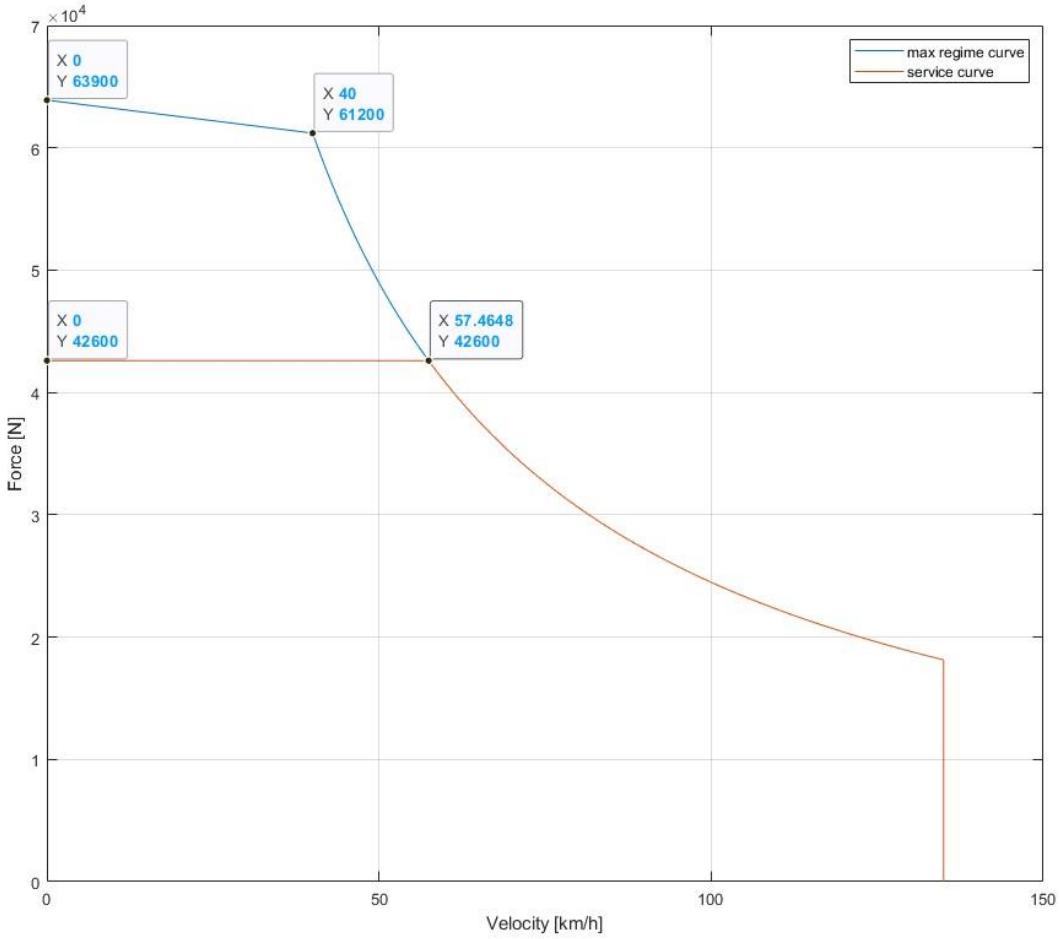

Figure 2.4 : Modelized mechanical characteristic

The full-function curve in the first section is not flat but inclined, because:

At zero speed it is considered the least permissive constraint relative to maximum acceleration:

$$F_{max0} = a_{\lim} * m_{\max} = 63.9\ kN \tag{2.2}$$

where:

- The first member is the maximum acceleration and is worth 0.9 m/s²
- The second is the highest mass among the various elements and at full load, it is worth 71t

At the point at "base speed" (that is, the speed for which you pass from the horizontal section, due to the limits mentioned above, to the constant power section vbase = 40 km / h) the force was calculated as the ratio between maximum train power (680 kW), as we are exactly at the point at maximum power, fraction the base speed itself, obtaining the value of 61.2 kN in the case at full speed; this is the point with the most binding constrain among the three mentioned above, and corresponds to the adhesion limit, considering a maximum friction coefficient of 0.25.

Once the curve was obtained at full capacity (the blue one), the service curve was also calculated (the red one), defined as, as regards the first almost constant section, two thirds of the curve at full speed at the base speed point, in order to have optimal results even in the case of "drive" losses caused by the loss of a possible element in the compartment.

In the case of "service curve" the base speed will be higher as clearly seen in the graph.

2.1.2. Resistance forces

The resistance forces are caused by various factors, generally grouped into two components: *straight and flat* resistances and *accidental resistances* [32]

To the *straight and flat* resistances belong those forces that are always present if the train is in motion and due to:

1. Vehicle-air
2. Wheel-road
3. Internal friction

RFI uses the following empirical formula for trains of this type: [33]

$$F_{ro} = m \cdot g \cdot [\ 1.94 + 2.65 \cdot \left(\frac{v^2}{100}\right)\ ] \tag{2.3}$$

where:

- m is the mass in tons
- v is the speed in m/s
- F_{ro} is the sum of all forces in straight and plane expressed in N

Other empirical formulas of losses have also been tested, and all have given comparable results. [34], [35]

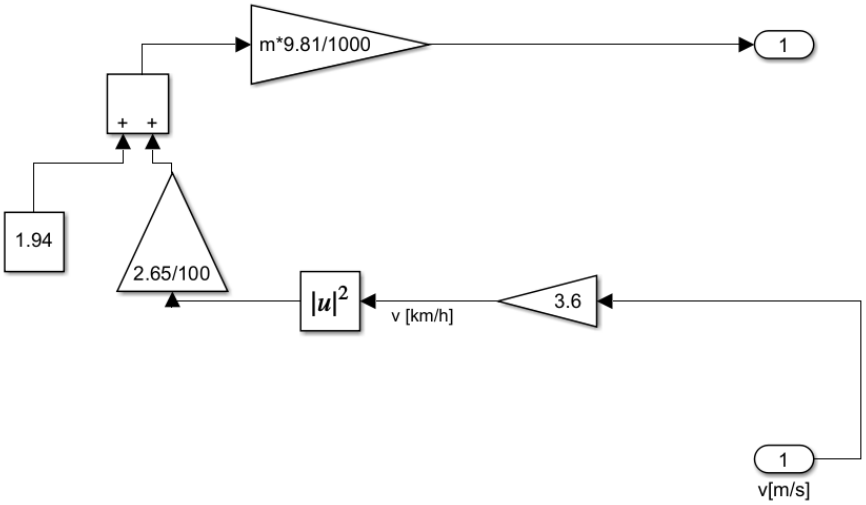

Figure 2.5 : Simulink modelized losses

Accidental forces, on the other hand, are composed of resistance in curves and slopes, those in curves have been neglected, as the route considered is mostly straight, while those for slope have been calculated as follows:

$$F_{ri} = m \cdot g \cdot sen(\theta) \tag{2.4}$$

Where:

- θ is the express slope of the path expressed in radians.

For the evaluation of α, a constant slope between one stop and another was considered.

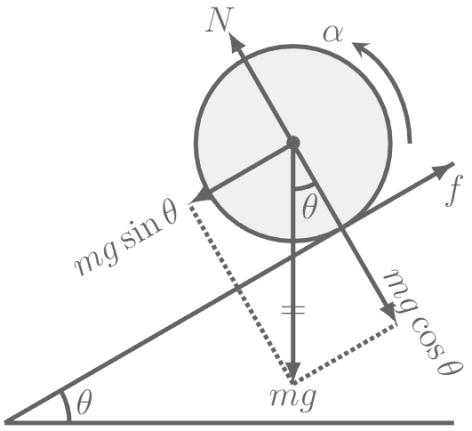

Figure 2.6 : Forces in an inclined plane

[[https://www.concepts-of-physics.com/mechanics/rolling-without-slipping-of-rings-cylinders-and-spheres.php]]

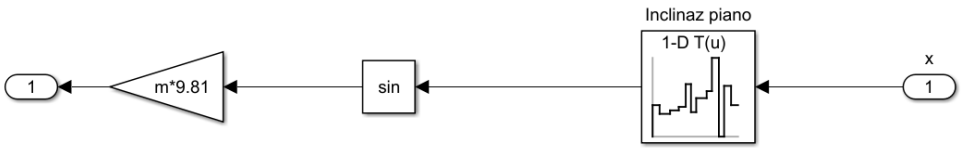

Figure 2.7 : Simulink vertical losses

For the calculation of the equivalent mass, reference was made to various papers that indicate a value with which the mass of the train must be increased to consider the rotating elements, in this study the value of 10% was taken as a reference. [4], [36]

2.1.3. Train model

Finally, the power, absorbed or transferred by each train, is simply the product between the traction forces of the train itself, and its speed.

$$P = F \cdot v \tag{2.5}$$

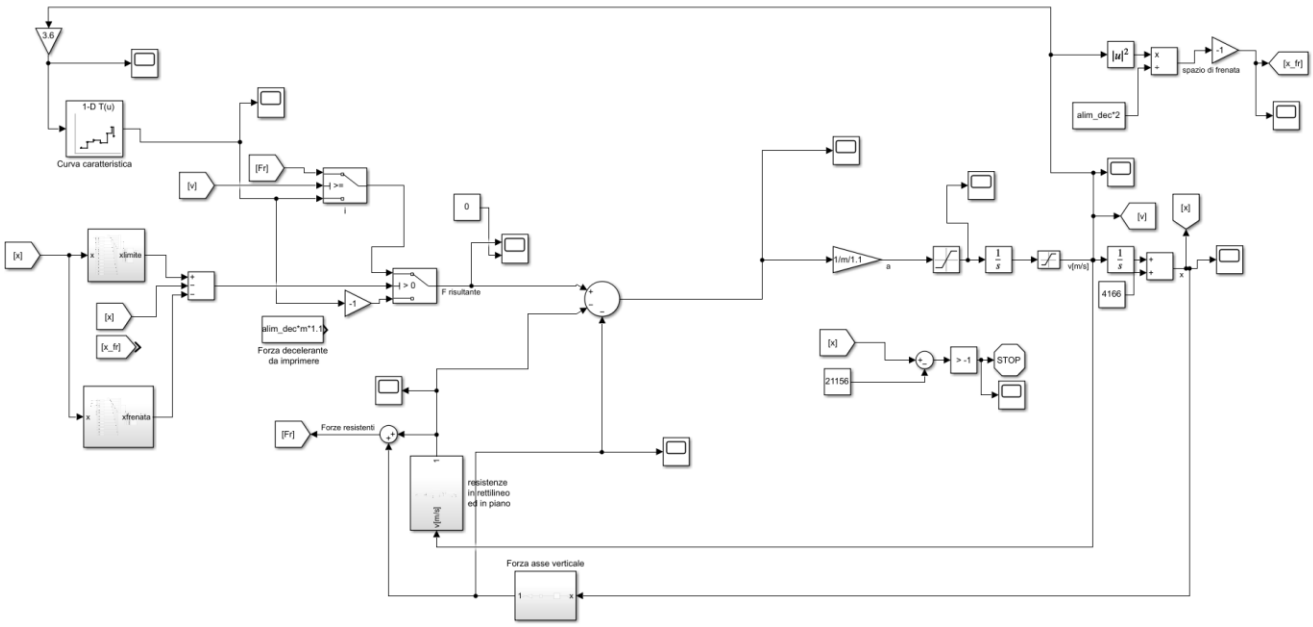

Figure 2.8 : Simulink train model

The results of a five elements train is the follows:

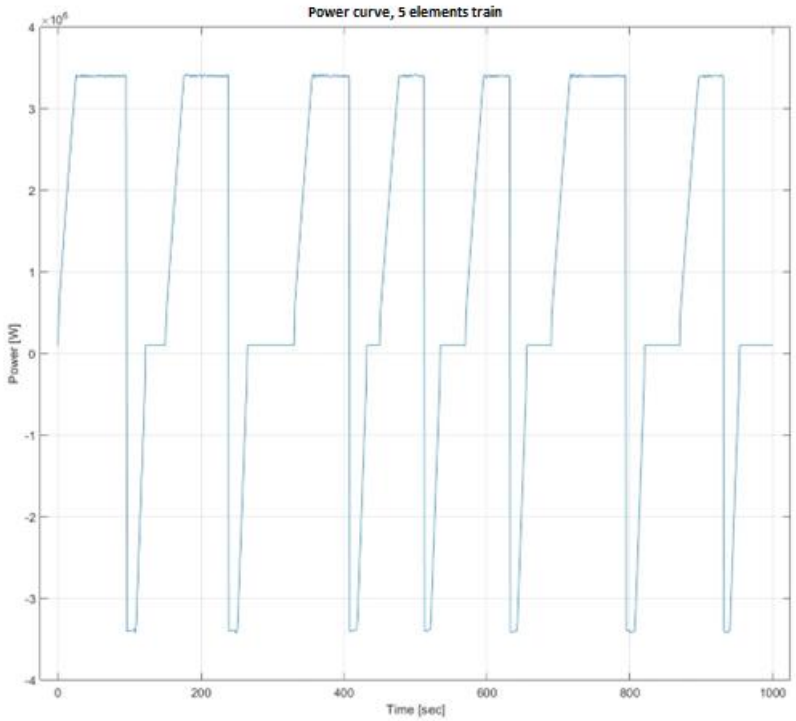

Figure 2.9 : Power curve of a five elements train

It is also important to underline that when a train brakes only part of that force or power can be recovered electrically.

In fact, it is only possible to electrically recover a force that respects the graph of the characteristic curve mentioned above. If the braking force is greater than that then part of this will necessarily be dissipated by heat.

It is therefore possible to imagine two scenarios, the first, closer to reality, where the train brakes with a single constraint the maximum deceleration and therefore it will take less time but will necessarily dissipate energy, the second where braking follows the characteristic curve of the TSR and therefore allows for potentially recover all the braking.

2.1.4. Train timetable

The passenger service of the railway line is carried out by two suburban lines, the S1 and the S3, and by four regional lines (Malpensa Express, Novara – Saronno - Milano Cadorna, Laveno – Varese – Saronno - Milano Cadorna and Como – Saronno - Milano Cadorna). The operation of all six lines is by Trenord on the basis of the service contract with the Lombardy Regional Administration (2009) [37].

The various train stops of the route considered are listed in the following Figure 2.10. It is also possible to note the distance between one stop and another and also the altitude of each of them (data used for the modeling of the system).

Figure 2.10 : Datas of the Cadorna - Saronno track.

The various train schedules are divided according to the following figure [38]

The tabular representation of the section considered is as follows:

Genere di treno	EX	S3	R	R	R	S1	S1	RE	EX	RE	S3	S1	S1	RE	EX	S3	R	R	R	S1	S1	EX	RE	S3	S1	S1	EX	S3	R	R	R	S1	S1	EX
Numero del treno	323	823	23	123	223	23130	523	25	325	125	825	23136	525	6027	327	827	29	129	229	23142	529	329	6129	829	23148	531	331	831	31	131	231	23154	533	333
Giorno di circolazione	G	G	G	G	G	G[1]	G[1]	G	G	G	G	G[1]	G[1]	P[12]	G	G	G	G	G	G[1]	G[1]	G	P[12]	G	G[1]	G[1]	G	G	G	G	G	G[1]	G[1]	G
Nota commerciale	[31] [37] [39] [43]	[31]		[31]	[31] [42]	[31] [36]	[31] [36]	[31]	[31] [37] [39] [43]			[36]	[36]		[37] [39] [43]				[42]	[36]	[36]	[37] [39] [43]			[36]	[36]	[37] [39] [43]				[42]	[36]	[36]	[37] [39] [43]
Classe	1	2	1-2	1-2	1-2	2	2	1-2	1	1-2	2	2	2	1-2	1	2	1-2	1-2	1-2	2	2	1	1-2	2	2	2	1	2	1-2	1-2	1-2	2	2	1
Milano Cadorna	8:27	8:32	8:35	8:40	8:45			8:50	8:57	9:00	9:02			9:20	9:27	9:32	9:35	9:40	9:45			9:57	10:00	10:02			10:27	10:32	10:35	10:40	10:45			10:57
Milano Domodossola	|	8:36	8:39	8:44	8:49			8:54	|	9:04	9:06			9:23	|	9:36	9:39	9:44	9:49			|	10:03	10:06			|	10:36	10:39	10:44	10:49			|
Milano Rogoredo p.						8:28						8:58								9:28					9:58							10:28			
Milano P.ta Vittoria						8:36						9:06								9:36					10:06							10:36			
Milano Dateo						8:38						9:08								9:38					10:08							10:38			
Milano P.ta Venezia						8:40						9:10								9:40					10:10							10:40			
Milano Repubblica						8:42						9:12								9:42					10:12							10:42			
Milano P.ta Garibaldi						8:45						9:15								9:45					10:15							10:45			
Milano Lancetti						8:50						9:20								9:50					10:20							10:50			
Milano Bovisa a.	8:33	8:39	8:42	8:47	8:52	8:54		8:57	9:03	9:07	9:09	9:24		9:26	9:33	9:39	9:42	9:47	9:52	9:54		10:03	10:07	10:09	10:24		10:33	10:39	10:42	10:47	10:52	10:54		11:03
Milano Bovisa p.	8:34	8:41	8:44	8:49	8:54		8:56	8:59	9:04	9:09	9:11		9:26	9:27	9:34	9:41	9:44	9:49	9:54		9:56	10:04	10:08	10:11		10:26	10:34	10:41	10:44	10:49	10:54		10:56	11:04
Milano Quarto Oggiaro	|	8:44	|	|	|		8:59	|	|	|	9:14		9:29	|	|	9:44	|	|	|		9:59	|	|	10:14		10:29	|	10:44	|	|	|		10:59	|
Novate Milanese	|	8:46	|	|	|		9:01	|	|	|	9:16		9:31	|	|	9:46	|	|	|		10:01	|	|	10:16		10:31	|	10:46	|	|	|		11:01	|
Bollate Centro	|	8:48	|	|	|		9:03	|	|	|	9:18		9:33	|	|	9:48	|	|	|		10:03	|	|	10:18		10:33	|	10:48	|	|	|		11:03	|
Bollate Nord	|	8:50	|	|	|		9:05	|	|	|	9:20		9:35	|	|	9:50	|	|	|		10:05	|	|	10:20		10:35	|	10:50	|	|	|		11:05	|
Garbagnate Serenella	|	8:53	|	|	|		9:08	|	|	|	9:23		9:38	|	|	9:53	|	|	|		10:08	|	|	10:23		10:38	|	10:53	|	|	|		11:08	|
Garbagnate Milanese	|	8:56	|	|	|		9:11	|	|	|	9:26		9:41	|	|	9:56	|	|	|		10:11	|	|	10:26		10:41	|	10:56	|	|	|		11:11	|
Cesate	|	8:58	|	|	|		9:13	|	|	|	9:28		9:43	|	|	9:58	|	|	|		10:13	|	|	10:28		10:43	|	10:58	|	|	|		11:13	|
Caronno Pertusella	|	9:01	|	|	|		9:16	|	|	|	9:31		9:46	|	|	10:01	|	|	|		10:16	|	|	10:31		10:46	|	11:01	|	|	|		11:16	|
Saronno Sud	|	9:04	|	|	|		9:19	|	|	|	9:34		9:49	|	|	10:04	|	|	|		10:19	|	|	10:34		10:49	|	11:04	|	|	|		11:19	|
Saronno	8:46	9:07	8:57	9:02	9:07		9:22	9:12	9:16	9:22	9:37		9:52	9:39	9:46	10:07	9:57	10:02	10:07			10:22	10:16	10:20	10:37		10:52	10:46	11:07	10:57	11:02	11:07		11:22	11:16
	MXP		VARESE	COMO	NOVARA			LAVENO	MXP	COMO				LAVENO	MXP		LAVENO	COMO	NOVARA			MXP	COMO				MXP		LAVENO	COMO	NOVARA			MXP

Figure 2.11 : Trains timetable

It was also decided to divide the day into Rush hours (when there is a greater number of elements for each train) and Off-peak. Rush hours range from 7.00 to 9.30 and from 17.00 to 19.30 with an estimated average of 8 elements per train. The rest of the day is modelled as Off-peak hours with an estimated average of 5 elements per train.

2.1.5. Time track

A time track is "*The graphical timetable is a Cartesian diagram x, y used by timetables to represent a transport service (usually rail) on a given line. In abscissa (x-axis) are represented the times (h, min), in ordinates (y axis), the spaces (km) and the stations of a railway line. [...] The track is an oblique break oriented from left to right and from top to bottom for trains running from the station at the lower end of the y-axis to the station at the upper end of the same axis and from bottom to top for trains in the opposite direction (see cadenced timetable).*

The slope of the track represents the average running speed of the train, therefore, in a space-time diagram executed at an appropriate scale, the more the track tends to the vertical, the faster the train, whatever the direction of travel." [39]

Horizontal lines represent a stationary train at a station.

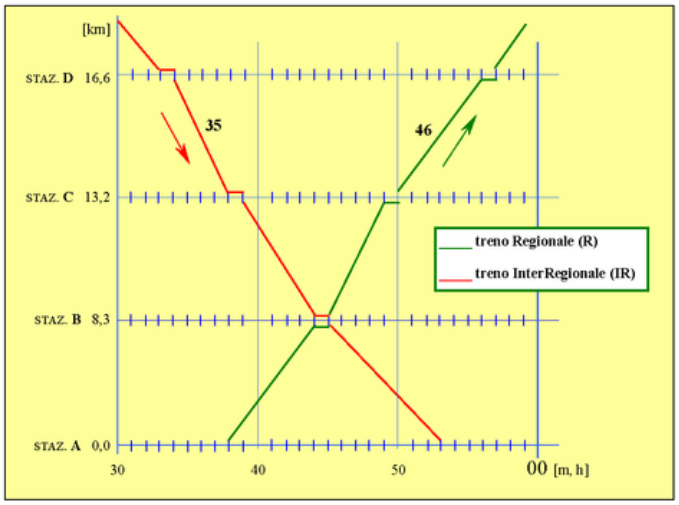

Figure 2.12 : Example of graphical timetable

As will be better explained in the chapter describing the network, the Novate Saronno sector consists of four tracks: two are fast and two are slow (more stops).

Figure 2.13 is the hourly track for each pair of tracks. Track 1 and 2 are slow tracks while track 3 and 4 are fast tracks. The odd numbers indicate direction to Saronno while the even numbers refer to the direction to Cadorna.

The four tracks not only have a different number of stops, but also have a different section of the overhead line: for the first two tracks has been assumed a section type FF4 (i.e. two contact wires and two messenger wire) of 610 mm^2 , while the last two a section of 460 mm^2 as they are assumed as type FF3 (i.e. two contact wires and one

messenger wire), however, refer to Figure 1.6 : Different kind of contacts lineFigure 1.6

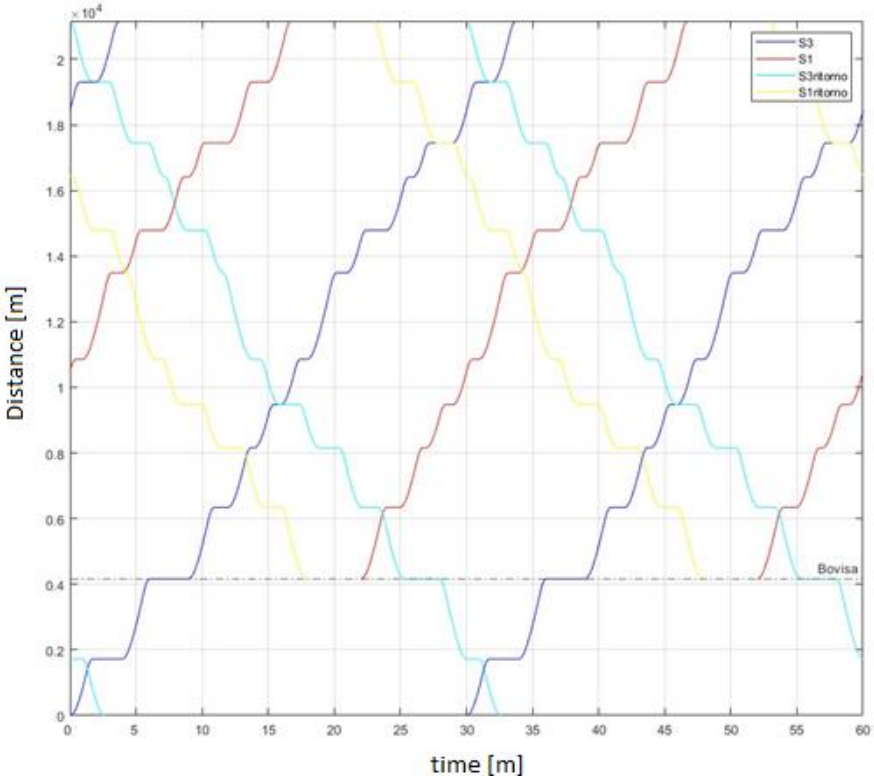

Figure 2.13 : Modelled graphical timetable of "Track 1 and 2".

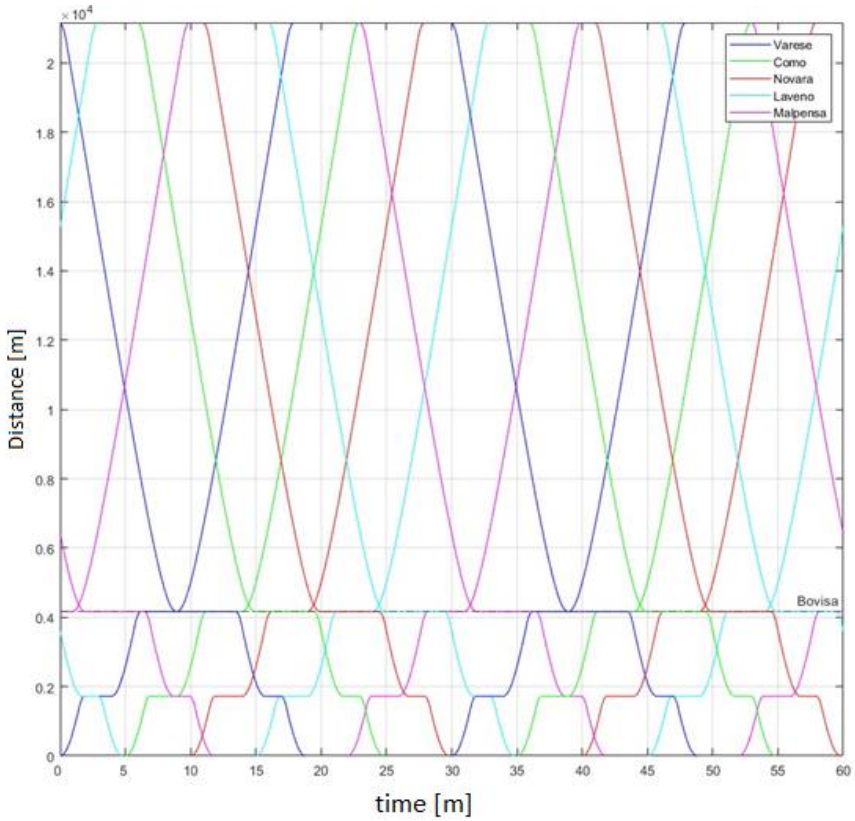

Figure 2.14 : Modelled graphical timetable of "Track 3 and 4".

The S1 trains, both round trips, do not reach Cadorna and therefore are modeled only for the Saronno – Bovisa route.

Bovisa is the stop where each train makes a scheduled break of about 3 minutes (which is not respected if the train has already accumulated delay)

The only trains that reach the maximum speed allowed are only those that travel on preferential tracks (track 3 and 4) and only in the Saronno - Bovisa section.

2.2. Railway electrical system modeling

The topology of the railway grid is a function of the position of the trains along the tracks. Two cases were considered: a simplified model and a more detailed and realistic.

The simplified model takes into account only the resistance of the through the overhead line, while the second one includes the modeling of return circuit through the rails (it was assumed that both rails take part in the return circuit) and the an ideal ground due to the leakage currents.

The following configurations are obtained Figure 2.15.

Below there are the two diagrams of the "simplified" and "detailed" models mentioned above: note that both schemes have been simplified, as they represent a single track with only one train travelling, (a 4-track representation would have been more complex and judged to be an unnecessary complication).

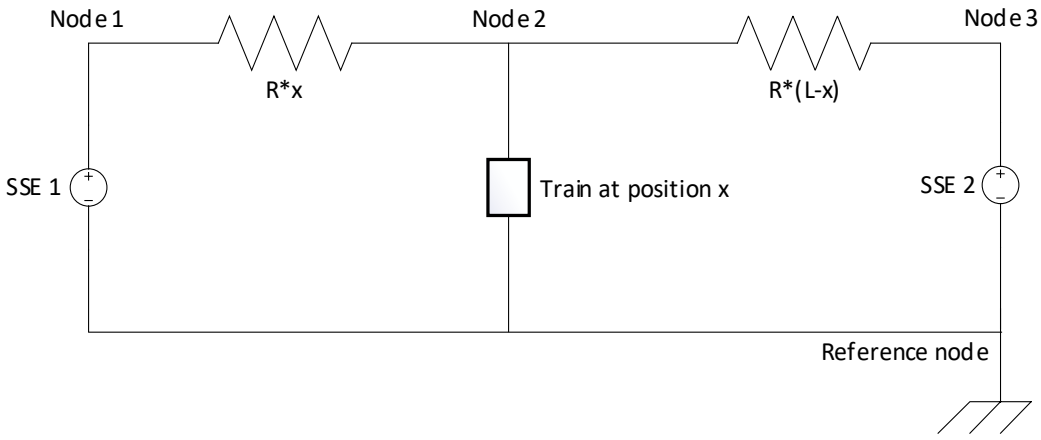

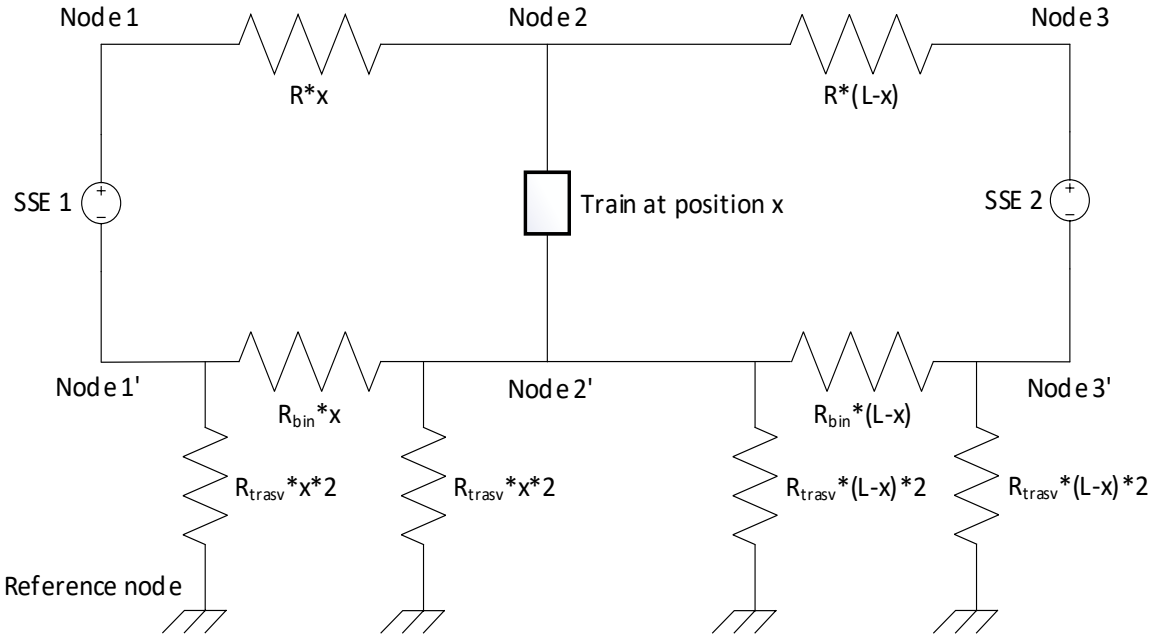

Figure 2.15 : Different models of a single track

It is important to note that the biggest difference between the two cases is the number of nodes doubling moving from the first to the second one. Also, the number of resistances/conductances involved changes (more than doubled).

To represent the electrical circuit, it is first necessary to identify the position of the trains for each track, for any time.

The electrical grid is then defined as follows and allows to calculate the conductance of the circuit.

2.2.1. Electric resistances

Given the position of the trains, the distance between it and the next electrical node (electrical substation or another train) is defined.

The per-unit-length line resistance is defined as follows:

$$r_{line} = \frac{\rho_{line}}{A_{cat}} \tag{2.6}$$

Where:

- ρ_{line} is the electrical resistivity defined in $[\frac{\Omega\,mm^2}{m}]$, in the case considered (copper) the value of is ρ 0.017 $\frac{\Omega\,mm^2}{m}$;
- A_{cat} is the overall section considered, being a overhead line of type 4 with two wires and two conductors (FF4 150 + 150 + 160 + 160)[13] the overall section is 610 mm^2 for the first two tracks, and a FF3 with a overall section of 460mm^2 for the last 2 two.

Once the per-unit-length line resistance is obtained, the resistance can be evaluated as follows:

$$R = r * x \tag{2.6}$$

Where:

- x is the distance in $[m]$ between two nodes.

For the per-unit-length resistance of the tracks

$$r_{rail} = \frac{\rho_{rail}}{2 * A_{rail}} \tag{2.7}$$

Where:

- $\rho_{binario}$ is the electrical resistivity defined in $[\frac{\Omega\,\mathrm{mm}^2}{m}]$, in the case considered (mild iron) the value of is $\rho = 0.13\,\frac{\Omega\,\mathrm{mm}^2}{m}$;
- A_{rail} is the overall section considered, the rail is UNI 60 [40] with section of 7686 mm^2.

The presence of the coefficient two in the denominator takes into account that both rails belong to the return circuit.

The ground conductance (inverse of the resistance) , or also called shunt conductance, can take on more values and also vary by orders of magnitude. In fact, it is a function of several parameters such as: construction parameters of the track, humidity, presence or absence of other elements that can discharge to the ground (such as other tracks) and environmental conditions etc.

In this study, the reference value of R = 0.5 ohms/km was therefore assumed, having considered the study in [41].

The difference compared to the two previous cases is that the shunt resistance is placed in parallel to the other resistances, as the π model has been used, for this reason in figure Figure 2.15 : Different models of a single trackthere is the multiplicative factor 2, as to represent the same phenomenon with the π model (and putting two resistances and not one) it is necessary to multiply the resistance by 2.

To obtain the conductance of each individual parameter, the conversion is immediate:

$$G = \frac{1}{r * x_{posix}} = \frac{1}{R} \tag{2.8}$$

Material	Resistivity $[\frac{\Omega\,mm^2}{m}]$
Copper	0.017
Gold	0.024
Iron	0.13
Carbon	35

Table 2.2 : Different materials resistivities[42]

2.2.2. Conductance matrix

Once the conductances of each branch are obtained, the circuit can be solved by knowing the voltages and/or currents thanks to the following relation:

$$[\bar{I}] = [\bar{G}] \cdot [\bar{V}] \tag{2.9}$$

Where:

- $[\bar{I}]$ is the column vector of external nodal current injections;
- $[\bar{G}]$ is the nodal conductance matrix;
- $[\overline{V}]$ *is* the column vector of nodal voltages with reference the reference node.

The matrix G is defined following the *Graph Inspection method:*

The diagonal terms, G_{ii} are the self-conductance terms, equal to the sum of the conductances of all branches incident to node i

$$G_{ii} = \sum_{(i.k)\in\beta_i} g_{ik} \tag{2.10}$$

Where:

- β_i is the set of branches connected to node i
- g_{ik} is the conductance of the branch connecting node i to node k

The off diagonal terms, G_{ij} are equal to the negative of the sum of the conductances of the branches directly connecting the two nodes i and j

$$G_{ij} = -g_{ij} \tag{2.11}$$

Next, some properties of the conductance matrix:

- Shunt terms, such as with the π line model, only affect the diagonal terms, in our case they are the shunt conductance;

When the number of nodes is high, G becomes a sparse matrix.

2.2.3. DC Power flow

As a first approximation, the two electrical substations can be considered as voltage sources with a constant voltage of 3000 V.

This simplifying choice allows the entire system to be easily modeled (compared for instance to a series of generator of equivalent resistance), even if at the cost of losing some information on the substations themselves a secondary effect out of the scope of this thesis.

Having already calculated the conductance matrix as described in the previous section and having determined the absorbed powers of the trains and the electrical powers actually regenerable by them (thanks to the Simulink model of chapter 2.1), it is possible to calculate current and voltage in each node of our network thanks to the *DC power flow* approach, defined in the following study [43], as illustrated in section 2.2.5.

Considering the DC railway having N_{nodes} (N_s substations and N_T trains), the electrical parameters of the nodal voltage, can be obtained moment by moment from a sequence of power flow solutions, with the trains frozen in time for each instant Is possible to well define the matrix G; remembering that every train is connected electrically between the catenary and the track(rail), whose running rails are used for traction current return. The earth leakage is represented by the equivalent π model.

Once the nodal voltage are obtained, the currents of the whole circuit can be evaluated.

To do this, the modified conductance matrix must be formulated [44].

2.2.4. Modified conductance matrix

The following relationship holds:

$$\mathbf{Ax} = \mathbf{z} \tag{2.12}$$

For a circuit formed by n nodes and two independent voltage sources (the 2 electrical substation):

- The **A** matrix is (n+2)x(n+2) in size, and is made of only by known quantities;
- The **x** vector is an (n+m)x1 vector that holds the unknown quantities (node voltages and the currents through the independent constant voltage sources);
- The **z** vector is an (n+m)x1 vector that holds only known quantities.

The A matrix will be developed as the combination of 4 smaller matrices, G, B, C, and D.

$$\mathbf{A} = \begin{bmatrix} \mathbf{G} & \mathbf{B} \\ \mathbf{C} & \mathbf{D} \end{bmatrix}$$

Where:

- **G** is the conductance matrix evaluated as described in the previous paragraph;

- **B** matrix is n×2 and is determined by the connection of the voltage sources; is matrix with only 0, 1 and -1 elements. Each location in the matrix corresponds to a particular voltage source (m) or a node (n). If the positive terminal of the i-th voltage source is connected to node j, then the element (i,j) in the B matrix is a 1. If instead is the negative terminal of the i-th voltage source is connected to node k, then the element (i,k) in the B matrix is a -1. Otherwise, elements of the B matrix are zero;
- the **C** matrix is m×n and if only independent voltage sources are present, C is simply the transpose of **B;**
- the **D** matrix is m×m and is zero if only independent voltage sources are considered.

The **x** matrix has all of the unknown quantities and it is composed by as the combination of all the unknown node voltages and the 2 unknown currents through the voltage sources.

The **z** matrix holds our independent current and voltage sources and will be developed as the combination of the n sum of the currents through the passive elements into the corresponding node (either zero, or the sum of independent current sources); and the 2 values of the independent voltage sources, in our case, 3000V.

$$\begin{bmatrix} G_{11} & 0 & \cdots & 0 & G_{1N} & 1 & 0 \\ 0 & G_{1'1'} & \cdots & G_{1'N'} & G_{1'N} & -1 & 0 \\ \vdots & \vdots & \ddots & \vdots & \vdots & \vdots & \vdots \\ 0 & G_{N'1'} & \cdots & G_{N'N'} & 0 & 0 & -1 \\ G_{N1} & 0 & \cdots & 0 & G_{NN} & 0 & 1 \\ 1 & -1 & \cdots & 0 & 0 & 0 & 0 \\ 0 & 0 & \cdots & -1 & 1 & 0 & 0 \end{bmatrix} \begin{bmatrix} v_1 \\ v_{1'} \\ \vdots \\ v_{N'} \\ v_N \\ i_{sse1} \\ i_{sse2} \end{bmatrix} = \begin{bmatrix} 0 \\ 0 \\ \vdots \\ 0 \\ 0 \\ V_{sse1} \\ V_{sse2} \end{bmatrix}$$

Where for the sake of clarity, in this case:

- $\boldsymbol{B} = \begin{bmatrix} 1 & 0 \\ -1 & 0 \\ \vdots & \vdots \\ 0 & -1 \\ 0 & 1 \end{bmatrix}$;
- $\mathbf{C} = \mathbf{B}^{\mathrm{T}} = \begin{bmatrix} 1 & 1 & \cdots & 0 & 0 \\ 0 & 0 & \cdots & -1 & 1 \end{bmatrix}$;
- $\boldsymbol{D} = \begin{bmatrix} 0 & 0 \\ 0 & 0 \end{bmatrix}$;

- **G** is the portion of the matrix with the relatives conductances.

D will always be a 2x2 empty matrix if the two electrical substations are the only constant voltage generator in the system.

2.2.5. Power flow

The electrical substation is connected to the positive bar (catenary) and the negative bar (rail), which in turn is connected to the ground. Consider a train connected between a catenary node *i* and a track node *j*; the train power is related to the voltages of the node and the current I^3_{ij} in the train by:

$$P_{Ti} = (V_i - V_j) \cdot I_{ij} \tag{2.13}$$

Where P_{Ti} is the power of i-th train evaluated thanks to the mechanical model.

The train can be represented as 2 current injections, one at node i (catenary) and the other at node j (rail); the following equations are derived:

$$I_i = I_{ij} = \frac{P_{Ti}}{V_i - V_j} \tag{2.14}$$

$$I_j = -I_{ij} = \frac{-P_{Ti}}{V_i - V_j} \tag{2.15}$$

Now it is clear how at the level of electrical circuit trains can be considered:

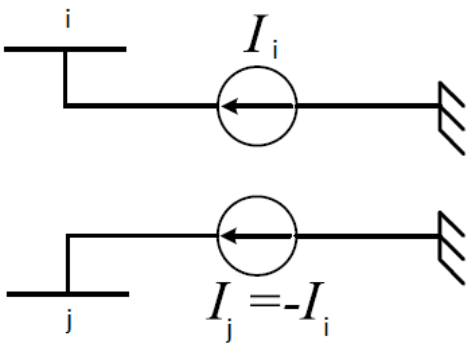

Figure 2.16 : Train electric model

In fact, the trains are represented as absorption (and therefore generators with negative current) of current if they require power, while as positive current generators, unknown in both cases, if instead they yield to the Power network.

The electrical substations lead the system to have also two other equations:

$$V_{pos} - V_{neg} = V_s \tag{2.16}$$

[3] in the previous chapters the rail nodes of the Detailed case have always been named with the superscript "i'", in this chapter instead of having the nodes i-i' it was chosen to have the pair i-j.

$$I_{pos} - I_{neg} = 0 \tag{2.17}$$

With V_s equal to 3000V.

The network voltage is obtained by iterating the current injection values from the power equation $P_{Ti} = (V_i - V_j) \cdot I_{ij}$ (2.13) with voltage output from the network from the equation with the modified conductance matrix, until the scheduled train power values are satisfied within the tolerance. The iterative procedure is defined as follows:

Step 0: Determine the [A] matrix and factorize it using optimally-ordered sparse LU matrix decomposition [45]. Initialize all catenary node voltages to Vs, all track node voltages to zero, and set the iteration counter k = 0.

Step 1: Increment k by 1 and compute the current injection vector $[I^{(k)}]$ at step k using:

$$I_i^{(k)} = -I_j^{(k)} = \frac{P_{Ti}}{V_i^{(k-1)} - V_j^{(k-1)}} \tag{2.18}$$

Step 2: Evaluate $[V^{(k)}]$ in the matrix equation $[\bar{I}] = [\bar{G}] \cdot [\bar{V}]$ (2.9) using forward-backward substitution.

Step 3: Tolerance check evaluating the power obtained with the new values of V and I with the power given by the mechanical model

$$\left| \left(V_i^{(k)} - V_j^{(k)} \right) \cdot I_i^{(k)} - P_{Ti} \right| \leq \epsilon \tag{2.19}$$

If the convergence test is satisfied, stop and this is the solution, otherwise go to Step 1 and repeat.

Below is the Flow Chart of what is described above:

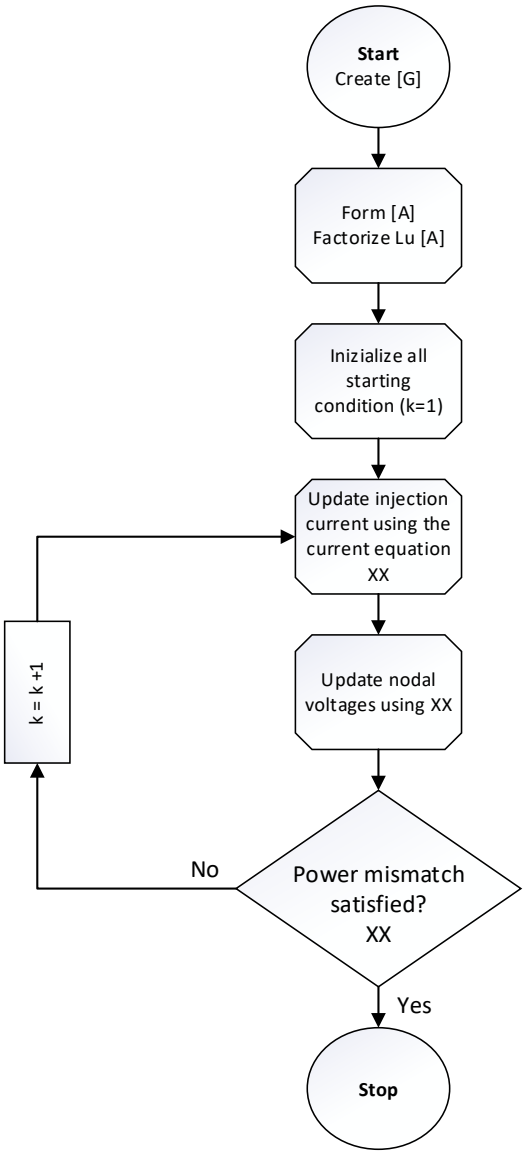

Figure 2.17 : DC power flow flow chart

The implemented model will tend to converge because the value of the required power of each individual train is a constant value within the power flow: therefore, if in a step there will be too high voltages, these will be compensated by the fact that lower currents will be produced (as per equation $P_{Ti} = \left(V_i - V_j\right) \cdot I_{ij}$ (2.13)); while in the next phase, re-evaluating the voltages, with the matrix A and the new currents , they will decrease. Below is a graphic representation of what has been said:

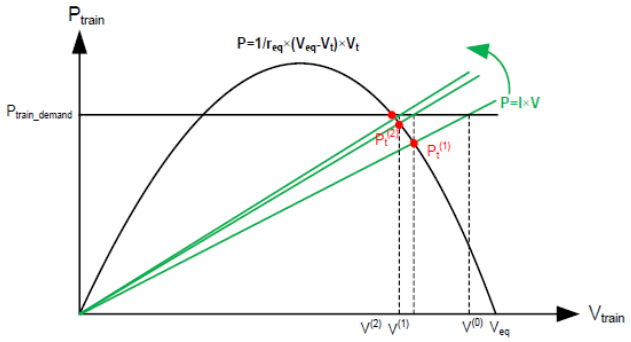

Figure 3.32 Geometrical interpretation for a traction train

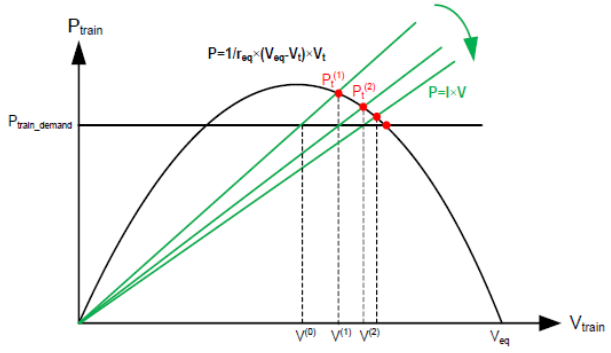

Figure 3.33 Geometrical interpretation for a traction train

Figure 2.18 : Graphical representation

The power flow previously presented needs some modifications to accurately represent the railway system; in fact, the constraints that must be respected by expanding the code described are the following:

1. the voltage at the pantograph cannot exceed 3600V;
2. Since the electrical substation is based on a unidirectional rectifier: current from ESS can only be supplied to the railway system.

To introduce these two constraints, some changes have been implemented: if a braking train leads to the introduction of a power driving the voltage at the pantograph above 3600V, the control system must necessarily dissipate that surplus of power. In this case, therefore, at the model level, the train will be considered as a constant voltage source at 3600V and therefore the modified conductance matrix will be suitably changed (following the rules mentioned above). Once converted, the train will no longer represent an unknown factor in the flow of power, but will have known and set voltage and, once the injectable power in the system has been calculated through the mechanical model, the current can be calculated accordingly.

For the second constraint, if at the end of the power flow, the current in one of the two electrical substations is negative, the electrical substation is turned off and a current equal to zero is imposed on it.

The modified conductance matrix will remove the rows and columns corresponding to the electrical substation as it will no longer be represented as a voltage generator; In practice, some rows and columns of the B and **C** matrix will be removed**.**

It is possible, that both electrical substations are switched off and therefore the power regenerated by the braking of the trains is greater than the loads existing at that particular time.

Below is the flowchart of the changes described above; the power flow described in the diagram above is called "PF base".

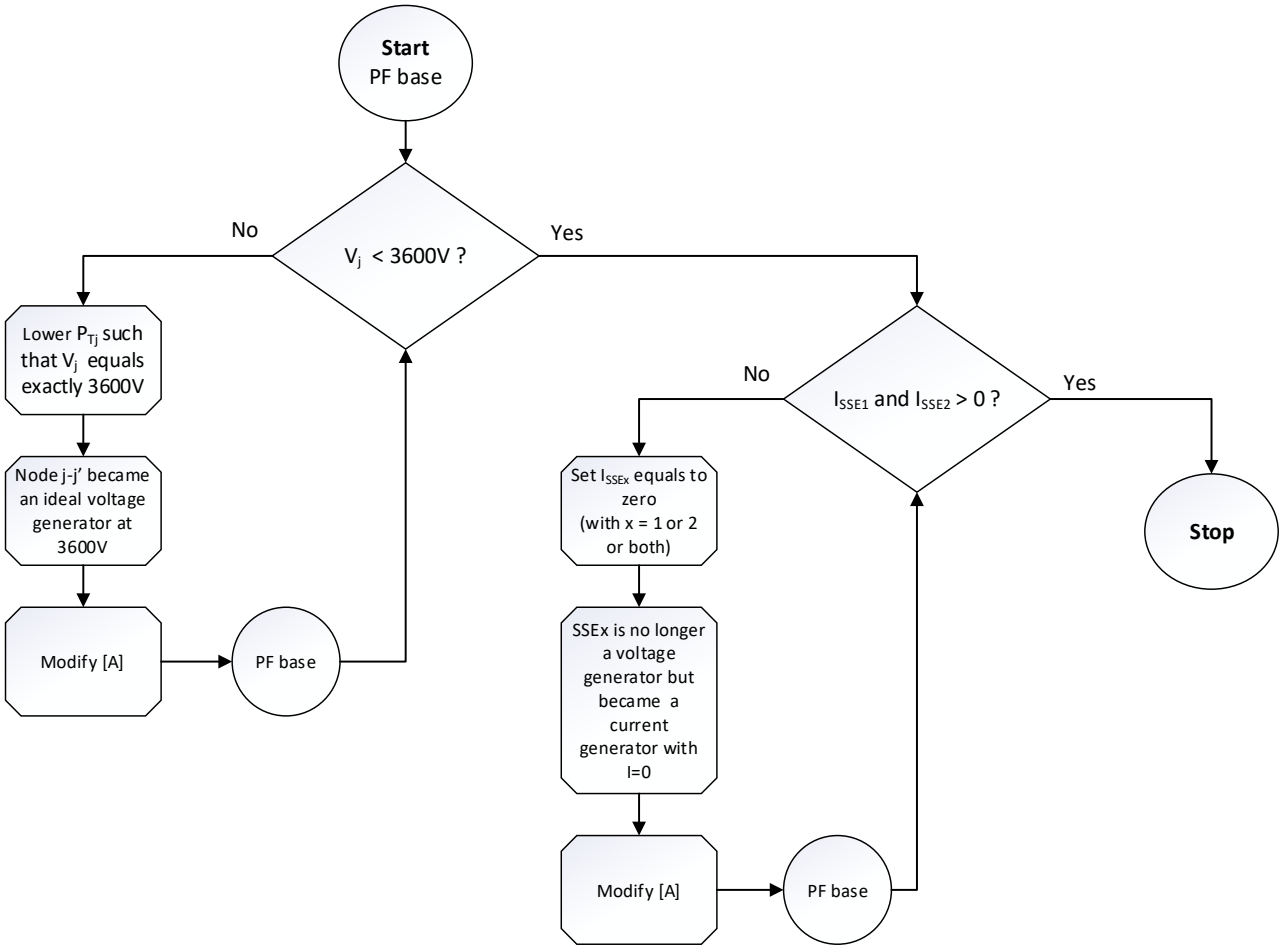

Figure 2.19 : Modified power flow, flow chart

2.3. Electric car parking modeling

This section describes the integration of electric vehicle parking lots with the railway power system.

Keeping in mind that - above all - the advantages of this connection are represented by:

1. exploitation of energy/power that would otherwise be unrecovered[4];
2. connection to a medium voltage network (3000V). This makes power transmission more efficient than low-voltage grids;
3. exploitation of a network that has important residual power carrying capacity most of the time during a day;
4. possible integrations of V2G logic to support trains and their network.

Taking into account the information contained in the introduction about chargers for electric cars (chapter 1.4), it was decided to place a charging points in every railway station along the Novate-Saronno line, with the exception of the stop "Garbagnate Parco delle Groane", as it has a tiny current parking lot of little interest. Current parking slots of each train stop were analyzed and an estimate of the available parking space for each of them was made.

Considering an European average of about 40 km/day of car use per day [46], [47] and a power consumption by car of about 150 Wh / km [48], it is estimated that 6 kWh are required each day per parked car.

The number of charging stations in each parking slot was also sized. The result is summarized in the following table:

Stop	Parking spaces	Charger size	Number of chargers	Total energy[5]
Novate	150	20 kW	13	1250 kWh
		100 kW	1	
		3.7 kW	6	
Bollate Centro	80	20 kW	9	670 kWh
		100 kW	0	
		3.7 kW	5	

[4] This concept will be better explained in the results chapter, 3.2

[5] The total energy is increased compared to what is described above (by about 40%), follow the rules given in the sheet below this.

Bollate Nord	100	20 kW	11	840 kWh
		100 kW	0	
		3.7 kW	5	
Garbagnate Mil.	60	20 kW	6	500 kWh
		100 kW	0	
		3.7 kW	6	
Cesate	150	20 kW	12	1250 kWh
		100 kW	1	
		3.7 kW	7	
Caronno Pertusella	120	20 kW	11	1000 kWh
		100 kW	0	
		3.7 kW	6	
Saronno Sud	50	20 kW	5	420 kWh
		100 kW	0	
		3.7 kW	5	
Saronno	100	20 kW	11	840 kWh
		100 kW	0	
		3.7 kW	5	

Table 2.3 : Charging stations

It should be noted the presence of 100kW columns (super fast) in the larger stations.

It is also important to note that each charging cycle is different and randomly generated from real data from existing charging stations. An average value of the charging time and the corresponding standard deviation were thus calculated.

In this work we will use data from existing charging stations, their size is: 3.7, 10, 20 and 100 kW. From these data the shapes of the charging curves (time-Power) are extrapolated, and they are of the following type:

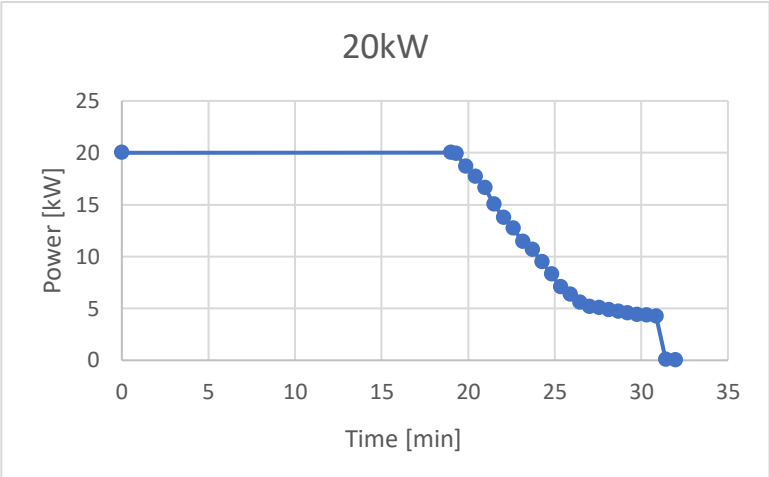

Figure 2.20 : Example of charging curve

These data have been processed as follows: considering that they are real charges, the recharges are not complete (from 0 100 state of charge), it was therefore decided to take the time interval for each curve for both Constant Power (CP) and Constant Voltage (CV) mode, with these values the average time and the associated standard deviation were calculated.

14 charging curves were analyzed and the following statistical parameters were obtained to generate a characteristic curve of a 10 kW charger, then every shape is resized to obtain the same area with different nominal power:

Standard deviation CP	Standard deviation CV
12 min	20 min
Mean CP	Mean CV
30 min	40 min

Table 2.4 : Statistical values of a 10 kW charger.

A random charging curve was generated for each charge starting from the mean and adding or subtracting the relative deviation with a corrective factor of 2;

The arrival time of the cars in the relevant parking lots is also generated randomly.

Each randomly generated parking demand curve is kept constant in the various simulations to better compare them.

It is estimated that the charging stations are put into operation at about 7:30 in the morning.

As for the connection to the railway network, it was decided to position each parking lot in a cyclical manner in each circuit of the trains considered: so, for example, that of Novate is placed in the circuit of the first track, that of Bollate Centro on the second, and so on.

To also represent as realistic as possible situation, a change of vehicles in the parking lot during the same day was considered equal to about 40% of the parking spaces present.
Accordingly, the energy value for each parking in the table is consistently increased: the total energy for each parking lot is no longer given by the number of parking spaces multiplied by the average daily request of a car, but by number of cars, equal to the number of places for about 1.4, per average request.

Below is the full-day demand curve of the Saronno car park.

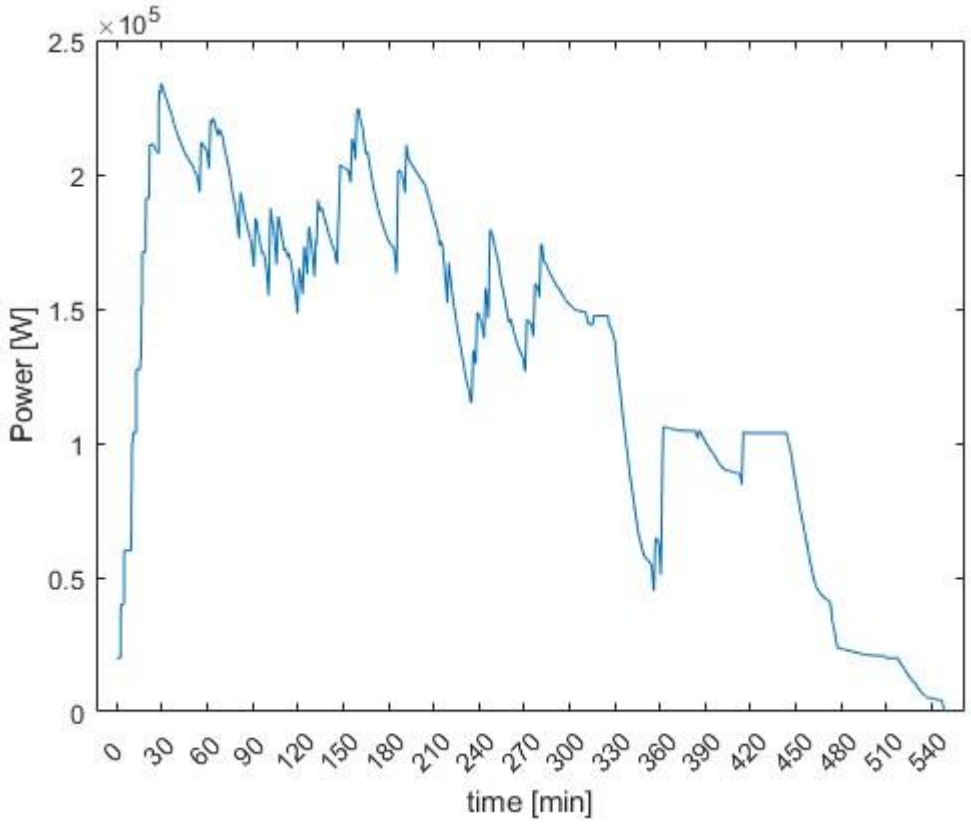

Figure 2.21 : Power demand of the car park in Saronno

The peak of about 230 kW reflects the fact that in about half an hour from the start of operations almost all the charging stations are in operation (remember that the curves have a delay time to start operating compared to 7:30 am, a delay that is calculated with a random normal function).

In conclusion a representation of all the car parks in each station power demand:

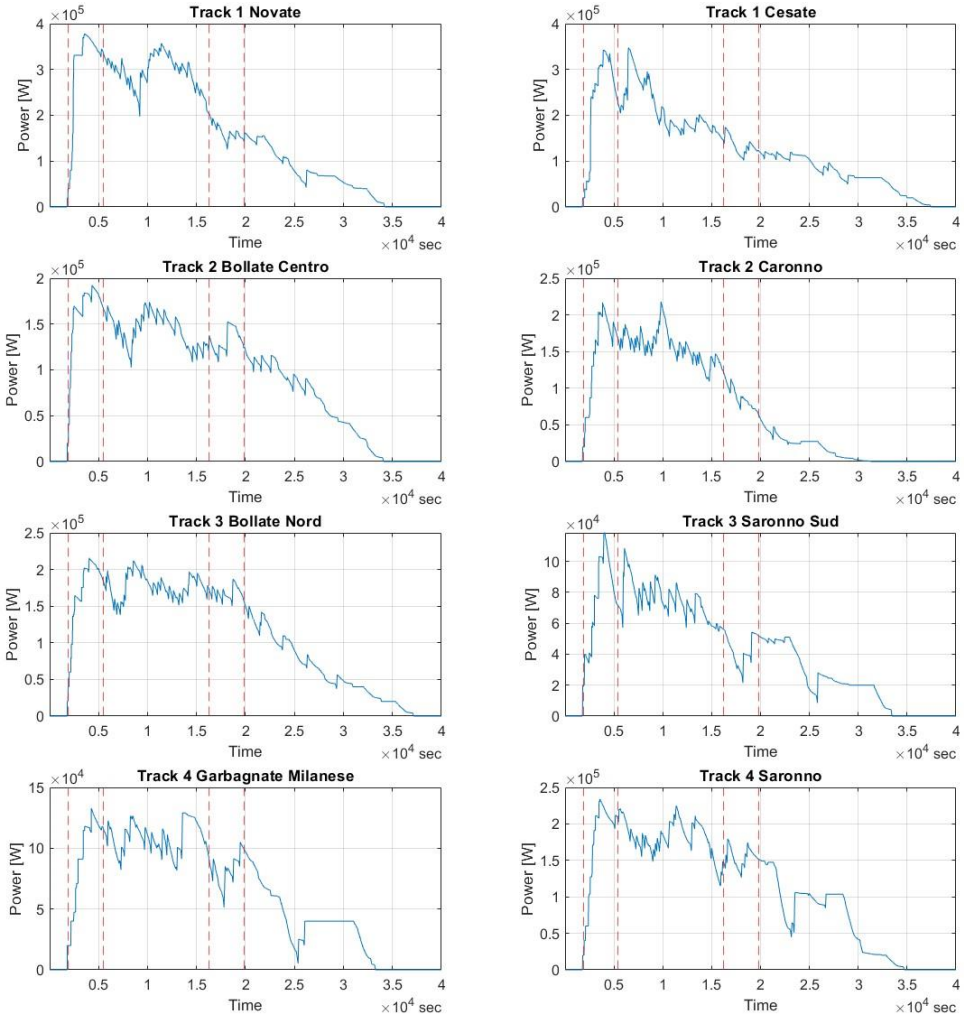

Figure 2.22 -Different power demand for each station car park[6].

2.4. Stationary battery energy storage system sizing and modeling

To introduce a stationary storage system in the various railway stations brings various benefits to the entire system including:

[6] Four vertical lines are in the graphs to represent the hours : 7.30-8.30 and 12.30-13.30.

- The absorption of part of the power that otherwise will be lost in the event that the power supplied by the trains under braking is greater than the request of the whole system at that specific times;
- the support of the network in the most critical moments, i.e. both in cases where the demand is high and then the stationary batteries can provide power to the railway electrical system and not operate only the electrical substations (with the additional advantage of obtaining higher voltages when the voltage drop is high due to too high loads), or, as already mentioned, when the electrical substation is switched off and there is an excess of power in the railway electrical system; in this case the batteries can absorb part of it and act as a load to lower the electrical voltage;
- support for systems installed in the immediate vicinity - both yielding and absorbing power for systems - such as parking for electric cars and any photovoltaic fields installed in the parking lot.

As already mentioned, the stationary batteries are located near the eight most important stations in the Saronno – Novate line.

For the sizing of the nominal power and the nominal energy of each battery pack, it was decided to determine an optimal pair of energy-power values that would make the network more stable among all pairs of values in the range of -50% + 200% of the energy-power characteristic of a braking of an eight-element train.

For the control system that governs the stationary storage system, as already mentioned, a two-input Fuzzy logic was used which, as output, gave the output power (in p.u.); the same Fuzzy logic was used for each car park.

This logic allows to determine control choices for devices that do not require immediate and mandatory requests, moment by moment, but for example for stationary batteries placed in support of the train network, which absorb power when the availability given by the network is high (trains braking) and yields to the network itself when it instead needs electrical power.

The boundary of these conditions is blurred and determining it is very complex, since it requires a coordinated evaluation of several parameters and involves the area of subjective interpretation also of experts in the field.

Exemplum: at 3050 V is the network already able to power the batteries and above all in what quantity? Or it is better to wait until the network is more able to provide power because the batteries are very charged. It is therefore not easy to determine when and how much to provide power, to do this we have chosen to use this particular logic to answer questions, once again *fuzzy*.

The voltage near the station and the SOC of the battery itself were used as input; The first parameter is used to balance the network itself: if the voltage is too low, for

example, the batteries supply energy to the grid and raise it, vice versa if it is too high they decrease it.

The SOC is a parameter also used to safeguard the health of the batteries themselves and not exceed the maximum or minimum values of them, which in this study are set at 20% and 80%. It also allows to constantly modulate the energy that can absorb or transfer to the grid.

The choice of the two parameters in question, used to govern the batteries and subsequently define the rules, is not uncommon in literature, where reference has been made to the following articles[49]–[52]

Fuzzy rules					
SOC / V	VL	L	M	H	VH
VL	Z	MP	MP	VP	VP
L	Z	Z	Z	SP	VP
M	SN	Z	Z	Z	SP
H	VN	SN	Z	Z	Z
VH	VN	VN	MN	MN	Z

Table 2.5 : Fuzzy rules

The set of rules used is the one presented in the table above, in which every rule has the weight equal to 1. The following formulation has been chosen for the membership functions:

The membership functions of the State of charge (SOC) and voltage (V) function are divided into: VL (Very Low), L (Low), M (Medium), H (High) and VH (Very High), in the following graphical representation:

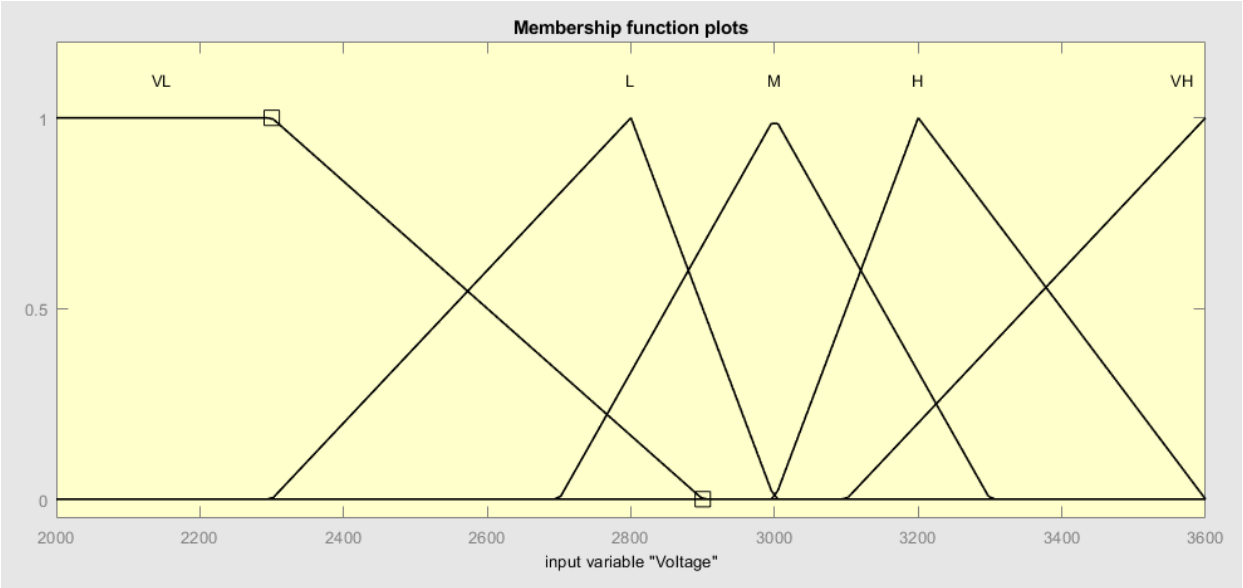

Figure 2.23 : Voltage membership function

Since the two maximum and minimum constraints for voltage are not symmetrical, even the membership functions with respect to 3000 V will not be symmetrical.

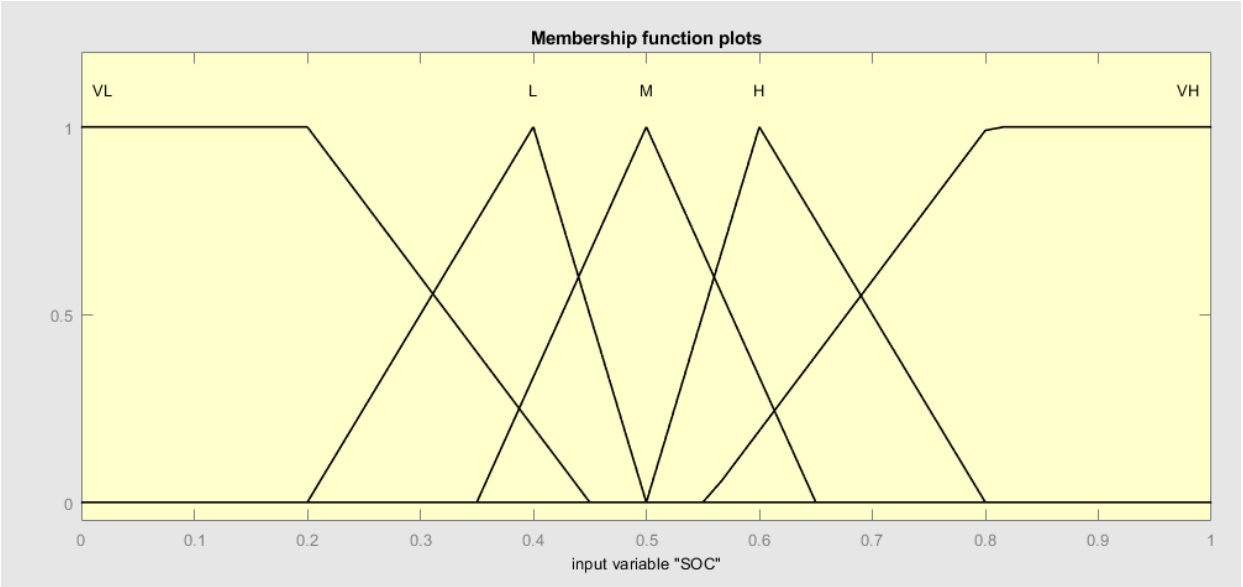

Figure 2.24 : SOC membership function

It should be noted that for values less than 0.2 or greater than 0.8 the fuzzy set will be equal only to "*Very Low*" or "*Very High*" respectively, this choice makes it easy to implement the fact that below or above these SOC values the battery can recharge or discharge respectively, regardless of the line voltage (if the network is not able to supply / absorb current, the control system will simply block any flow of power in the batteries for that moment.)

As for the output function, i.e. the power in per unit compared to the nominal one to be supplied or requested at that particular moment of the batteries is divided as follows:

Where the membership function is divided into 7: VP (Very Positive), MP (Medium Positive), SP (Small Positive), Z (Zero), SN (Small Negative), MN (Medium Negative) and VN (Very Negative).

The choice of such a kind of variables and the corresponding membership functions produces a type of nomenclature that remains faithful to the literature on the subject. [50], [51]

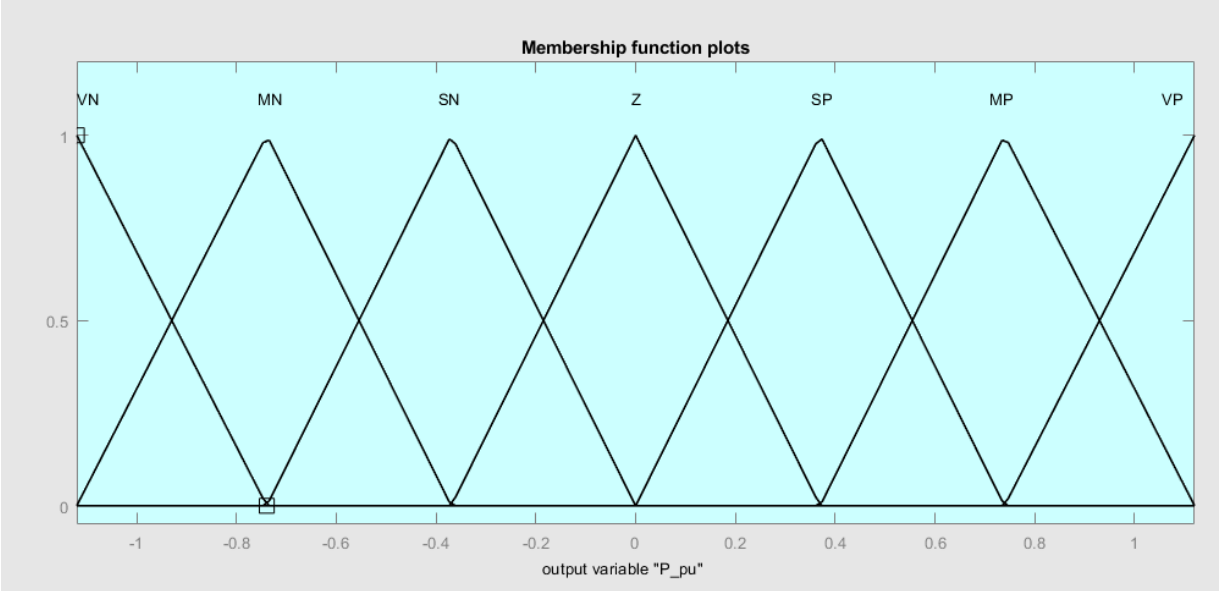

Figure 2.25 : Power output membership function

It should also be noted that the "*positive*" nomenclature refers to a flow of power leaving the stationary batteries that supply the network, while the "*negative*" one, on the contrary, has regard to the incoming power flow.

Furthermore the membership function of the output variable "*P_pu*" is defined for values less than -1 and greater than 1; This is because the defuzzification process is based on the centroid method, this method, giving as a solution the barycenter of gravity of the membership functions active at that time, to give as a result -1 or 1, requires the fact that the membership functions are defined beyond the range [-1 1].

It was also decided, as can be seen from Table 2.5, to set many rules equal to "Zero", this is because the first task of stationary batteries is to induce stability in the network, intervening especially when the network requires it, or both if you move considerably away from the nominal voltage (at least in the case in which the batteries are half charged, specifying that this rule is no longer valid when the batteries are on average more discharged or charged). Only in the event that the batteries are overcharged or too discharged (SOC values greater than 0.8 or less than 0.2 respectively), they will not take part in the power flow of the system to support it,

even if there is a real need, but can only discharge or charge respectively when the conditions of the train network allow it; it is precisely for this reason that the SOC columns in the table of rules of " Very Low" and "Very High" have only zeros and negatives in the case of low charge and only positives and zeros in the case of maximum charge.

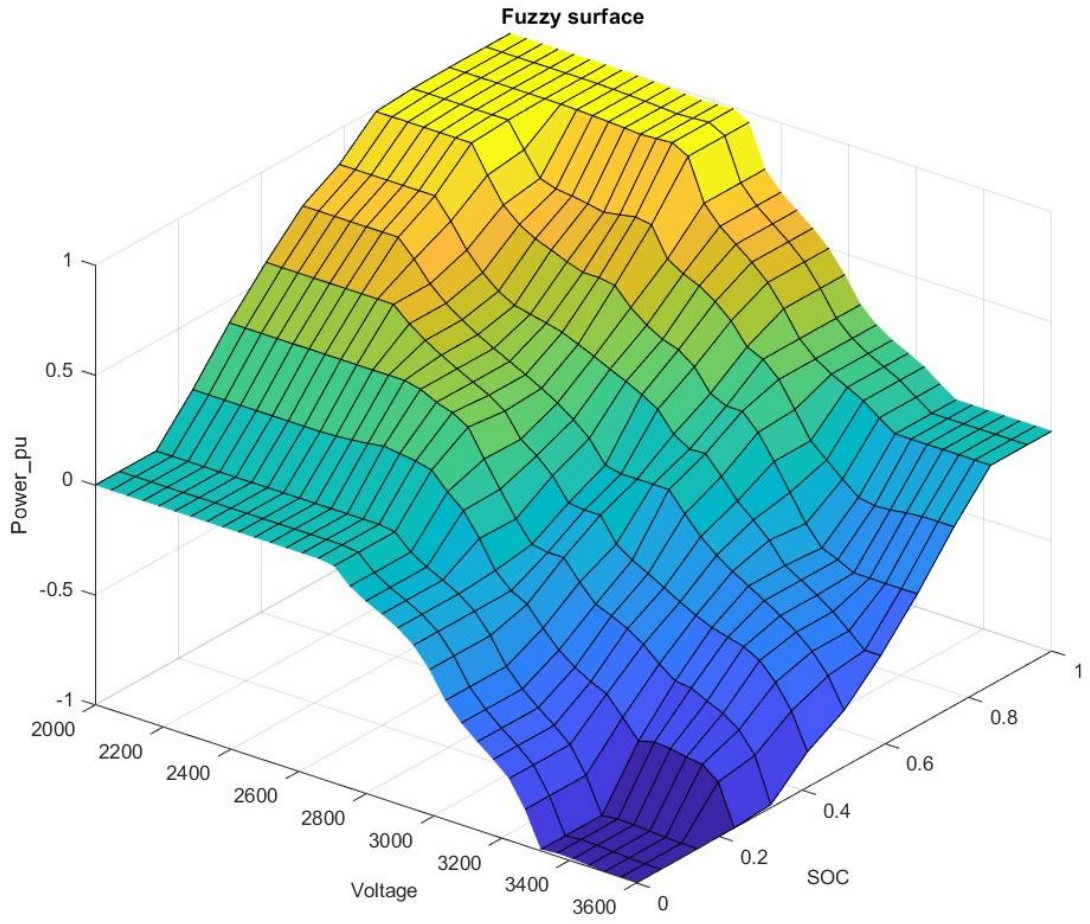

Figure 2.26 : Fuzzy surface

This graph represents the final solution of all fuzzy logic, in fact after obtaining this surface, it is possible for each possible input pair simply to interpolate the solution and not go through the various membership functions and all the various steps of fuzzy logic. We also want to point out that there are five plateau in the surface:

- SOC less than 0.2 and high voltages, the output power will be fixed at the maximum value (in absolute value);
- SOC less than 0.2 and medium or low voltages, the output power will not be positive (the battery with SOC less than 0.2 can only recharge) and will be worth at most zero;

- SOC greater than 0.8 and low voltages, the output power will have maximum value;
- SOC greater than 0.8 and high voltages, the output power will not be negative, at minimum zero;
- SOC around 0.5 and medium voltages, the batteries will not work as they are designed to support the train network, which in these particular conditions does not need help (the plateau in question is hardly perceptible in the figure, but if you increase the points where the surface is evaluated it would be more evident).

2.5. Photovoltaic systems sizing and modeling

A generation of renewable energy was also introduced. Given the place of study (Lombardy, Italy), it was decided to adopt a photovoltaic system for each parking of electric cars, given the existing space.

A generation system can lead to several benefits for the network, such as:

1. The fact that the generated energy is supplied in a place where it is directly needed (parking of electric vehicles);
2. In the case of a greater production of photovoltaic generators compared to the absorption of nearby loads, the latter can help the railway network at times when it absorbs from the national grid, or they can directly recharge the stationary storage system mentioned in the previous chapter.

It is therefore important to underline how we are going in the direction of a DC hub with this elaborate, where users and generation, connected to each other and in proximity, rely on the railway network and not on the national one, which, it is repeated, can bring considerable advantages: first of all, a network is used sized for very high maximum peaks and that last for a few hours within a day; moreover, a better quality and greater efficiency of the power flow is guaranteed, given the voltage to which the user interfaces, which is 3000 V and not 220 V as in domestic networks.

To introduce photovoltaics into the model, reference was made to the meteorological conditions measured in the station present in the laboratory of the BL25 building of the Politecnico di Milano, from which the irradiation and temperature values were extracted.

Figure 2.27 : Politecnico di Milano laboratory rooftop [53]

These data were considered valid for the entire route between Saronno (45°37'32"N 9°01'49"E) and Novate (45°31'58"N 9°07'56"E) as the geographical coordinates with respect to Bovisa (45°30'10"N 9°09'24"E), where the measurements were taken, differ by a negligible amount.

It has also been assumed, since these are parking lots, that the laying of the modules is horizontal thanks to the large existing space and the fact that it fits itself well due to the characteristics of the parking lots themselves: this simplifies the calculations as the data provided are also "horizontal".

For each station, the cell temperature was calculated as a function of irradiance with the following formula:

$$T_c = T_{amb} + \frac{NOCT - T_{amb@NOCT}}{G_{NOCT}} * G \qquad (2.20)$$

Where:

- T_c is the cell temperature;

- NOCT is the *Normal Operating Cell Temperature* which is the cell operating temperature at given conditions $T_{amb@NOCT}$ = 20°C, G_{NOCT} =800 W/m² in the absence of thermal convection on the back of the module; in this case NOCT = 48 °C;
- G is the irradiance measured at that particular moment in the weather station of Politecnico di Milano.

The definition of the NOCT is dependent on the type of module chosen, for this work we used the S18K250 from ALEO SOLAR with the following rating reported in [54].

Finally, to calculate the power of the single module as a function of irradiance and temperature, the following formula was used:

$$P_{el} = P_{el,ref} * \frac{G}{G_{ref}} * [\, 1 + \gamma * (T_c - T_{amb,ref}) \tag{2.21}$$

Where:

- P_{el} is the electrical power actually extracted;
- $P_{el,ref}$ is the reference electrical power, in our case 250 W;
- G is irradiance, as in the first formula;
- G_{ref} is the reference irradiance for the calculation of the power (different from the one before) and by the value of 1000 W/m²;
- γ is the *power factor* given in the datasheet and in our case by the value of - 0.43 %/°C;
- T_c is the cell temperature calculated with the above equation;
- $T_{amb,ref}$ is the reference ambient temperature from which it is calculated γ, by the value of 25°C.

As a last step, the area of a single module is 1660 x 990 mm² = 1.6434 m² and taking into account the spaces of each individual parking lot, how many modules per car park is obtained.

In the case considered, all the car parks of each station studied, have an outdoor parking space of standardized dimensions of about 5 m x 2.5 m = 12.5 m², also considering the space to be able to proceed between the cars on foot.[55]

With these data, and chosen a system to lay the photovoltaic modules positioned above the parking spaces in a horizontal direction, about 7 modules were calculated per single parking lot, as 12.5 m²/ 1.6434 m² is equal to 7.6 using then the *floor* approximation, also taking into account the spaces that must be left free and the various obstacles that may exist.
For each station the number of seats considered is that shown in the table Table 2.3, obtaining the following results:

Stop	Novate	Bollate centro	Bollate Nord	Garbagnate Mil.	Cesate	Caronno Pertusella	Saronno Sud	Saronno
PV modules	1000	560	900	420	1050	800	350	700

Table 2.6 : number of modules for each station

It was checked, through the Google Maps site [56], if there were obstacles and / or objects that did not allow the installation of the modules in certain parking lots. The numbers were then adjusted accordingly.

Below are some views of the existing stations and parking lots from above:

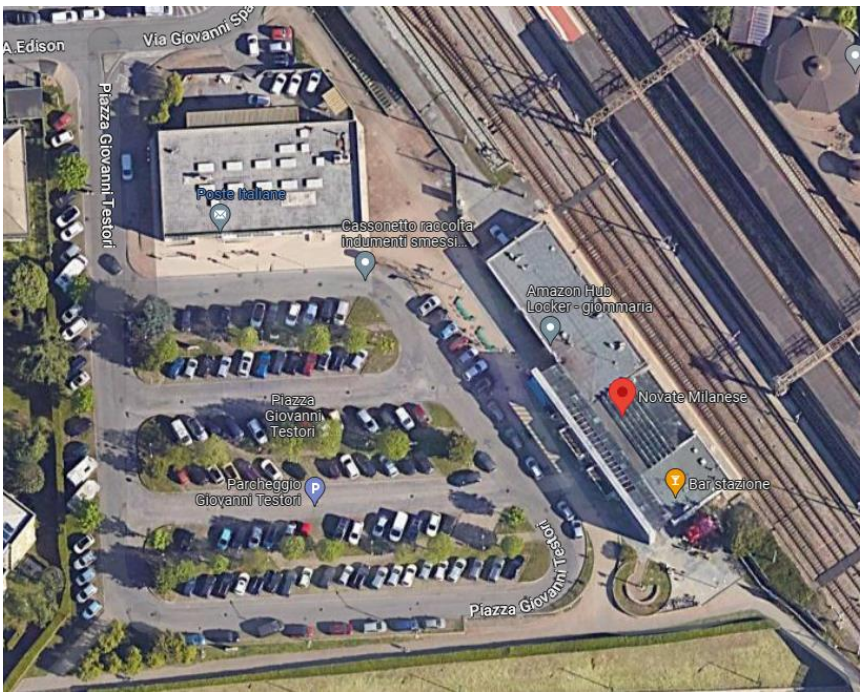

Figure 2.28 : Novate station car park

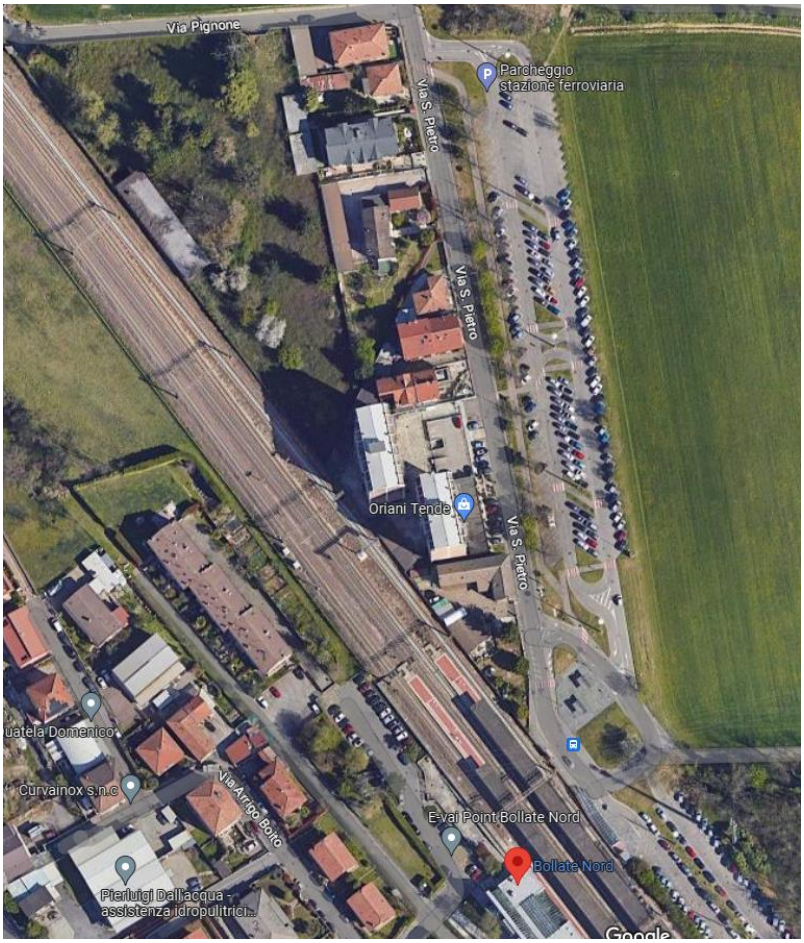

Figure 2.29 : Bollate Nord station car park

To obtain the final power of each photovoltaic field the relation is as follows:

$$P_{el,TOT,i} = P_{el} * N_{p,i} \tag{2.22}$$

Where:

1. $P_{el,TOT,i}$ It is the total electrical power provided by the entire photovoltaic field of the i-th car park.
2. P_{el} is the power calculated in the previous equation.
3. N_p is the number of modules in the i-th parking lot.

Moreover, for the measurements carried out in the meteorological station of the Politecnico di Milano, the *typical* days that could best characterize a solar year were selected; the days were analyzed following this logic: a clear day and a cloudy day near both solstices and only at an equinox (as the two equinoxes differ little if not at most for the temperature of the cell / environment, but they would still give absolutely comparable results). The choice of those six days is to represent in the best way possible with the minimum number of days, the whole solar year.

The days with the best data to better describe the problem are the following:

- spring equinox: 23 March 2022 as clear day and 15 March 2022 as cloudy day;

- winter solstice: December 27, 2022 as clear day and December 22, 2022 as cloudy day;
- summer Solstice: June 19, 2022 as Clear Day and June 23, 2022 as Cloudy Day.

All the simulations in a day that is between the cited ones, will give as results simply a middle way of the solutions of the two nearest implemented days.

With the datas extracted in Standard Test Conditions, the power in each panel has been evaluated.
In the Figure 2.30 the per-unit of irradiance and the power of a single module has been reported (G_{STC} = 1000 W/m² and P_{STC} = 250 W)

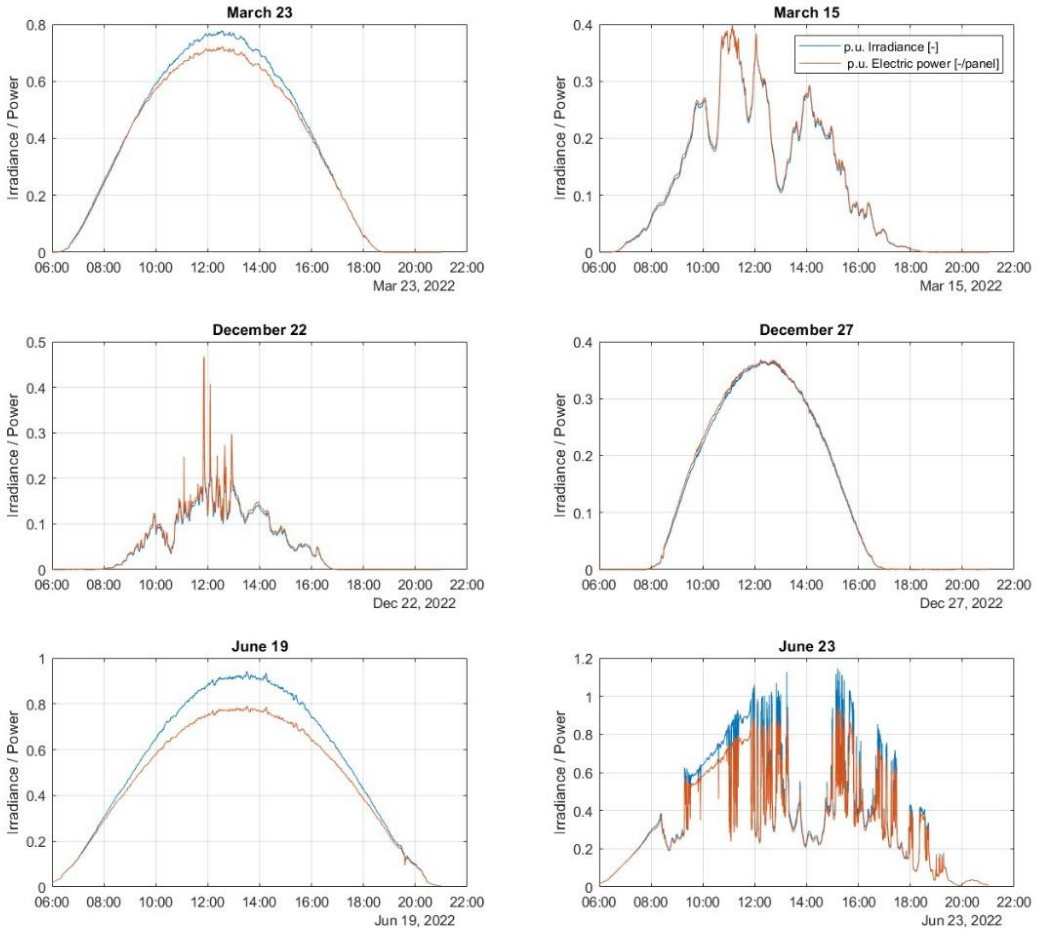

Figure 2.30 - Per-unit irradiance and power for each day considered.

The temperature effect on the extracted power is clearer on the warmer days.

Irradiance and Electric power has also been reported not in per-unit.

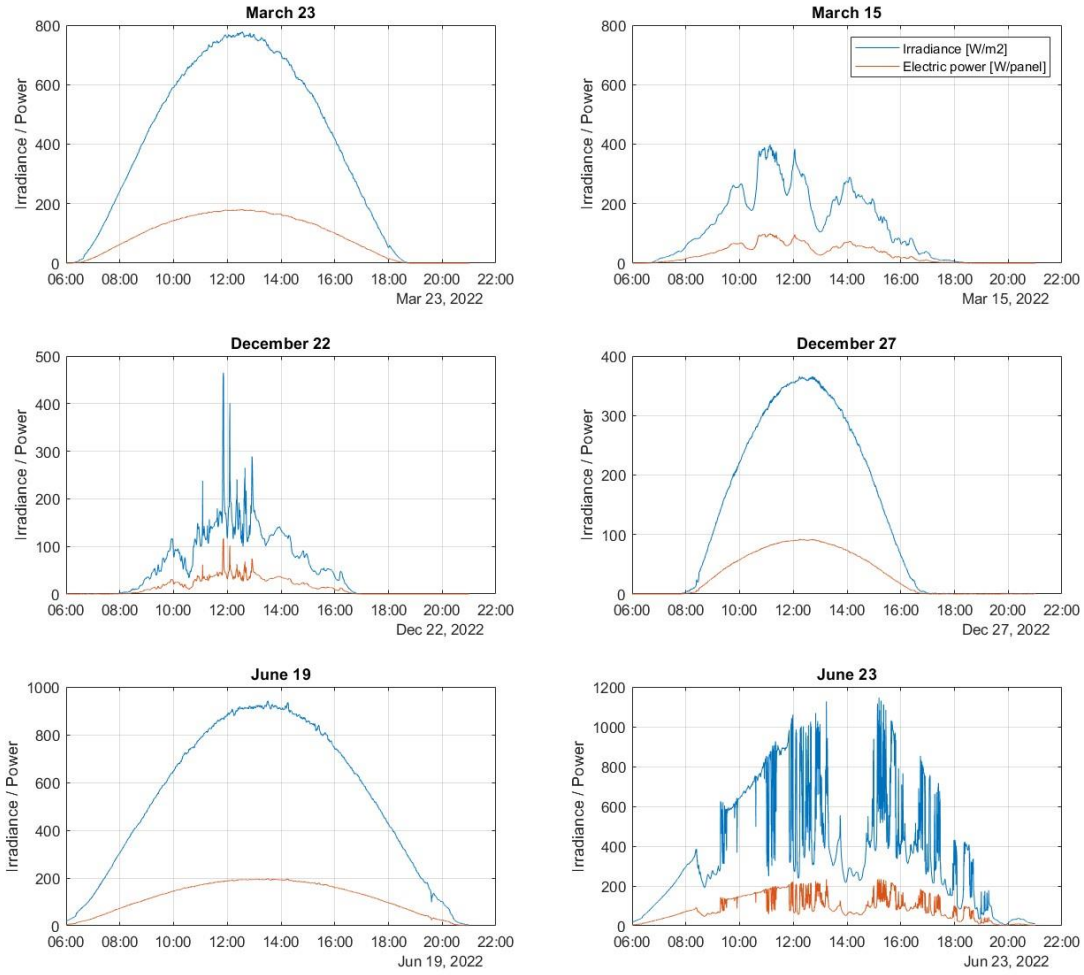

Figure 2.31 : Irradiance and Power for each day considered.

Note the different scales on the various days reported.

Below are the temperature profiles of the days described above:

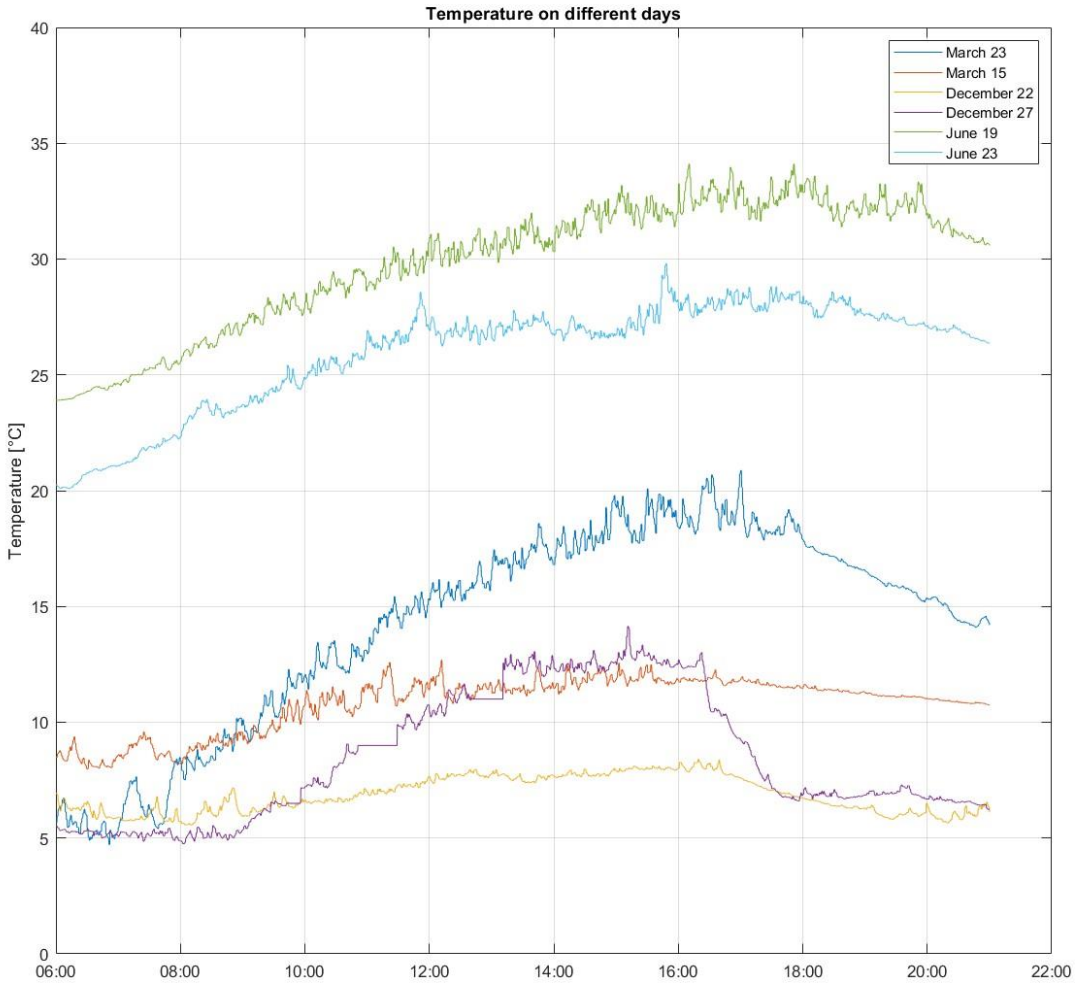

Figure 2.32 : Ambient temperature

3 Simulations

This chapter contains a presentation and the analysis of the results obtained. As mentioned, the simulations start from a baseline network with only the bare railway power system.

A first case named “Case 1” considers the baseline network and parking systems dedicated to the electric vehicles. The regenerative braking system of the trains may recharge the electric cars. When the power of the regenerative braking system is not available, it is the national grid through the train network to power the parking of electric cars.

A second case named “Case 2” considers an additional (compared to Case 1) storage system located close to the electric car parking nearby the railway stations under consideration. The storage system allows to store energy and stabilizes the grid.

A third case named “Case 3” considers an additional PV system added for power peak shaving to the Case 2 accumulation system previously described. It aims to recharging electric cars in the first place but also feeding the train network itself.

3.1. Baseline network

The simulations are run take into account either "Simplified" or "Detailed" models (whether or not a return circuit is considered - see Chapter **Errore. L'origine riferimento non è stata trovata.**) and for "Rush hour" or "Off-peak" traffic. Unless otherwise indicated, simulations are made on either Rush and Off-peak hours i.e. respectively between 7.30 – 8.30 in the morning and 12.30 – 13.30 in the afternoon. During Rush hours trains run with eight elements, during Off-peak hours only five.

3.1.1. Simple Network at Rush Hour

As said, this simulation represents railway network (as operated today) modeled in a *simplified* way and during Rush hours (eight trains).

Being the simulation used as a baseline, results are highlight in depth pointing out how far the various constraints are respected and how far network nominal values are deviated.

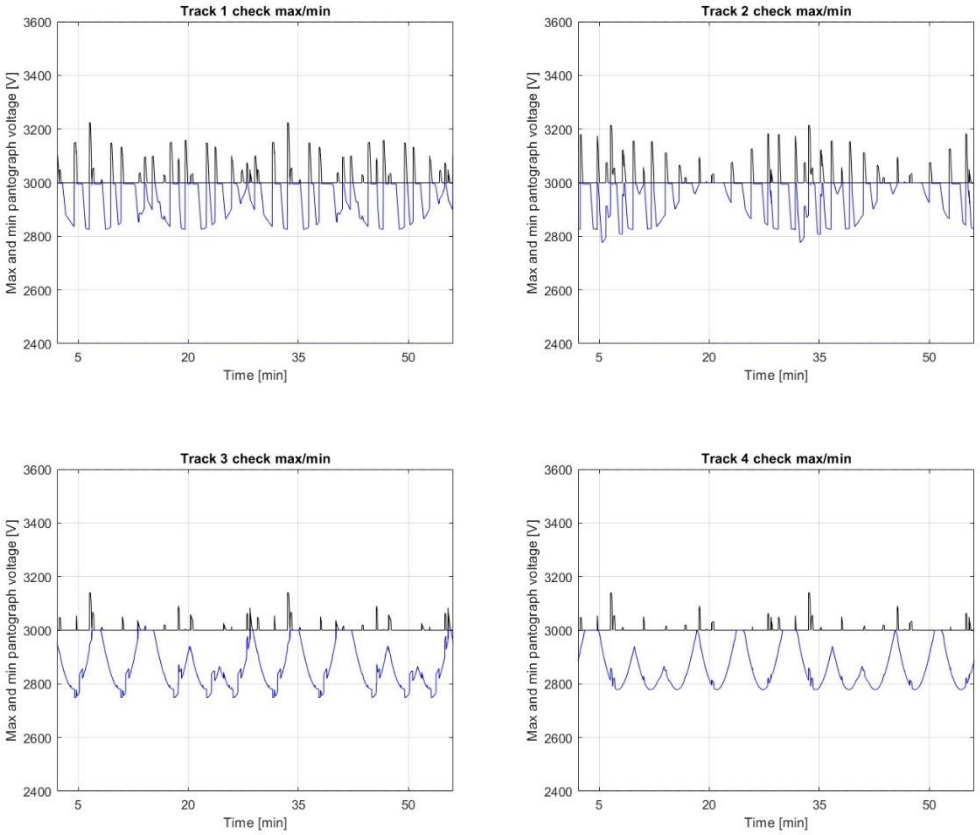

Figure 3.1 : Maximum and minimum voltage across the tracks

These results are the maximum (black line) and minimum (blue line) voltage across the whole track at any given time, it is so possible that from an instant t to the next one, the maximum/minimum change position along the track.

It is important to underline that the electrical load is quite important, but the voltage drop is within the limits. This is indeed far below its limits (3600V and 2000V) which in the graphs are represented by the two horizontal limits of the y-axis (for clarity the lower limit was represented at 2400 V: so that it is more symmetric and the graph less flattened). The black lines represent the maximum and the blue lines represent the minimum voltage for each track.

Figure 3.1 shows that the voltage drop is within the constrains.

On the base of these results, it is easy to imagine scenarios where networks are subject to additional loads (or even new generations, given that the maximum voltage is well within its constraints).

This is the case with fewer nodes and that neglects the return circuit: as we will see, in this latter case the constraints are slightly more stressed.

Below are the maximum and minimum values among all tracks at all times considered.

Track Maximum Voltage	Track Minimum Voltage
3225 V	2750 V

Table 3.1 : Maximum and minimum voltage

In terms of currents there are two different checks, one for the lines (Figure 3.2) explained in chapter 1.2.2, and the other one for the ESS (Figure 3.3) explained in chapter 1.2.1 :

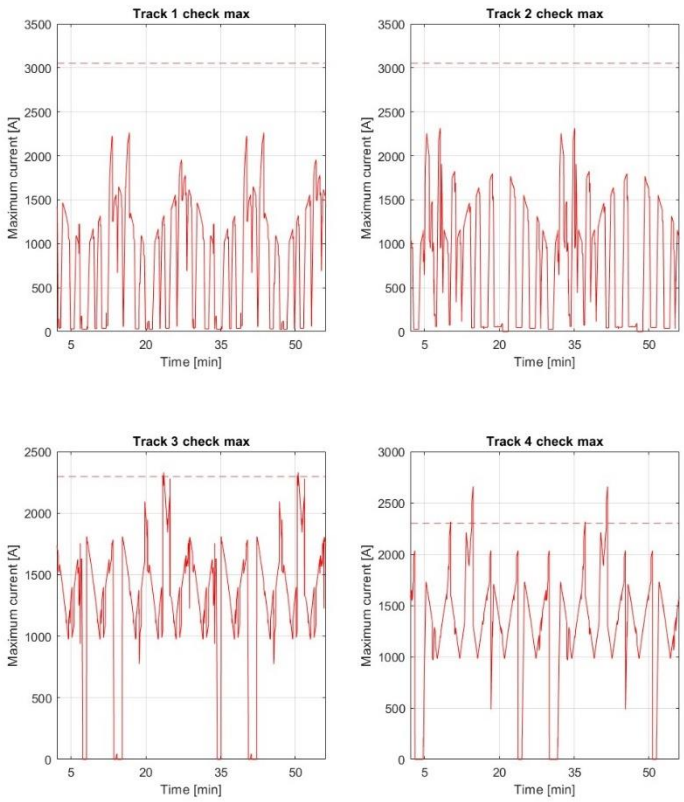

Figure 3.2 : Maximum current across the tracks

These graphs represent the maximum current, in any given moment, for each considered track.

The dashed horizontal lines represent the thermal limit that can be supported by the lines.
This value corresponds to 5 A /mm 2 * 610 mm^2 = 3050 A, where:

- 5 A/mm^2 is the maximum current corresponding to an overtemperature of 40 ° C compared to the ambient temperature;

- 610 mm^2 is the section of the contact system of the first two tracks;

For the "fast" tracks (track 3 and 4), the section is smaller (460 mm^2). The limit current is 2300 A.

It should be noted that this is a thermal constraint that represents the electrical "history" of the component (in this case catenary system) and it is therefore important not to exceed this limit for long periods of time.

In this simulation - which corresponds to the Rush hours of the day – for the "slow" tracks (track 1 and 2), the thermal constraint is absolutely respected with a wide margin. For the last two tracks, it is exceeded only for a few moments. The fact that the first two tracks better satisfy the current constraint is due to the fact that these two tracks have catenary system with different sections (the first two are FF4, the second two FF3), as all four tracks support absolutely comparable currents.

Simulation results for the electrical substations are:

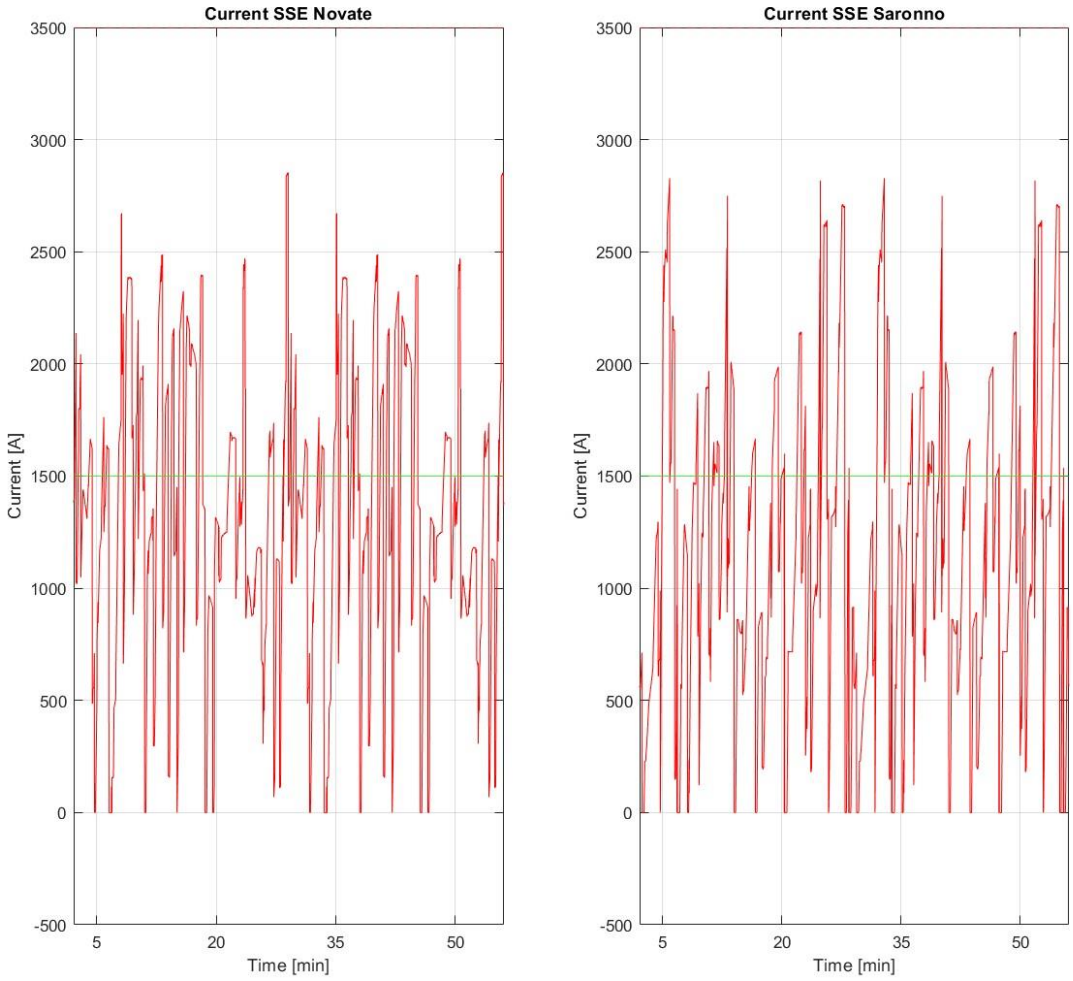

Figure 3.3 : ESSs instantaneous current

The graphs above describe the current trend in the two ESSs considered (Novate and Saronno).

In the graphs there are two horizontal lines: a green one at 1500 A and a red one at 3500 A. These lines represent the two acceptable limits for the electrical substations. The first indicates the nominal current value. The two electrical substations are able to produce that current value continuously. The second is the peak current: this high value can be produced by each substation for a maximum of five minutes without technical problems mainly because of overheating.

All limits are fully respected, the nominal current is exceeded in several instances, but as already mentioned, for values higher than the nominal current (and lower than the peak current) the quadratic mean current is considered in (determined as explained in chapter 1.2.2), using the formula $I_{ESS,rms} = \sqrt{\frac{1}{T_2-T_1}\int_{T_1}^{T_2}\left[I_{ESS,t}\right]^2 dt}$ (1-1).

The two values are well below the 2250 A limit thanks to the fact that each substation is equipped with two conversion units in parallel (if only one the current values would be double, exceeding the constraints significantly):

Quadratic mean current ESS Novate	**Quadratic mean current ESS Saronno**
1478 A	1353 A

Table 3.2 : Quadratic mean current of the two electrical substations

As it may be noted, often the ESSs does not supply the railway system (current equal to zero in Figure 3.3).

It is instead rare when both ESS do not supply power the lines i.e. when the network supplies itself with no need of external power because of the power generated by the regenerative breaking of the running trains. Being a very busy route, with many different trains running at the same time, it occurs only for just 16 seconds on the entire hour considered. During this very short period of time, a total of **36 MJ** are anyway unrecovered (and are potentially recoverable).

The three-dimensional surfaces of voltage and current of track 1 are shown here below (the next three tracks will have very similar graphs):

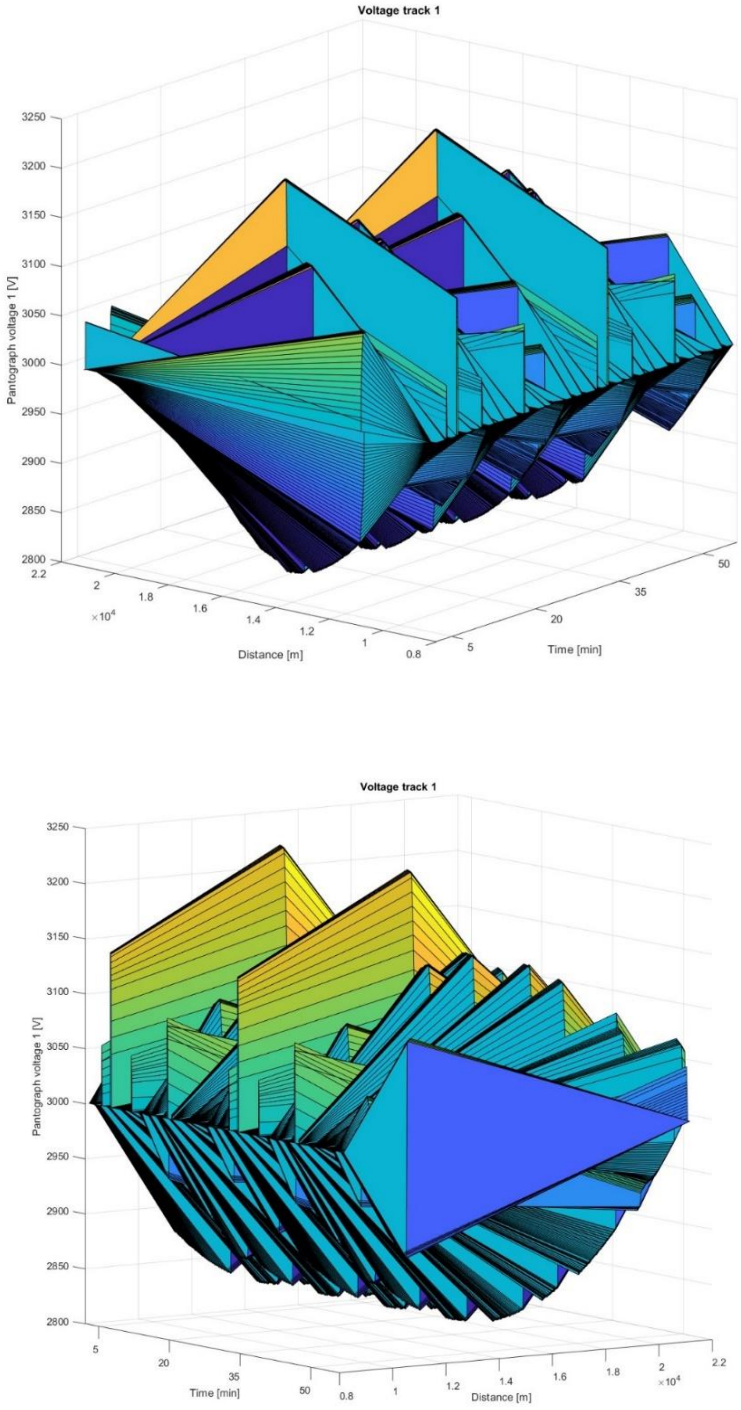

Figure 3.4 : 3D representation of the voltage in track 1

The two graphs represent the same curve simply turned with respect to the time axis, to point out that: during acceleration - and therefore at voltages below 3000 V - the network decreases its voltage less rapidly than when it begins to decelerate. This can be seen in the first of the two figures above taking also into account the characteristic Power Curve.

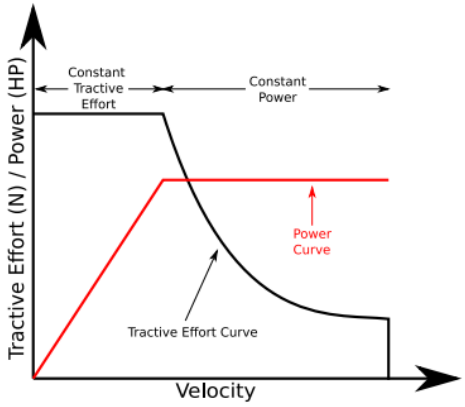

Figure 3.5 : Mechanical characteristics with power curve

At the start of the train acceleration (and therefore at low speeds) the absorbed power is minimal. Instead at the start of the train deceleration (and therefore at high speeds) significant powers is injected into the network.

The 3D graph of line currents is not easily readable. It is anyway included here below and shows the line values moment by moment.

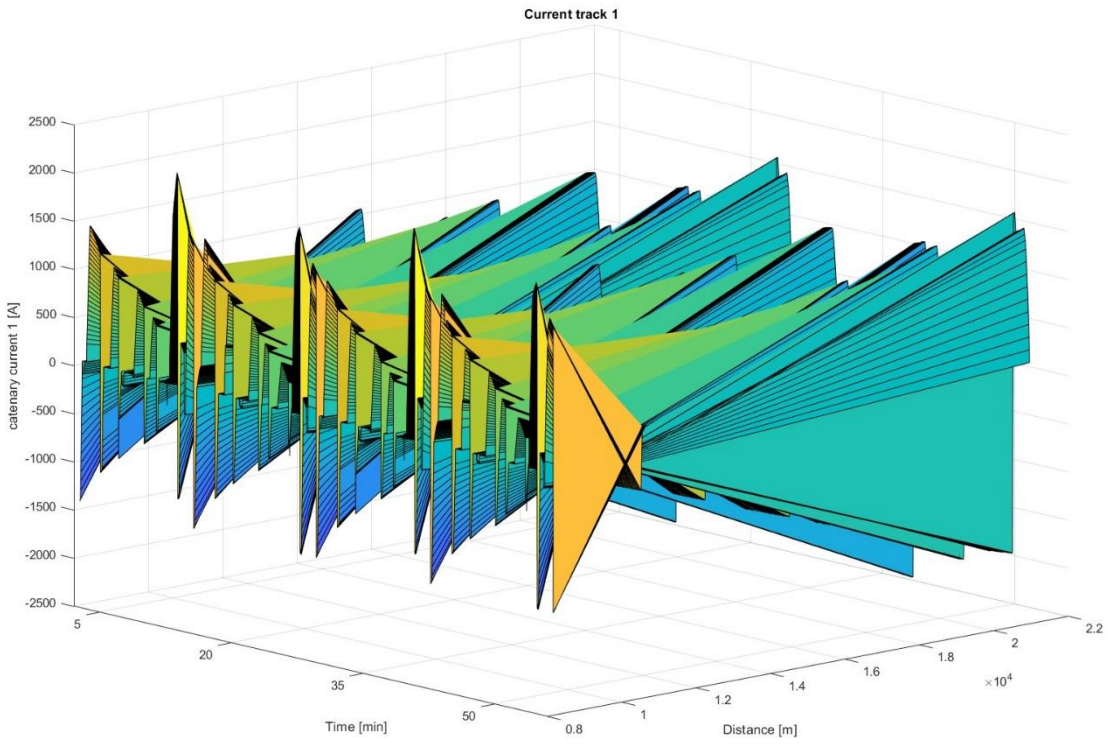

Figure 3.6 : 3D representation of the current in track 1

The abscissa in the axis starts at about 8 km, that is the point km of Novate station (km 8+162), being the reference placed in Cadorna station.

These graphs can be represented in two dimensions if the an instant of time t is considered, this representation (presented in Figure 3.7) is useful to see the voltage drops across the lines.

Finally, the two-dimensional graphs at an instant in time (7:34:02) where all the trains are absorbing power:

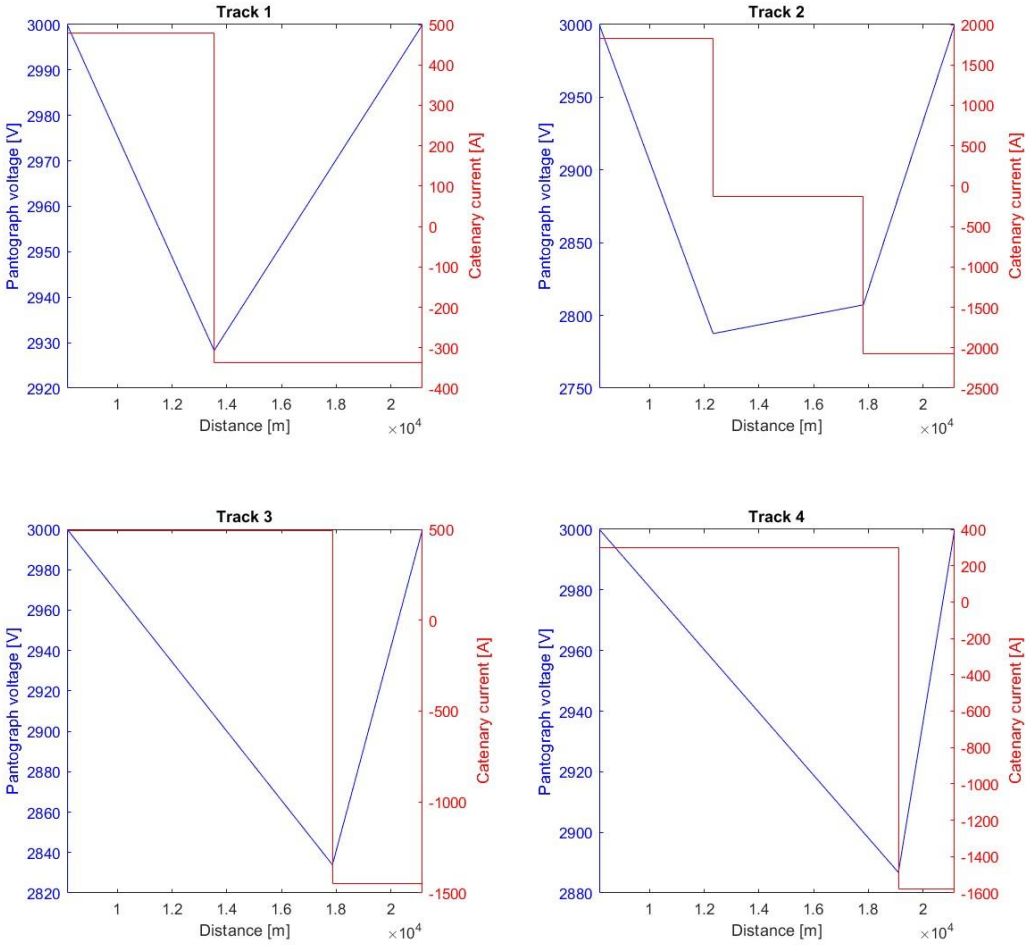

Figure 3.7 : 2D representation of the voltage.

By convention it has been chosen to use a positive current when it circulates from Novate to Saronno (positive direction of the abscissa axis).

3.1.2. Simple Network at Off-Peak Hour

This simulation has the same input parameters of the Simple Network Case at Rush Hour but runs between 12:30 and 13:30. The same graphs are reported to highlight how the lines and electrical substations are differently charged.

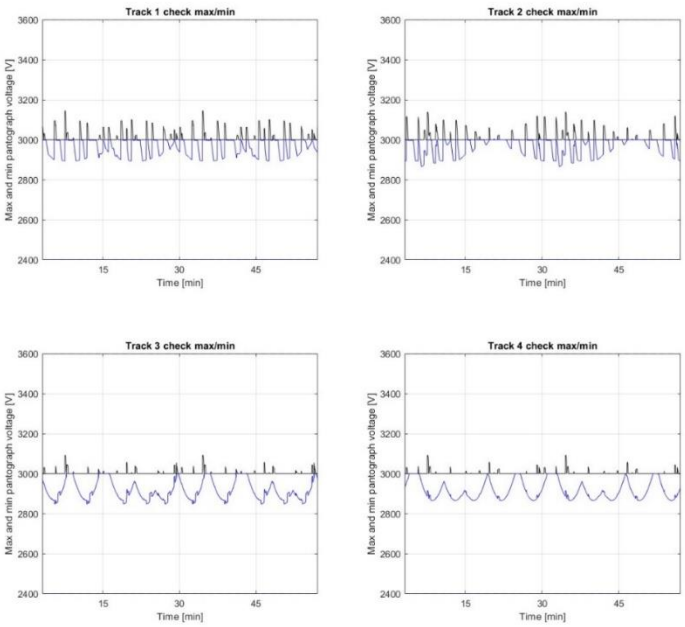

Figure 3.8 : Maximum and minimum voltage across the tracks

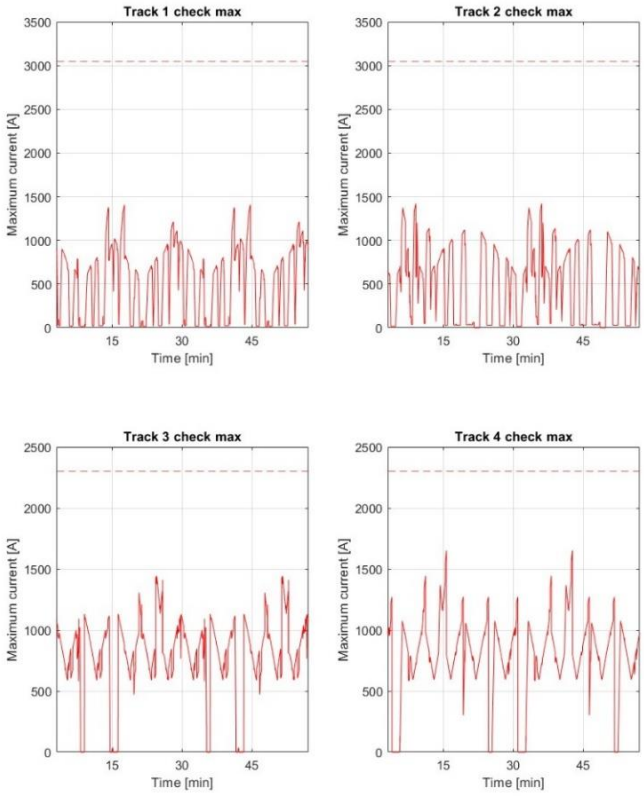

Figure 3.9 : Maximum current across the tracks

As expected, the limits are well respected as it was the case for the Rush Hour.

Track Maximum Voltage	Track Minimum Voltage
3145 V	2848 V

Table 3.3 : Maximum and minimum voltage

The same considerations apply to the ESS's:

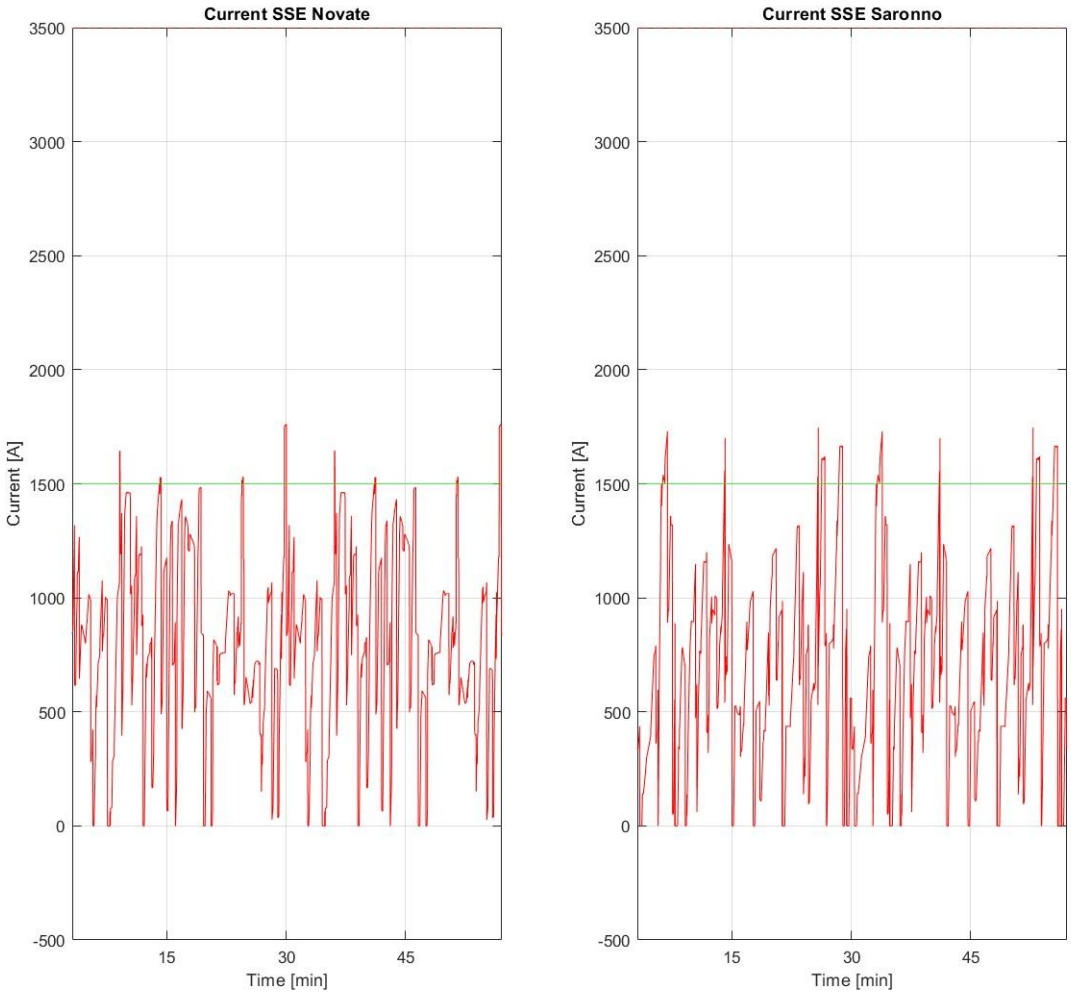

Figure 3.10 : ESSs instantaneous current

Also in terms of quadratic mean current, the value reached are well below the limits.

Quadratic mean current ESS Novate	Quadratic mean current ESS Saronno
906 A	828 A

Table 3.4 : Quadratic mean current of the two electrical substations

The unrecovered energy is lower than the rush hour case and it is **22.8 MJ** distributed once again in just 16 seconds throughout the considered hour (the times are identical as the train schedule is the same).

The results of this simulation are, as expected, even more compliant with the technical limits.
This demonstrates that the railway electrical system is sized for the "Rush hour" and so, for the rest of the day, has an extremely huge carrying power potential which leads to speculate that the network can be better exploited by connecting different types of infrastructure.

3.1.3. Detailed Network at Rush Hour

The model of the railway electrical system considers the return circuit (rail and ground).

Results are very similar to those obtained for the Reduced model Network as all input parameters are the same. For this reason the model "Reduced" has the aim to validate the more complex "Detailed" model, and from now on, the latest model will be used.

The results graphs are included here below:

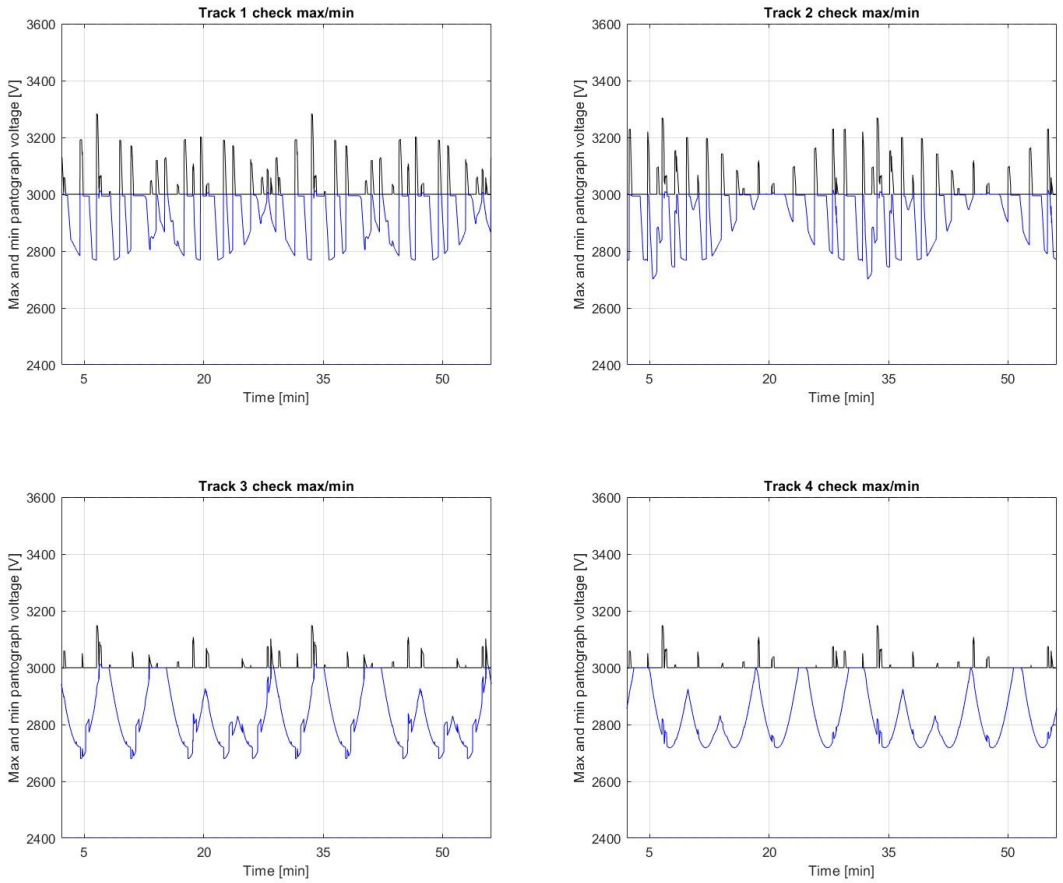

Figure 3.11 : Maximum and minimum voltage across the tracks

The maximum and minimum voltages are increased and decreased by about 70 V respectively.

Track Maximum Voltage	Track Minimum Voltage
3289 V	2680 V

Table 3.5 : Maximum and minimum voltage

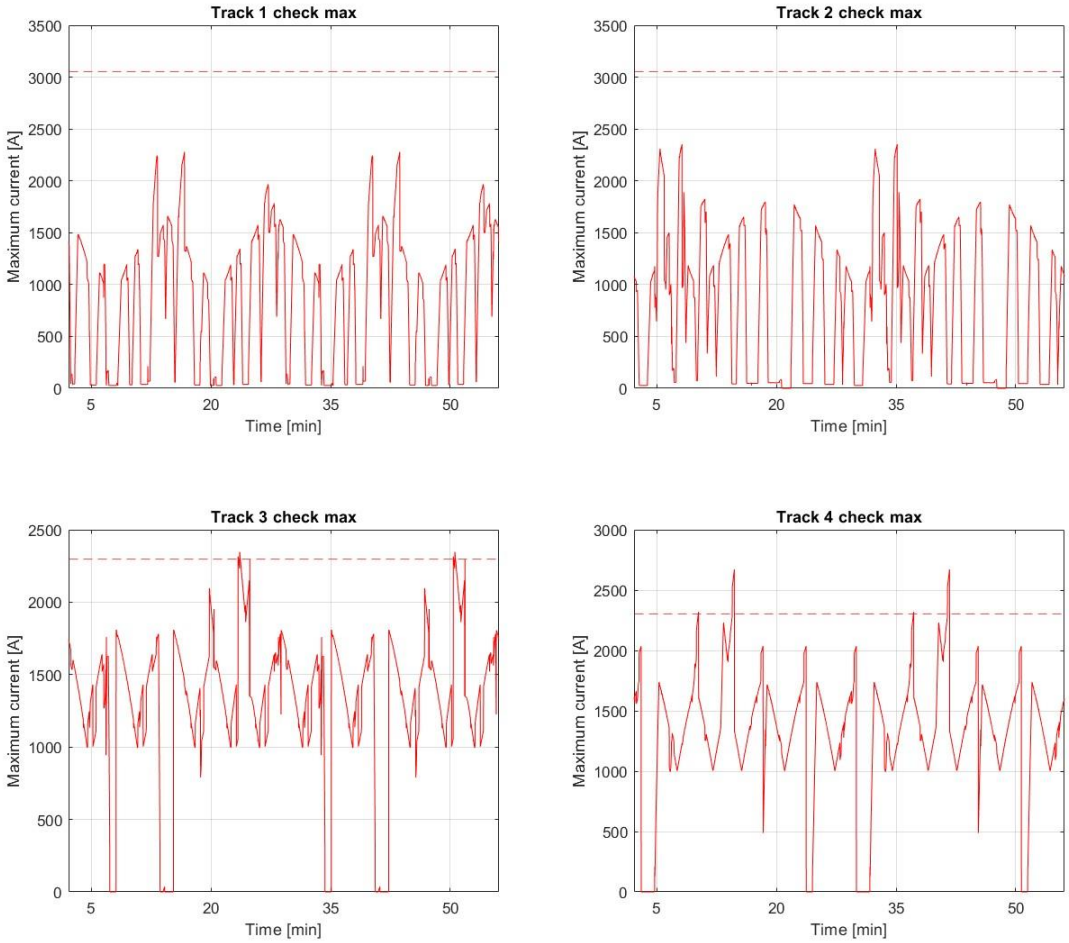

Figure 3.12 : Maximum current across the tracks

The thermal limit in the fast tracks is reached for a few moments due to their smaller section (a larger section would reduce the current and above all would raise the constraint by 750 A).

Electrical substations will also be a little more loaded than before, mainly because of the losses in the return circuit.

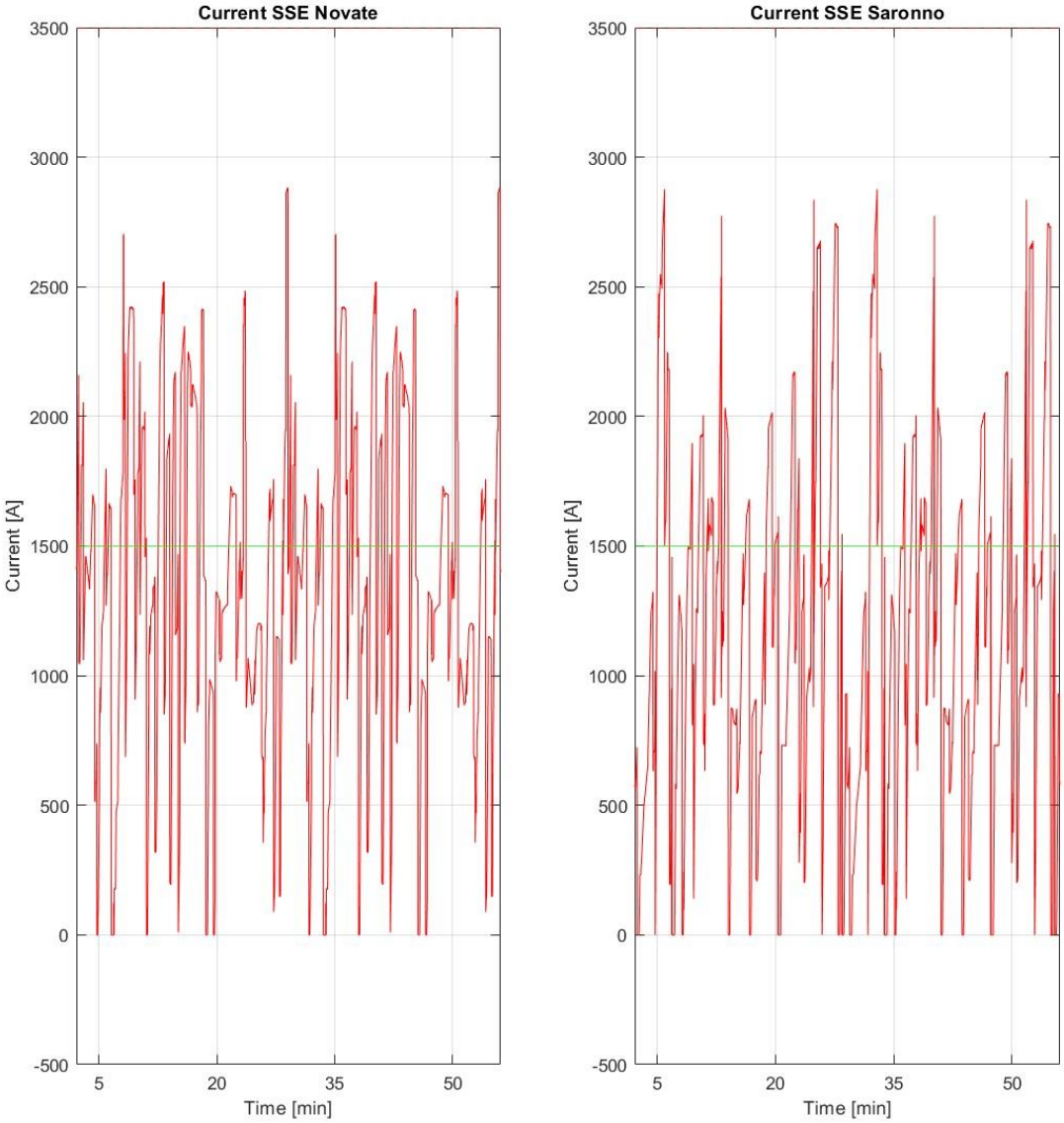

Figure 3.13 : ESSs instantaneous current

Quadratic mean current ESS Novate	Quadratic mean current ESS Saronno
1499 A	1373 A

Table 3.6 : Quadratic mean current of the two electrical substations

The quadratic mean values are about 20 A greater than the Simplified Network case in Rush hours but still well below the constraint of 2250 A.

The unrecovered energy is now only **34.8 MJ** (always for 16 seconds) as part of this energy is used to overcome the major dissipations having adopted the "Detailed" model.

3.1.4. Detailed Network at Off-peak Hour

This simulation has the same input parameters of the Detailed Network Case at Rush hour but runs during Off-peak hours. Similar graphs are reported to highlight how the lines and electrical substations are differently charged.

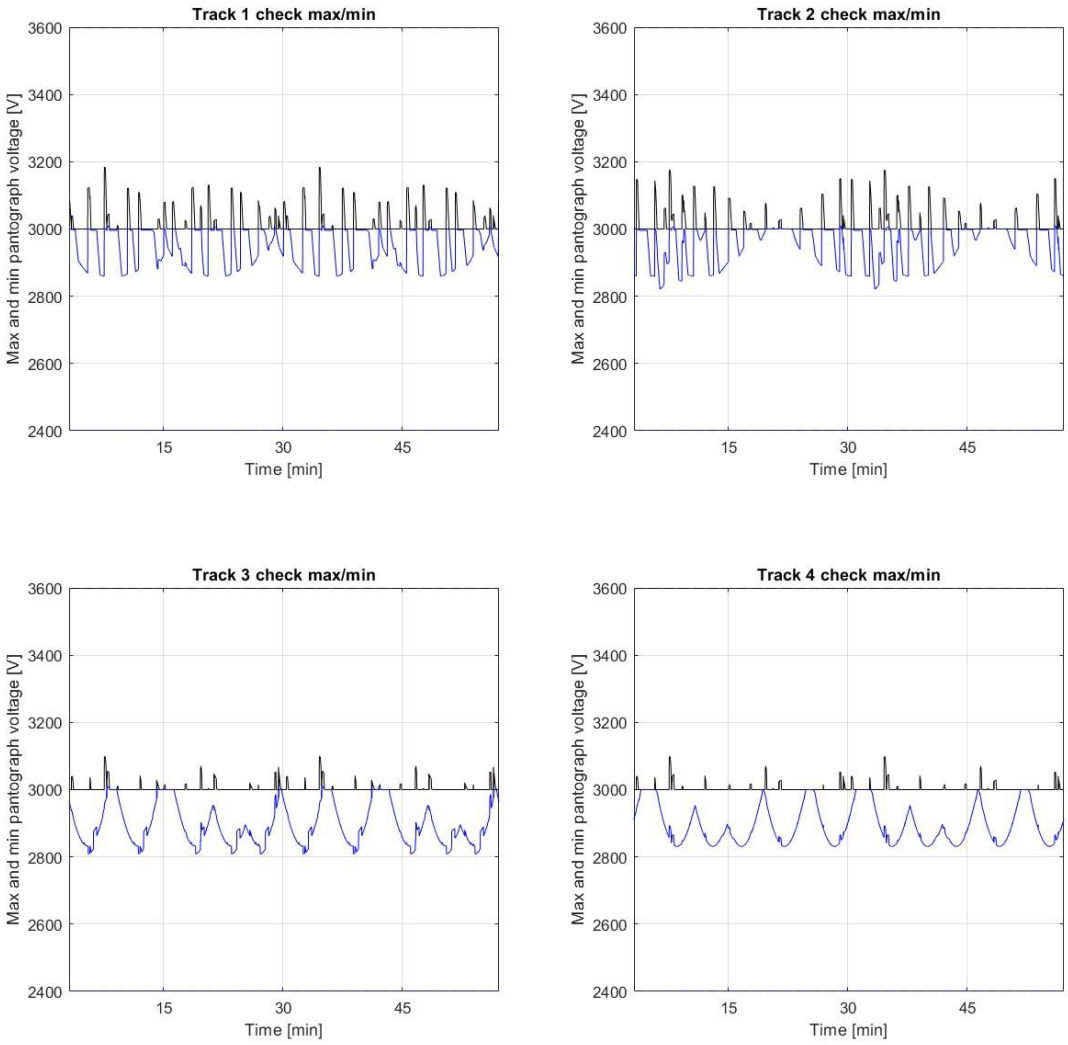

Figure 3.14 : Maximum and minimum voltage across the tracks

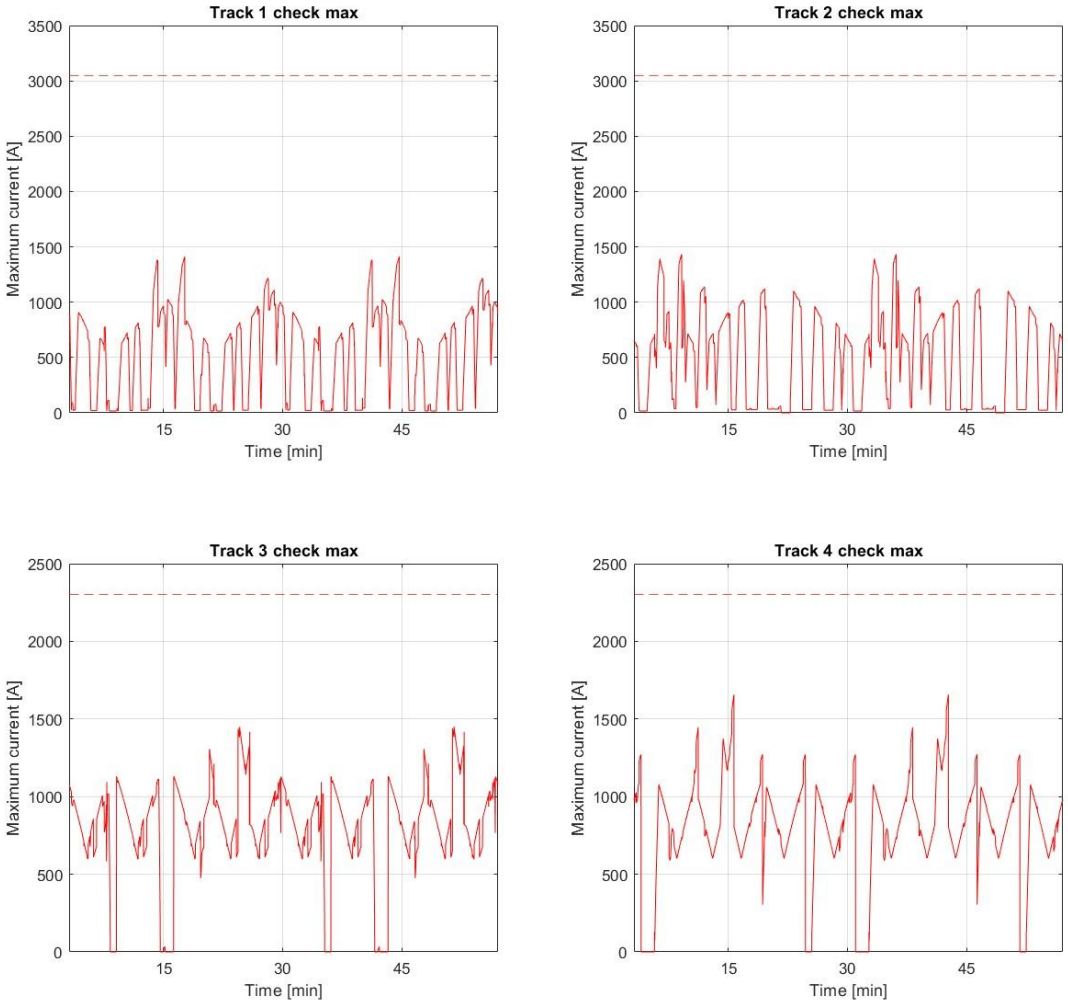

Figure 3.15 : Maximum current across the tracks

As expected, the limits are well respected as it was the case for the Rush Hour.

Track Maximum Voltage	Track Minimum Voltage
3185 V	2810 V

Table 3.7 : Maximum and minimum voltage

The same considerations apply to the ESS's:

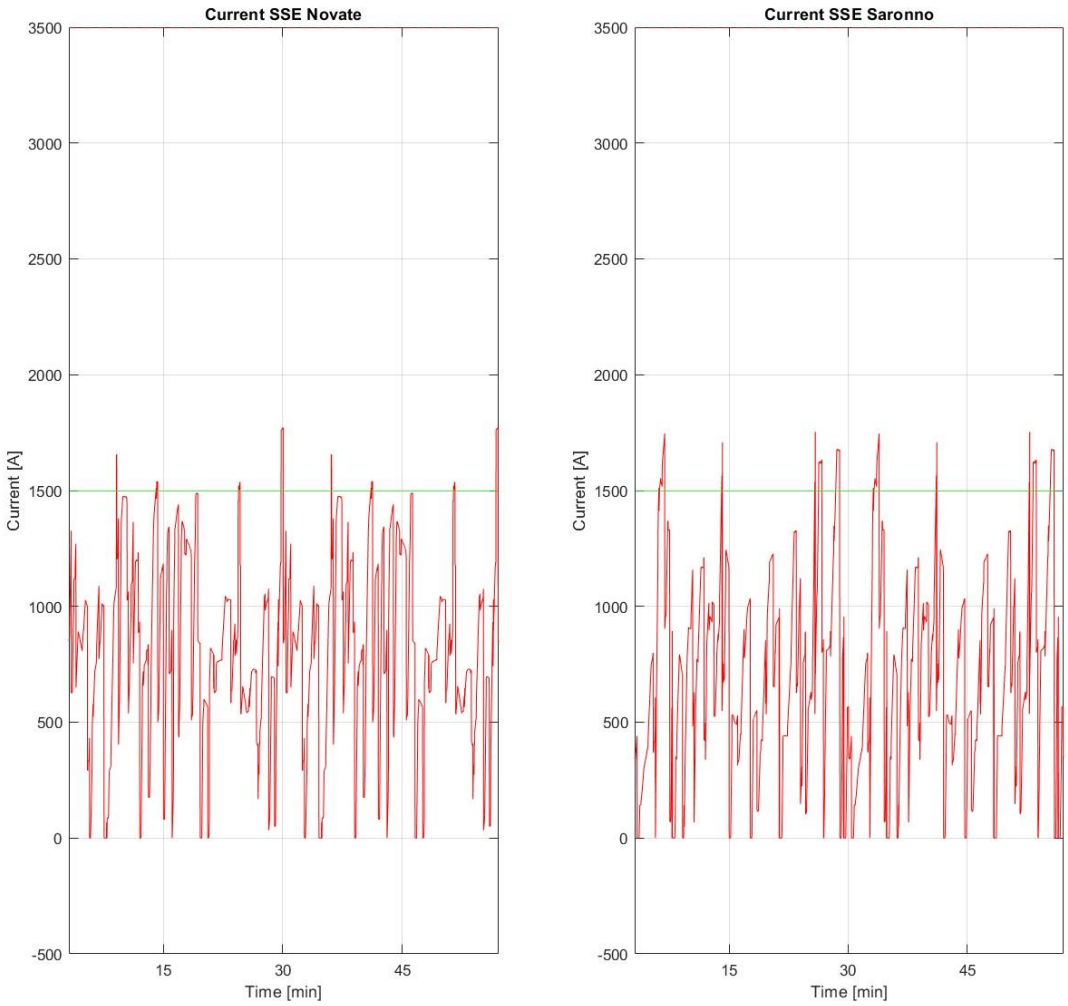

Figure 3.16 : ESSs instantaneous current

Also in terms of quadratic mean current, the value reached are well below the limits.

Quadratic mean current ESS Novate	Quadratic mean current ESS Saronno
914 A	836 A

Table 3.8 : Quadratic mean current of the two electrical substations

The unrecovered energy is now as low as **22.4 MJ** (always for 16 seconds).

3.1.5. Results

The following table summarizes the result of the four simulations runs for the Novate - Saronno sector.

	Vmax [V]	Vmin [V]	$I_{ESS,rms}$ Novate [A]	$I_{ESS,rms}$ Saronno [A]	Unrecovered Energy [MJ]
Simple Network Rush Hour	3225	2750	1478	1353	36
Simple Network Off-peak Hour	3145	2848	906	828	22.8
Detailed Network Rush Hour	3289	2680	1499	1373	34.8
Detailed Network Off-peak Hour	3185	2810	914	836	22.4

Table 3.9 : Comparison of different parameters

The impact of a greater number of elements per train during Rush hours than the Off-peak hours (8 against 5) is evident: Rush Cases are always nearly 60% larger than the Off-peak ones.

In terms of voltage, the same increase is more or less generated when the difference in respect to the nominal voltage of 3000 V is considered (not the absolute value).

In summary, the Detailed Network cases give results higher but not significantly different in respect of those of the Simple Network one. **Because of this, the Detailed Network has been chosen as baseline network in the following simulations**.

3.2. Addition of electric car parking recharging system (Case 1)

The railway electric system is integrated with 8 parking slots (out of 9 stations) for two principal reasons.

Firstly to exploit a great potential of the railway network to withstand additional loads during most hours of the day and secondly the electric car batteries can absorb the regenerative breaking energy of the trains.

To better compare the various cases, the same two reference hours of the baseline network has been selected (Rush and Off-peak hours).

Figure 2.22 shows the two selected timeslots and the power demand of the electric car parking, this two represents the higher electric car parking demand (7.30-8.30 Rush hour) and an intermediate situation (12.30-13.30 Off-peak hour).

3.2.1. Case 1 at Rush Hour

The following graphs may be used for comparison with the baseline network.

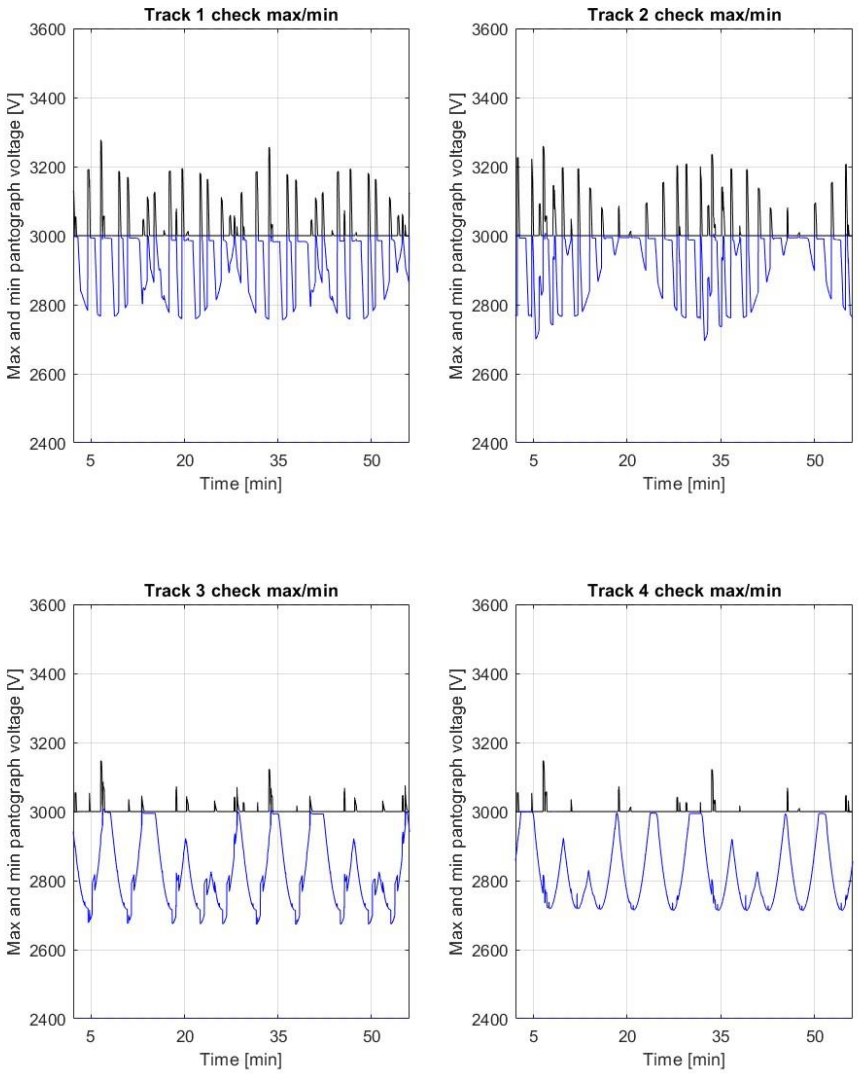

Figure 3.17 : Maximum and minimum voltage across the tracks

The difference with the corresponding baseline network at Rush Hour (but no Car Parking) is more evident in the blue lines which represent the minimum voltages of the given track at that certain moment of time. The network is definitively more loaded as it must provide energy to all electric car parked.

These minimum voltages appear to show less irregularities than before, as the load imposed in the simulation is almost constant, if we consider short periods of time. This case is the most stressful for the whole day as in the first half hour or so the parking lots reach their relative peak of demand adsorbing more power from the railway network.

	Maximum Voltage [V]	**Minimun Voltage [V]**
Baseline Network with Car Parking at Rush Hour	3281	2670
Baseline Network at Rush Hour (no Car Parking)	3289	2680

Table 3.10 : Comparison of different voltages

There is a small Voltage drop as the additional loads represented by the electric car parking is relatively low compared to the Railway network. It is to be noted that these maximum and minimum values are relative to specific points of the network where there is only one parking lot.

Track currents are:

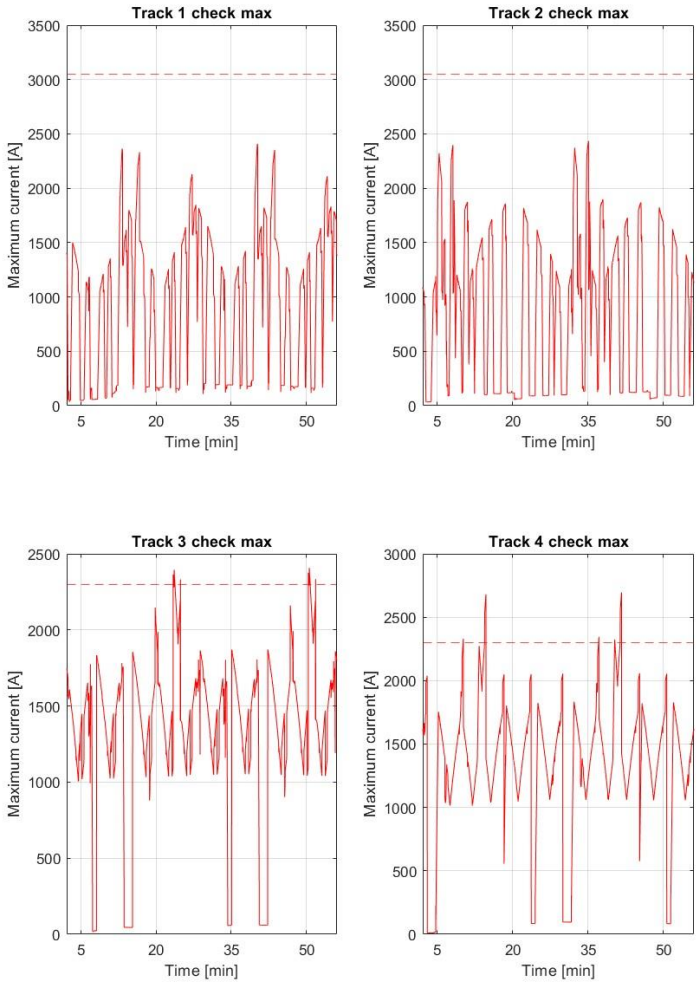

Figure 3.18 : Maximum current across the tracks

There are two peculiarities compared to Figure 3.12 of Baseline Network at Rush Hour (no Car Parking):

1. The railway lines, as expected, are more charged and the current is greater. Now even track 3 touches the thermal limit, only for a few moments that are within the overload limits.
2. With no Car Parking when no train is running along the track, the current is nil if the substations are at the same potential. From this simulation onwards, there is no longer the possibility of having a totally empty track, even if there is only one car inside the parking lot, as the car parks themselves are connected directly to the different tracks.

The most remarkable result, however, is the one that represents the electrical substations, which certainly at higher power than in other simulated cases:

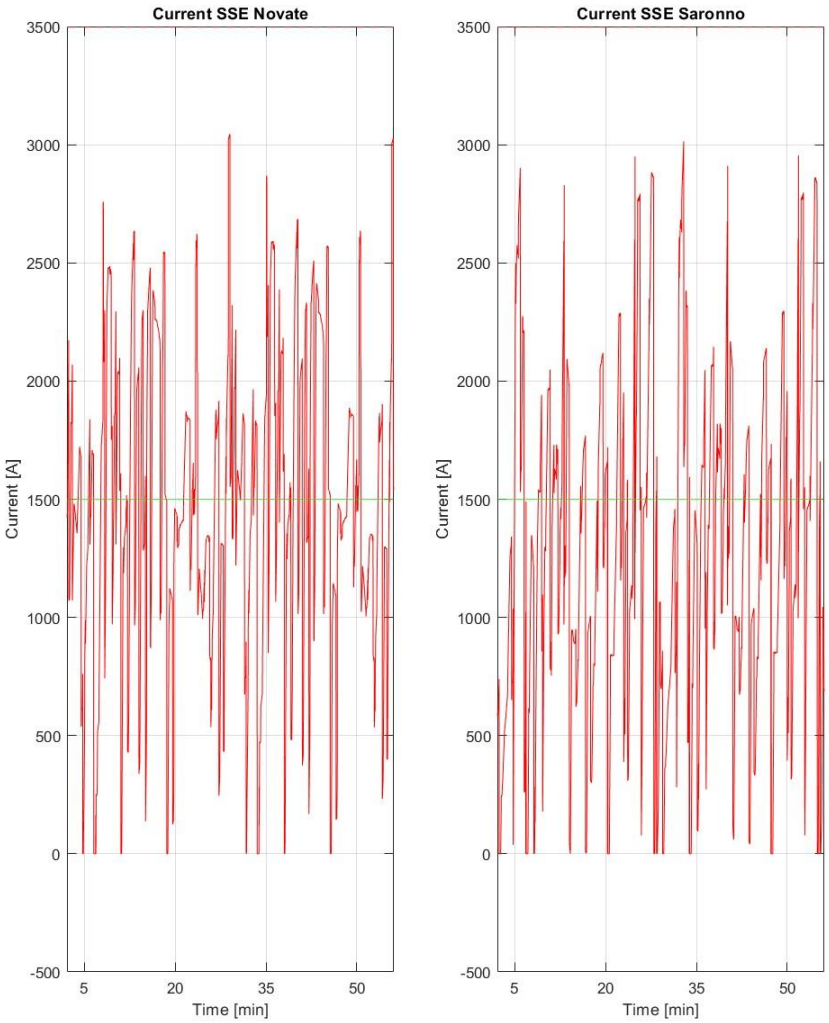

Figure 3.19 : ESSs instantaneous current

The substations have peaks of even 3000 A but only for a few moments of time, values still below the technical constraints. In terms of currents in quadratic mean:

	Currents in Quadratic Mean Novate [A]	**Currents in Quadratic Mean Saronno [A]**
Baseline Network with Car Parking at Rush Hour	1630	1471
Baseline Network at Rush Hour (no Car Parking)	1499	1373

Table 3.11 : Comparison of different currents

Current Values are higher of about 130 A and 100 A.

Unrecovered energy is now **20.2 MJ** significantly lower than the 34.8 MJ of the No Car Parking Case. This implies that about 14.6 MJ are recovered in just one hour during which (high traffic line at Rush Hour). It is important to underline that this energy is recovered in only sixteen seconds.

3.2.2. Case 1 at Off-peak Hour

This simulation assumed the same input parameters but runs at Off-peak Hour (12:30 – 13:30).

Compared to the case without electric parking, it should be noted that the latter can affect the railway network at a time of day when it is far from being overloaded. Therefore, being used more becomes an advantage for the analysis study.

As in the previous cases, the line voltages are illustrated first:

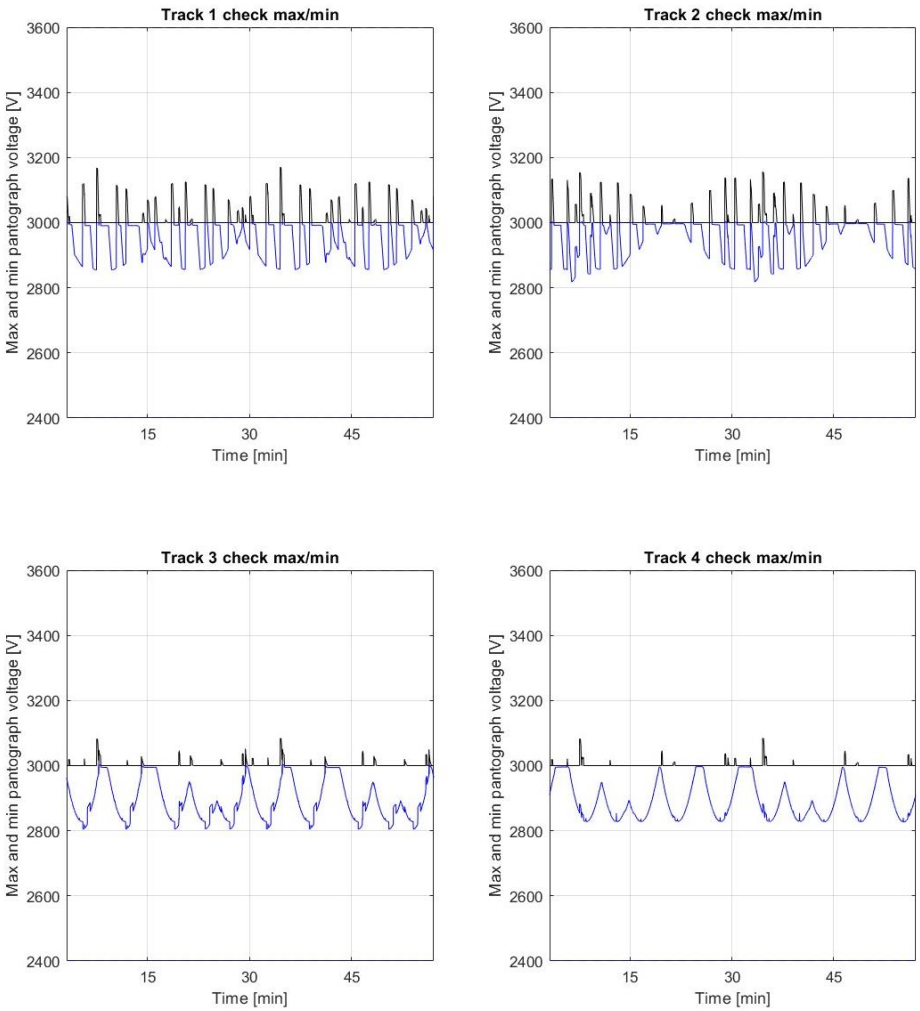

Figure 3.20 : Maximum and minimum voltage across the tracks

In terms of Voltages there is no significant difference with the Not Car Parking case reported in chapter 3.1.4

	Maximum Voltage [V]	Minimun Voltage [V]
Baseline Network with Car Parking Off-peak	3173	2805
Baseline Network at Off-peak (no Car Parking)	3185	2810

Table 3.12 : Comparison of different voltages

In terms of currents:

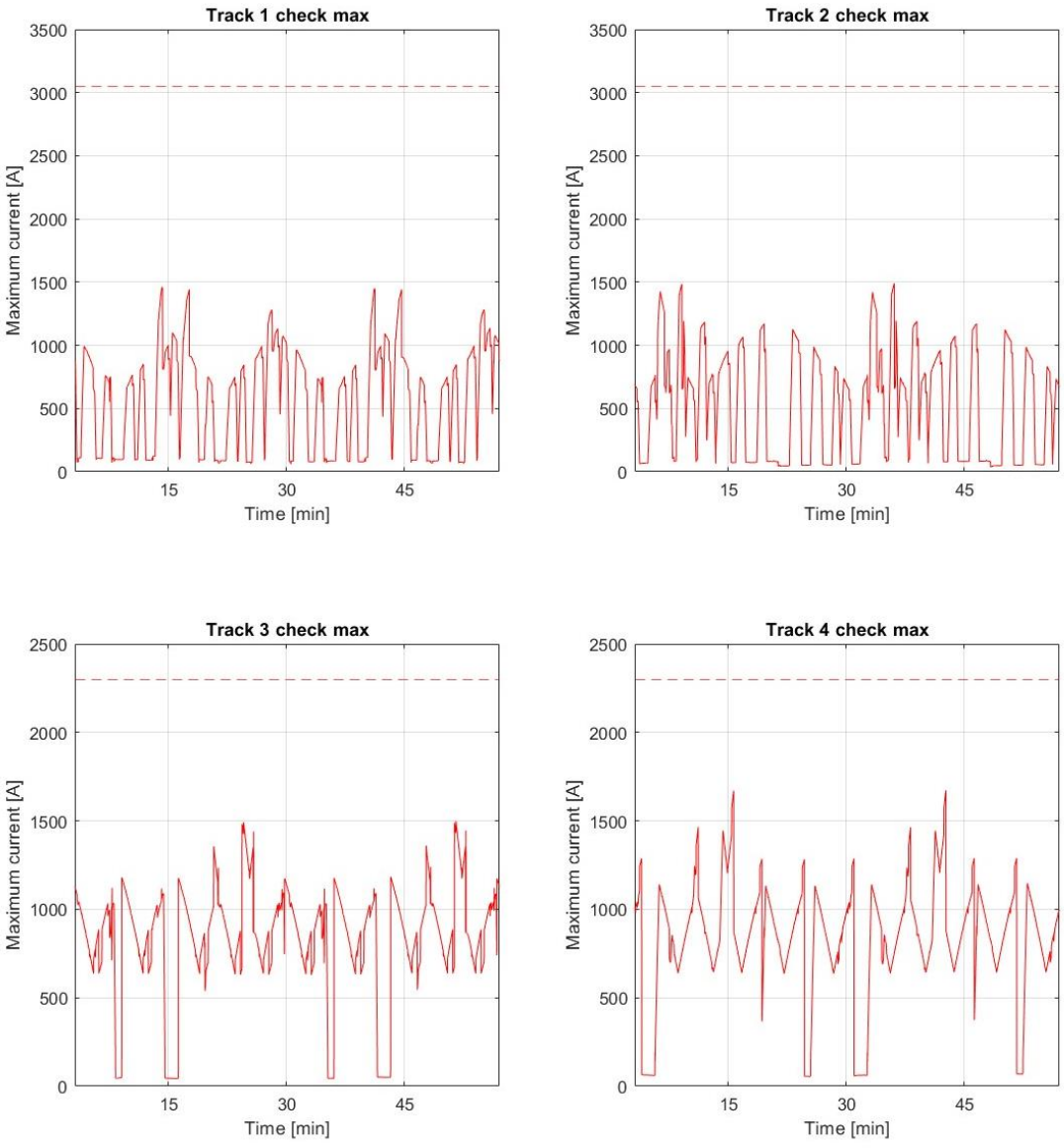

Figure 3.21 : Maximum current across the tracks

Currents are always far below the imposed thermal limits. There is no track without load during the Off-peak Hours.

As far as the ESS's are concerned:

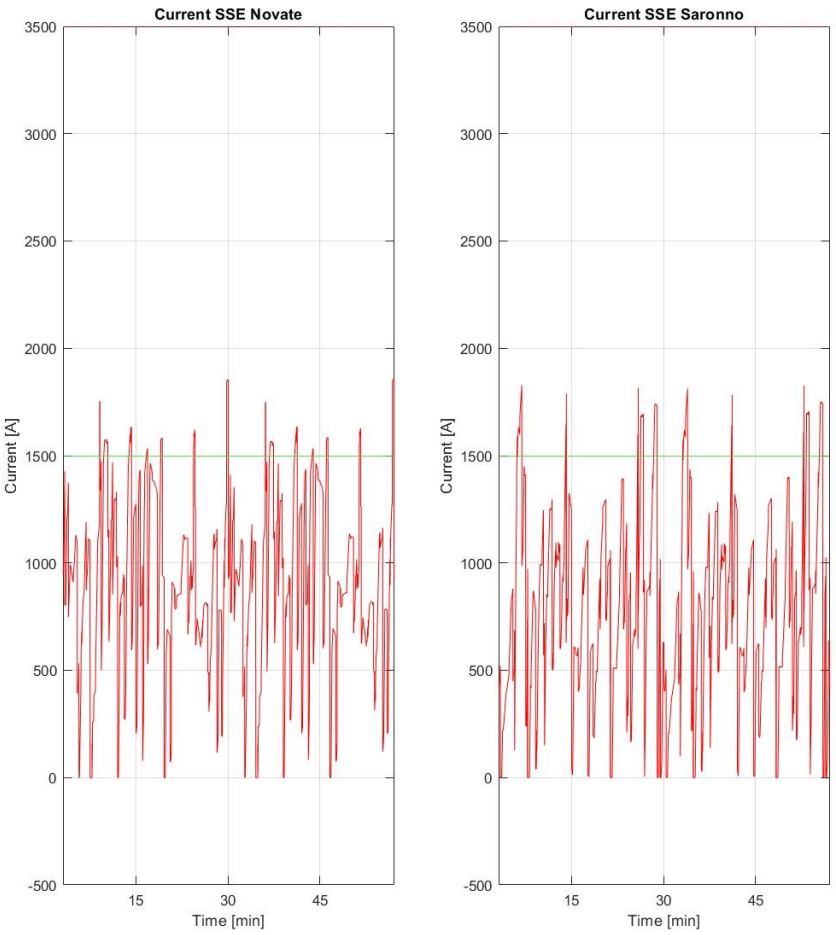

Figure 3.22 : ESSs instantaneous current

Once again they are below the constraints imposed but more than in the reference case.

In terms of currents in quadratic mean:

	Currents in Quadratic Mean Novate [A]	Currents in Quadratic Mean Saronno [A]
Baseline Network with Car Parking Low Traffic	1005	904
Baseline Network Off-peak (no Car Parking)	914	836

Table 3.13 : Comparison of different currents

Current Values are higher of about 90 A and 70 A which is a little less than the increase registered for the Rush hours (130A and 90A respectively). This is due not only to the fact that the current in the square mean is not a linear value function but also to the electric car park power absorption is lower during Off-peak hours as it has been assumed that cars have been parked in the parking few hours before. Focusing on how the Car Park charging changes during the day:

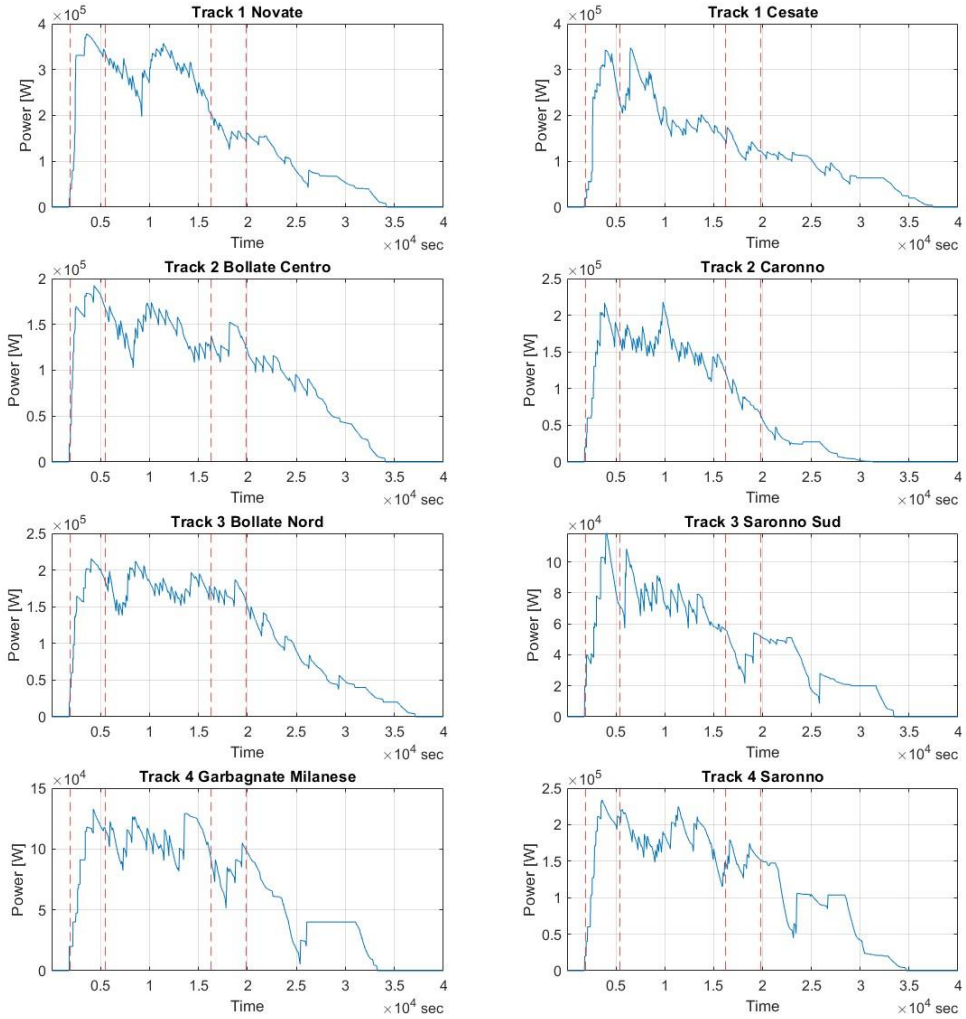

Figure 3.23 : Different power demand for each station car park

The red vertical lines highlight the 7:30 – 8:30 (Rush Hour) and 12:30- 13:30 (Low Traffic).

The unrecovered energy is now **9.7 MJ** significantly lower than the 22.4 MJ of the No Car Parking Case.

3.3. Addition of stationary battery energy storage system (Case 2)

The railway electrical system may be further expanded by installing a stationary storage system in each of the eight stations considered for the Car Parking. The goal is

to stabilize the grid and recover part of the energy generated during braking so that this may be released further on.

The battery system has as control system (or Energy management system) a fuzzy logic control explained in chapter 462.4

The batteries are sized with a nominal power and a nominal energy with the same *characteristics* to the train network i.e. the power of a train during Rush hours (eight elements) and the calculated total energy of a single train brake during the same Rush hours.

The following results were obtained:

Power characteristic = 680 kW * 8 elements =5.44 MW.

Energy characteristic = 100 MJ (as braking takes place in about twenty seconds and 100 is taken as a reference value).

With these reference values, simulations were carried out throughout the range from -50% to +100% of the characteristic power / energy, to find that pair of values representing, in first approximation, the optimal case to define the magnitude of the storage system.

Starting from the Rush hour case representing the higher load condition among the whole set of analyzed cases, the following values were obtained, first expressed in tabular form (reference values – no batteries – are Maximum Voltage 3280 V – Minimum Voltage 2670 V – Unrecovered Energy 20.2 MJ):

Maximum Voltage [V]				
Energy / Power	0.5	1	1.5	2
0.5	3253	3257	3259	3260
1	3253	3242	3243	3244
1.5	3293	3291	3278	3270
2	3265	3281	3284	3292

Table 3.14 : Maximum voltage with different Energy and power

Minimum Voltage [V]				
Energy / Power	0.5	1	1.5	2
0.5	2685	2684	2684	2684
1	2685	2684	2684	2684
1.5	2684	2684	2684	2683
2	2588	2598	2619	2622

Table 3.15 : Minimum voltage with different Energy and power

Unrecovered Energy [MJ]				
Energy / Power	0.5	1	1.5	2
0.5	19.68	17.99	17.28	16.53
1	25.67	22.06	19.64	18.51
1.5	45.38	32.96	27.36	23.97
2	91.11	64.04	45.97	36.11

Table 3.16 : Unrecovered energy with different Energy and power

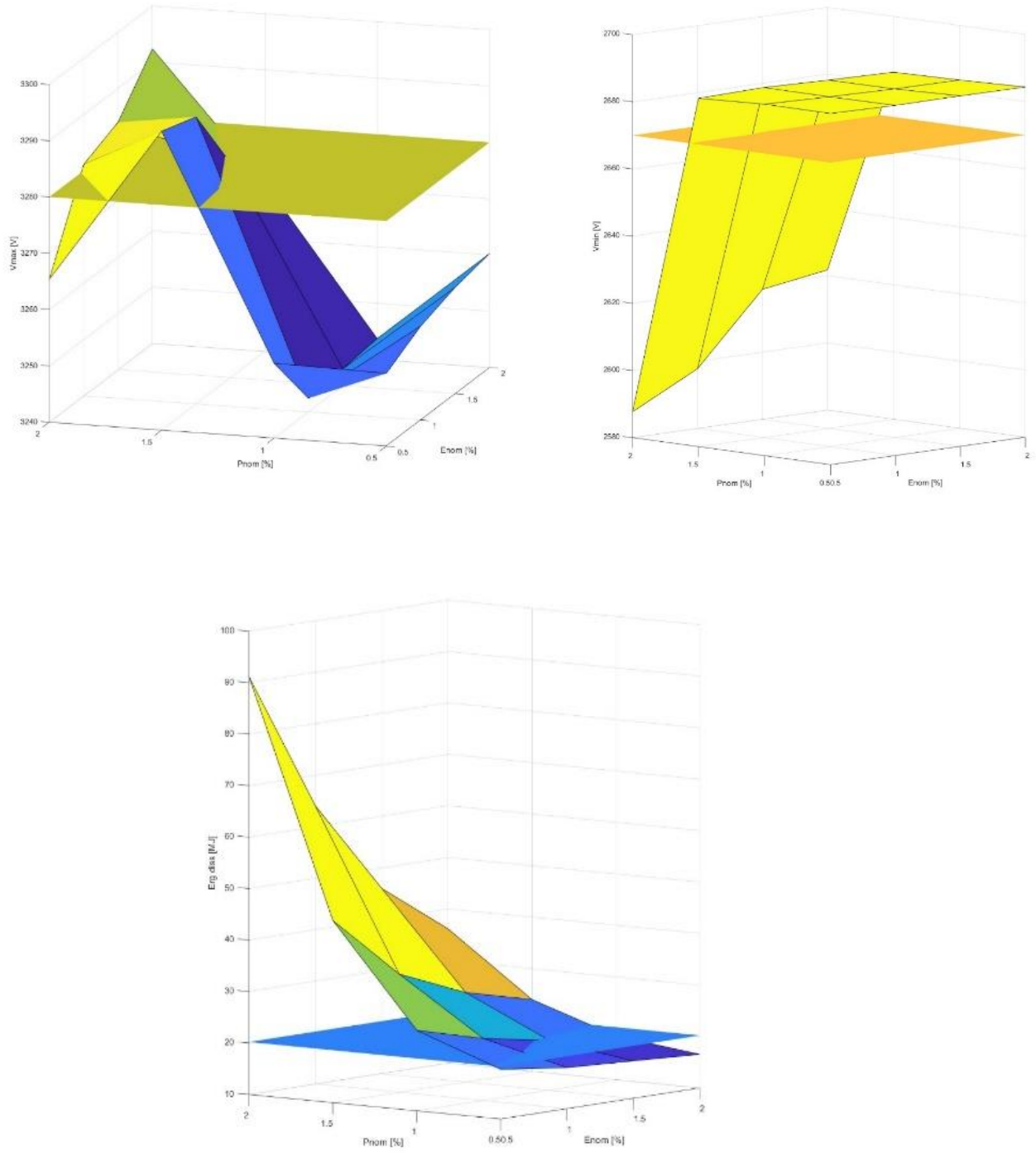

Figure 3.24 : Graphical representation of the tables: Maximum voltage, minimum voltage and unrecovered energy

The choice of the optimal combination is not immediate.

It was then decided to opt for the solution that would involve less unrecovered energy:

Nominal power = 50%P characteristic and Nominal energy = 200%E characteristic.

Even if other solutions appear to have a lower maximum voltage (3243 V - of the case 100% Pnom and 150%Enom - against 3260 V), since there is only a small voltage difference it was selected a solution that better met the demands of the whole system in terms of energy, unrecovering then *only* 16.53 MJ. This choice also has the advantage that, as with the integration of a photovoltaic system will show, it is better coupled to the photovoltaic system, later added to the network, as the powers are more comparable than other options.

The system has also been better discretized to simulate the optimal simulation, but the chosen solution remains the optimal case. It was also tried to further enlarge the battery park, which would lead to a non-significant reduction in the unrecovered energy, but also to an ever higher maximum voltage, causing the batteries to lose the possibility of stabilizing the whole system.

There are also boundary solutions, such as maximum power and minimum energy: as expected, since the power is too close in value to the energy of the batteries, the system worsens significantly rather than improves.

In addition, the greatest differences between the maximum and minimum voltages compared to the reference case without batteries, are obtained at the maximum voltage; This is because Rush hours are simulated, during which the system is more subject to higher loads; As a result, the batteries will be below 50% state of charge for longer periods of time recovering energy rather than feeding the system; therefore, supporting it especially when it is at maximum voltages.

Finally, it is important to underline that the same procedure was adopted to find the optimal power/energy even for the Off-peak hours, reaching identical conclusions.

3.3.1. Case 2 at Rush Hour

As mentioned, the battery characteristics are:

Nominal Power = 50% P characteristic = 2.72 MW.

Nominal energy = 200% E characteristic = 200 MJ.

The missing parameters and graphs are as follows:

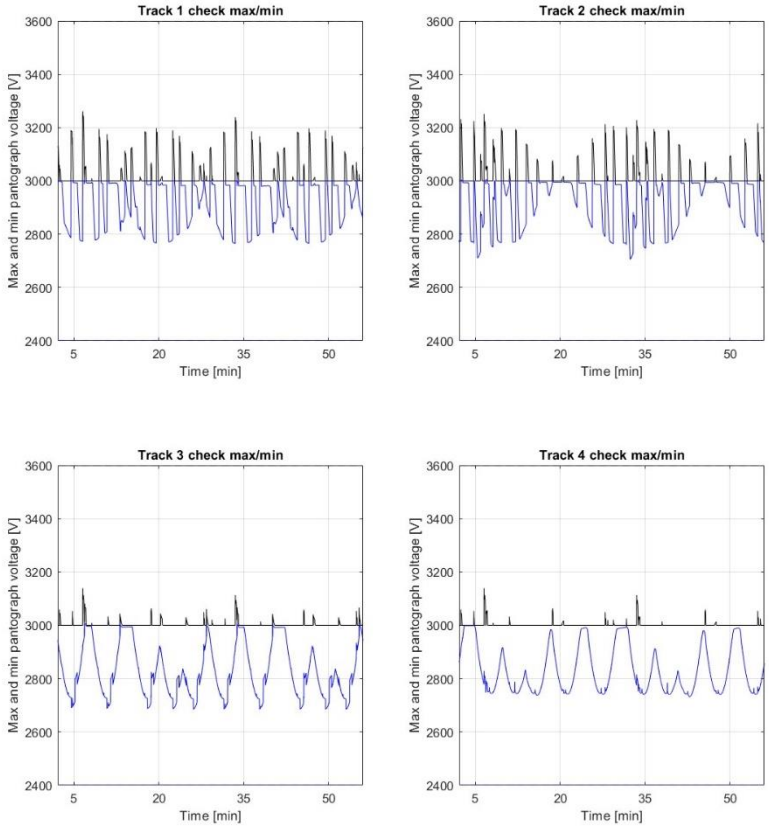

Figure 3.25 : Maximum and minimum voltage across the tracks

Compared to cases without batteries, voltage lines are similar even if they are more narrow for the minimum curves.

Track Maximum Voltage	Track Minimum Voltage
3260 V	2684 V

Table 3.17 : Maximum and minimum voltage

The maximum and minimum voltages are closer to the nominal voltage than in cases without a storage system (3280 V and 2670 V respectively).

Comparable currents circulate in the lines.

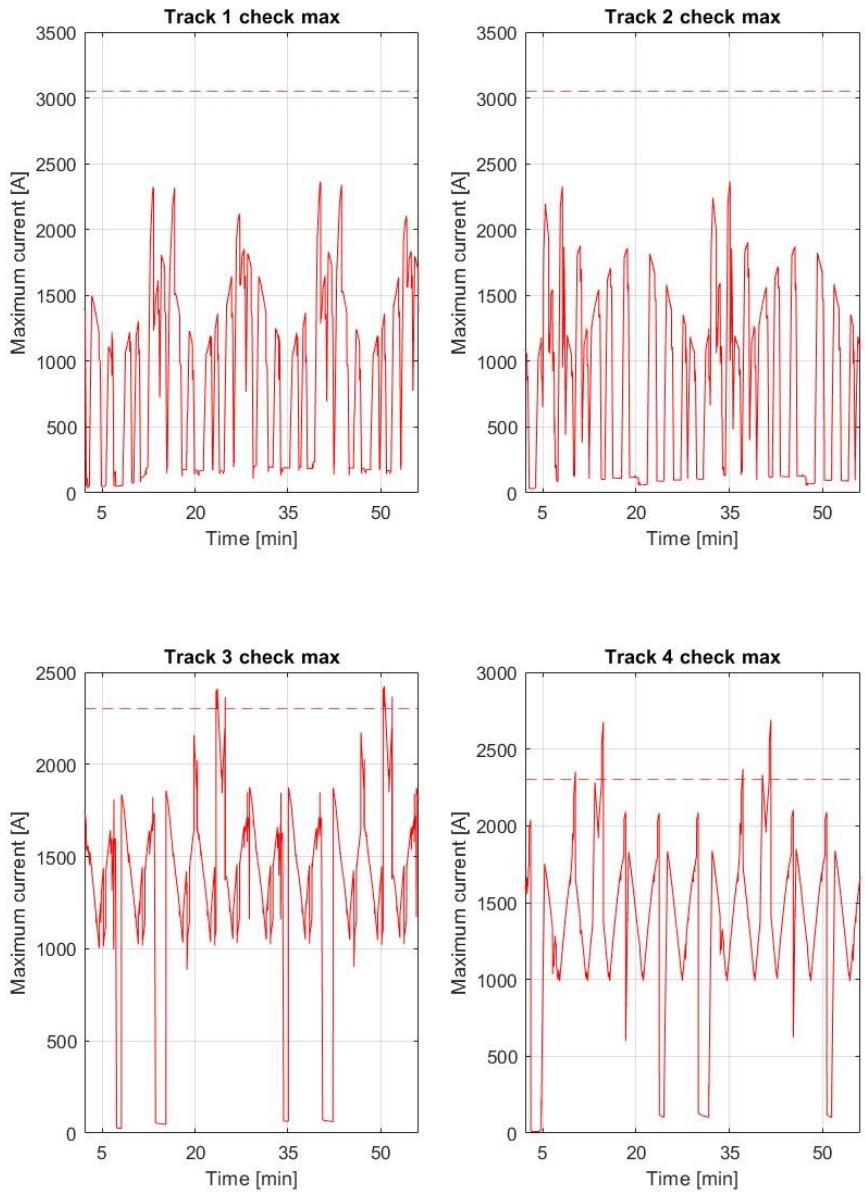

Figure 3.26 : Maximum current across the tracks

As far as the ESS's are concerned:

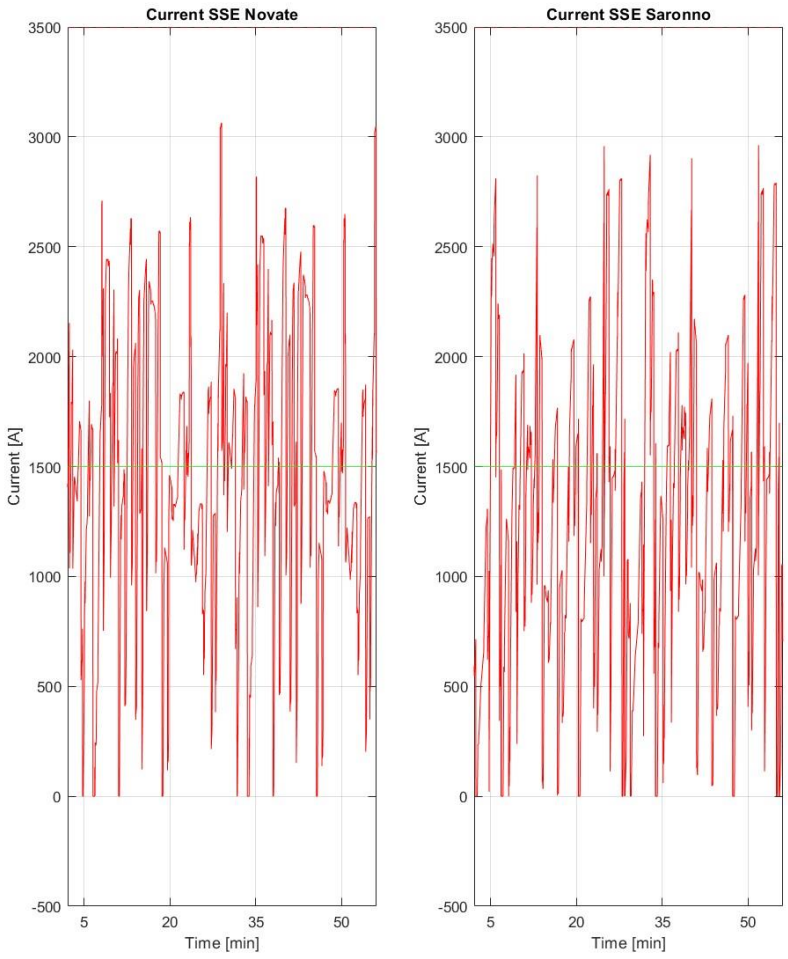

Figure 3.27 : ESSs instantaneous current

In both cases there are no substantial differences.

Quadratic mean current ESS Novate	Quadratic mean current ESS Saronno
1617 A	1450 A

Table 3.18 : Quadratic mean current of the two electrical substations

A drop of about 15-20 A is registered for the current in the square mean, compared to the case without a storage system.

The unrecovered energy, as said, decreased to 16.53 MJ.

The trends of the newly introduced batteries are also reported:

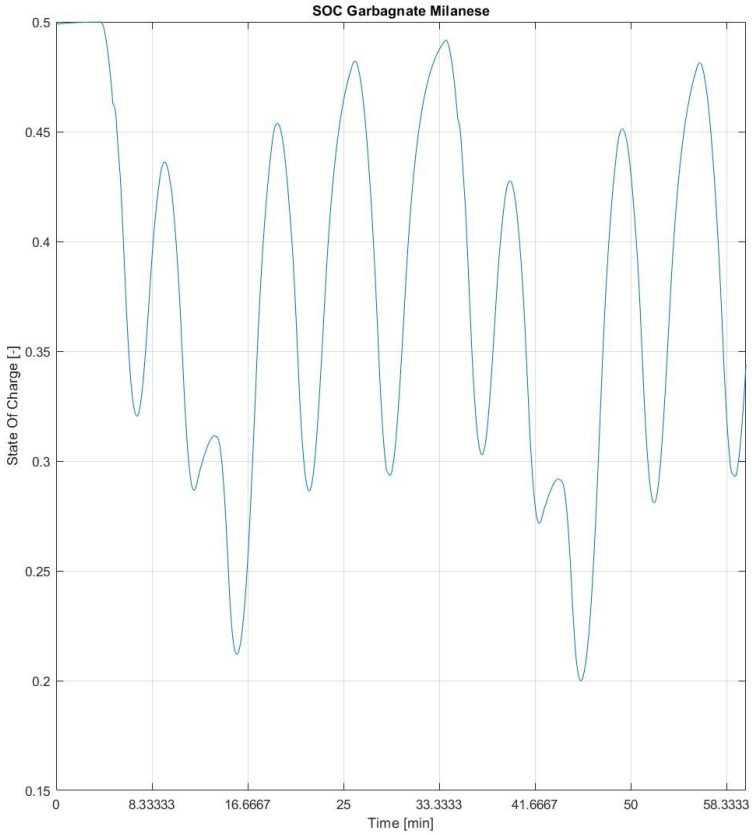

Figure 3.28 : Battery system with the wider SOC range.

What shown is the set of batteries subject to the highest loads of the entire network, and is the system installed in Garbagnate Milanese.

An initial State Of Charge of 0.5 has been imposed, but it always stabilizes below this threshold.

The trend of the less stressed batteries corresponding to the Bollate Centro:

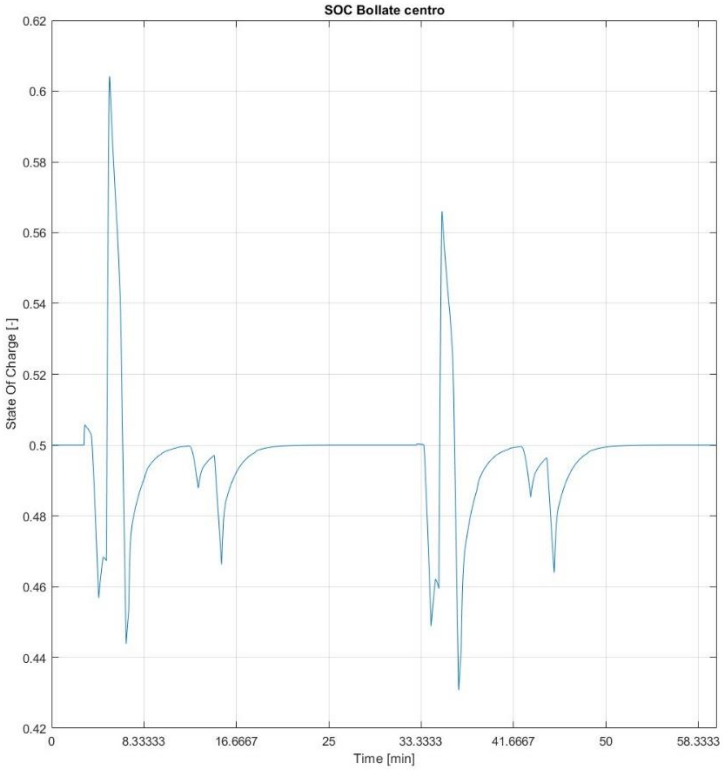

Figure 3.29 : Least stressed battery system.

3.3.2. Case 2 at Off-peak Hour

Results of the maximum/minimum line voltages, the maximum/minimum line current and the currents supplied by the electrical substations appear with no significant variations compared the corresponding case with no batteries (paragraph 3.2.2). Therefore only the following tabular solutions are here reported:

	Maximum Voltage [V]	**Minimun Voltage [V]**
Baseline Network with Batteries Off-peak	3164	2811
Baseline Network No Batteries Off-peak	3173	2805

Table 3.19 : Comparison of different voltages

	Currents in Quadratic Mean Novate [A]	Currents in Quadratic Mean Saronno [A]
Baseline Network with Batteries Off-peak	998	895
Baseline Network No Batteries Off-peak	1005	904

Table 3.20 : Comparison of different currents

The unrecovered energy is now **8.1 MJ** versus the 9.7 MJ in the case "Baseline Network No Batteries Off-peak".

The reductions registered in the Off-peak hours are low and therefore the improvement on the voltages is even less than in cases without batteries. This is to be explained by the fact that the batteries, based on fuzzy logic, increase their output / input power also depending on the mains voltage at that specific point. If the network has minor voltage deviations during Off-peak hours, the batteries are still of use but less responsive in terms of power output (the absolute value of the power output of the batteries will be lower due to smaller voltage drops and SOC closer to 0.5).

The graphs of the same stations shown above for the Off-peak hour are also reported where they are less active because the system, in terms of voltage, is much more stable:

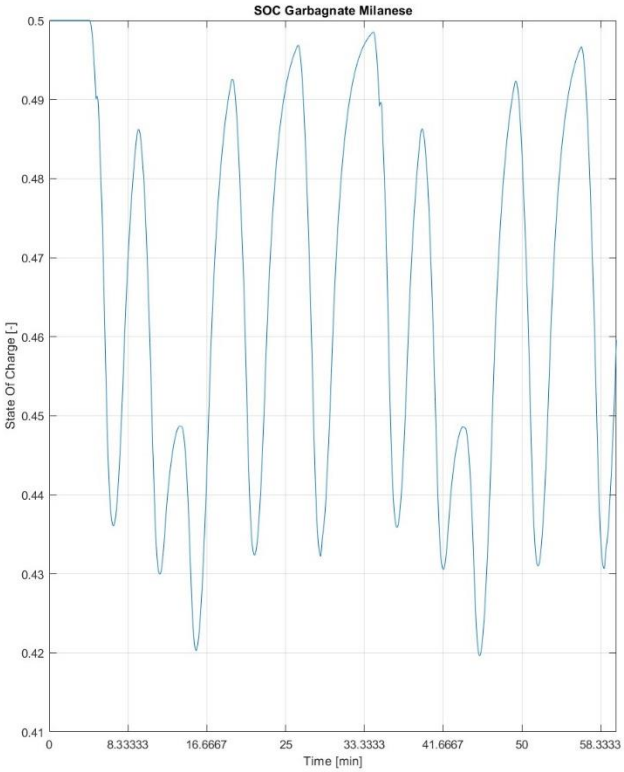

Figure 3.30 : Battery system with the wider SOC range.

In Bollate instead the voltage varies little from the nominal 3000 V, moving the state of charge rarely out of the value of 0.5.

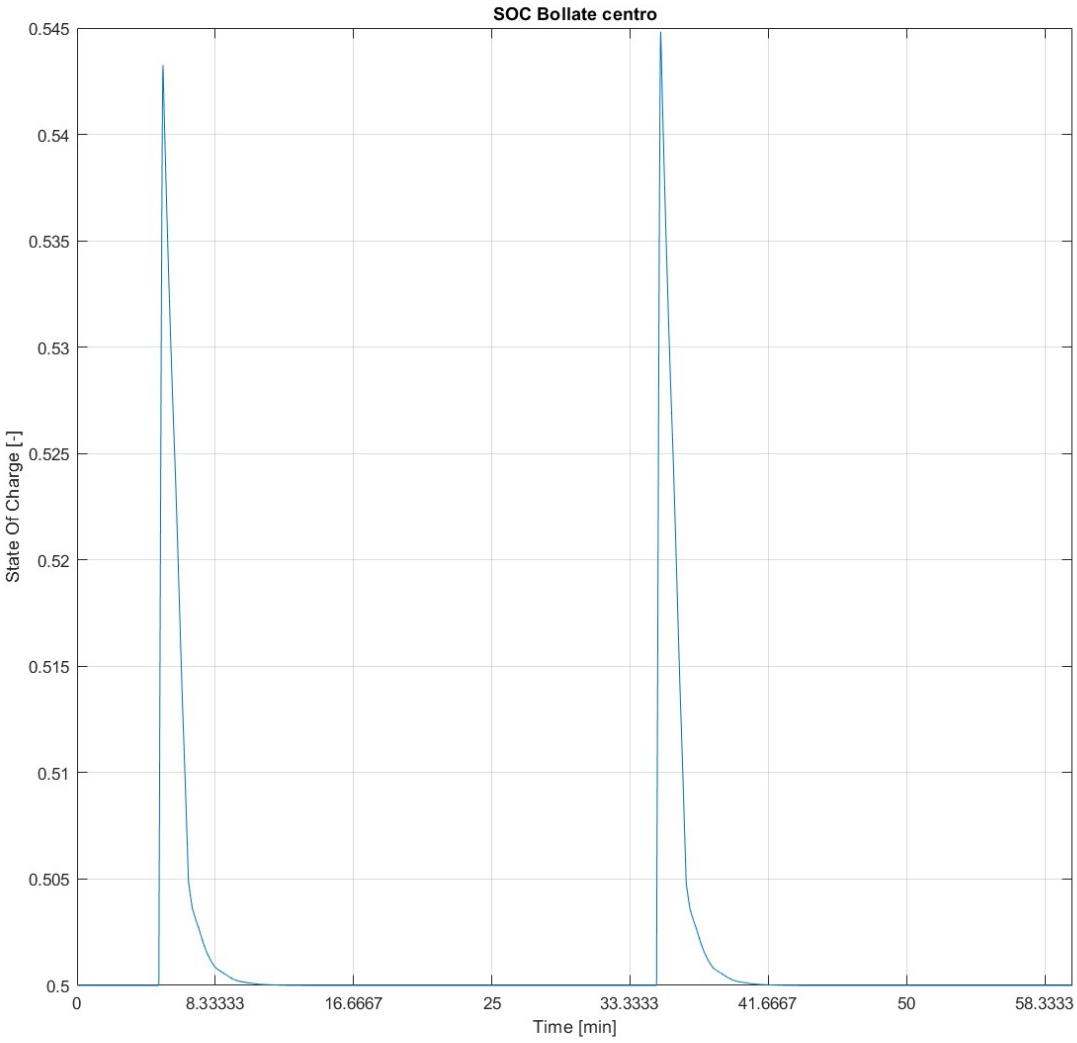

Figure 3.31 : Least loaded battery system

3.4. Addition of photovoltaic system (Case 3)

Finally, photovoltaic systems have been added to the network. The network is now complete with all the infrastructures creating a sort of *DC smart microgrid.*

The photovoltaic modules generate energy for the charging of the electric cars, the stationary batteries and the trains lowering the load on the two ESSs.

3.4.1. Case 3 at Off-peak Hour

This simulation presents the results obtained for the June 19, 2022, that is the day with the higher availability of sunlight.

Here are the results graphs:

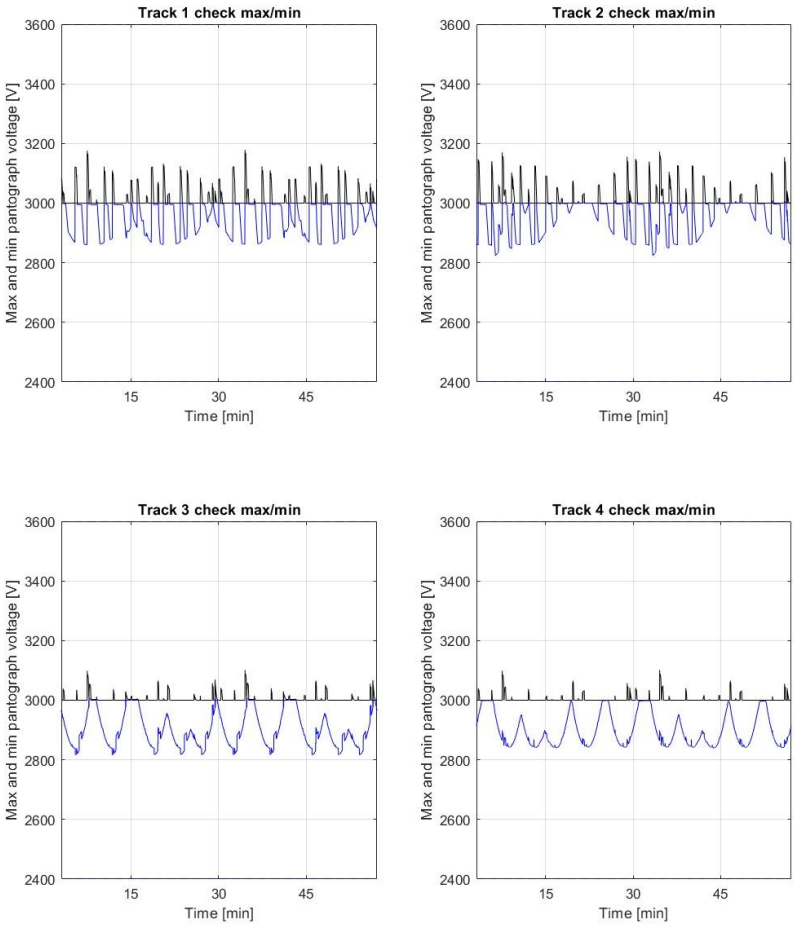

Figure 3.32 : Maximum and minimum voltage across the tracks

The chapter to which reference must be made is that relating to the hours of low traffic. The train lines, at least as far as voltages are concerned, are slightly higher than before (case 3.3.2 and 3.2.2), as reported:

	Maximum Voltage [V]	**Minimun Voltage [V]**
Baseline Network with Batteries/PV Off-peak	3180	2818
Baseline Network No Batteries Off-peak	3173	2805
Baseline Network Off-peak (no Car Parking)	3185	2810

Table 3.21 : Comparison of different voltages

There is a small increase due to the power generation introduced into the system that has raised the voltages (both maximum and minimum), albeit by a few units, as the network respect every constraint and the voltage drops are small.

Instead, in terms of line currents the following results shows a quite interesting result.

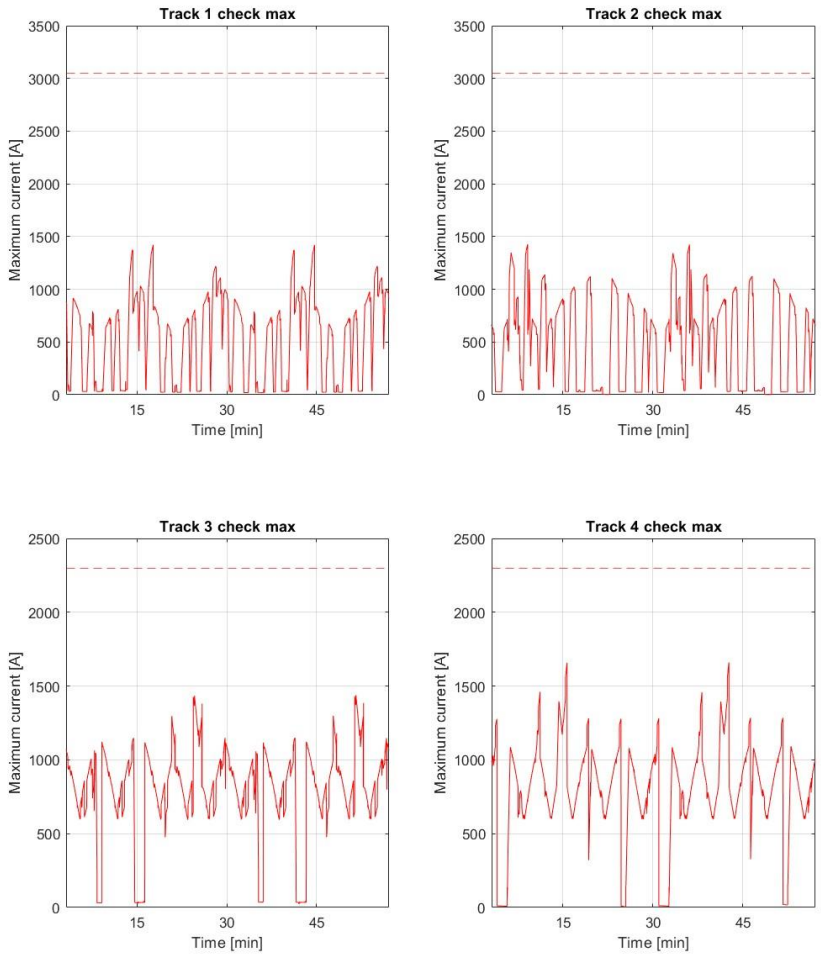

Figure 3.33 : Maximum current across the tracks

Currents are in general lower and there are cases where the current is almost zero, and not a few dozen like the previous cases because the PV supplies power the car park even with no train in the track.

The ESS's show significantly lower values:

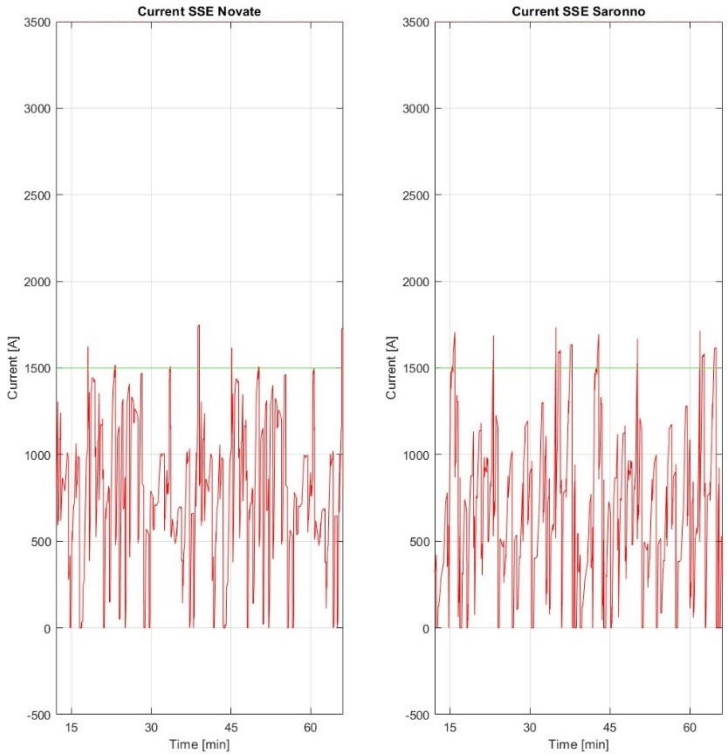

Figure 3.34 : ESSs instantaneous current

The currents in quadratic mean are even more significant:

	Currents in Quadratic Mean Novate [A]	Currents in Quadratic Mean Saronno [A]
Baseline Network with Batteries/PV Off-peak	886	807
Baseline Network No Batteries Low Traffic	998	895
Baseline Network Off-peak (no Car Parking)	914	836

Table 3.22 : Comparison of different currents

The determined values are well below the values registered in other corresponding simulations including the one with no car parking (case 3.2.2)

The unrecovered energy is slightly higher than in the last case as the batteries are at a higher charge when they are required to absorb more power. In this condition, the fuzzy logic let them absorb less power due to the higher SOC.

We thus obtain a value of **8.63 MJ**.

Moreover, the charging period is now of 20 seconds (versus 16 seconds).

The increase in voltage of the system partly counterbalances this phenomenon (few Volts) which certainly has a limited effect on the fuzzy logic.

As already mentioned, simulations during different days throughout the year have been run and once again the system remains very robust with different solar input data. It was therefore decided to illustrate the parameter that changes most from simulation to simulation, as the others are comparable: the current in quadratic mean.

First, the series of graphs is proposed again to better compare the days:

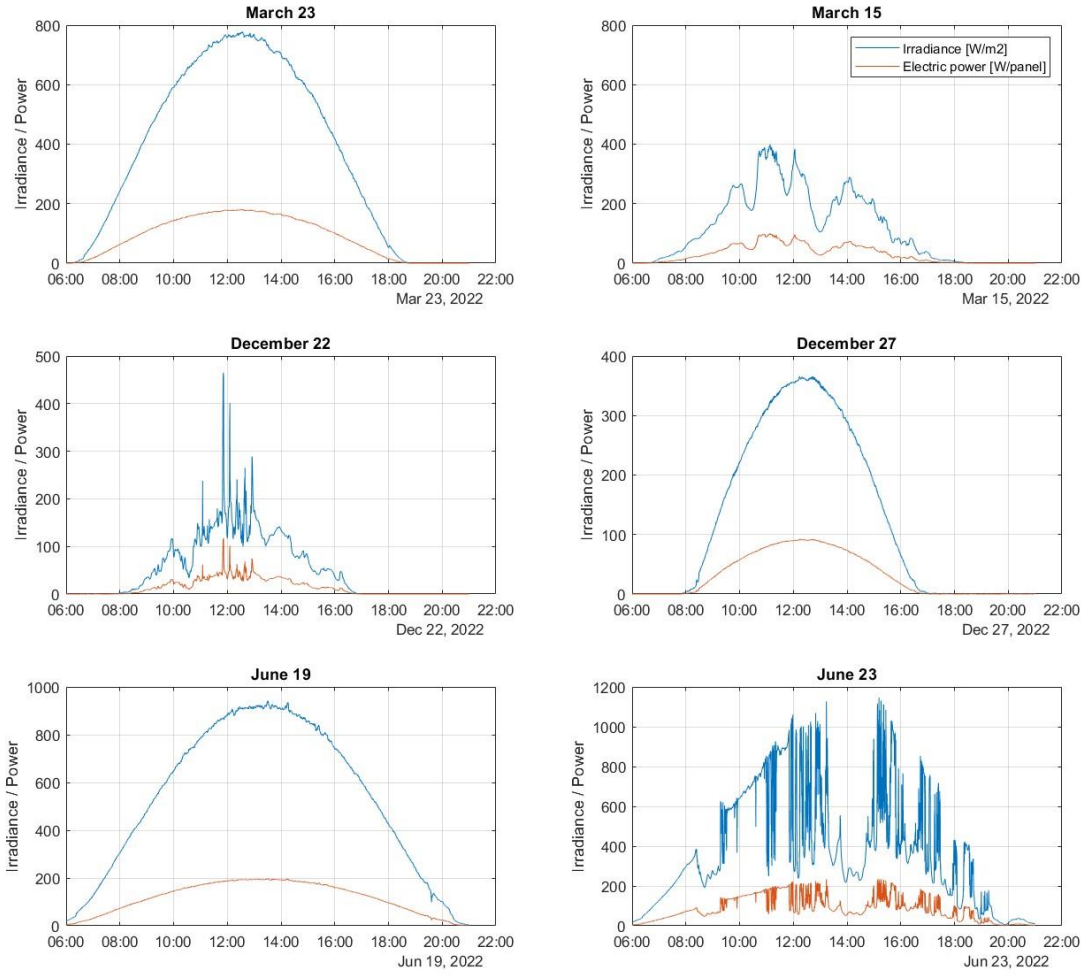

Figure 3.35 : Irradiance and Power for each day considered

The average square current of the electrical substations represents also how much the national network supplies power the train network: it was decided to report the values of this parameter in the Off-peak hour (12:30 – 13:30).

winter	Currents in Quadratic Mean Novate [A]	Currents in Quadratic Mean Saronno [A]
December 27 (clear)	938	847
December 22	963	866

Table 3.23 : Comparison of different currents in winter

Spring	Currents in Quadratic Mean Novate [A]	Currents in Quadratic Mean Saronno [A]
March 23 (clear)	898	820
March 15	962	865

Table 3.24 : Comparison of different currents in spring

Summer	Currents in Quadratic Mean Novate [A]	Currents in Quadratic Mean Saronno [A]
June 19 (clear)	886	807
June 23	920	832

Table 3.25 : Comparison of different currents in summer

Two important considerations:

Despite the *not completely* sunny day, June 23 provides results similar to those with a clear sky. March 23 provides results comparable to those of June 19. This is due to: firstly sun radiations of the two days are not so dissimilar (in per-unit the irradiance is 0.93 in June 19 versus 0.78 in March 23), moreover the temperatures in March are much lower than those of June and this has a beneficial effect on the power generated.

The graphs of the state of charge of the most significant battery energy storage systems are reported:

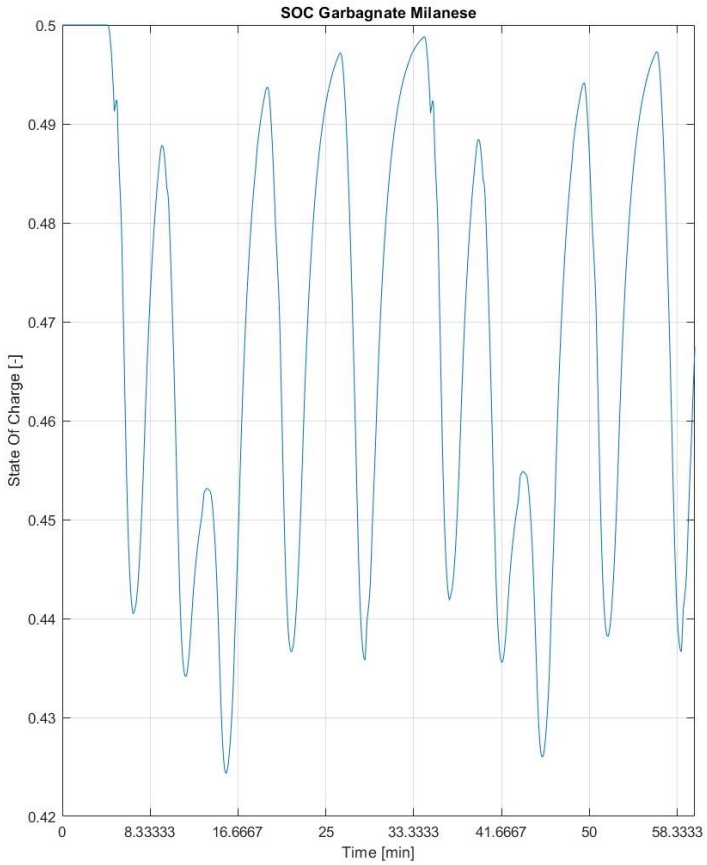

Figure 3.36 : Battery system with the wider SOC range.

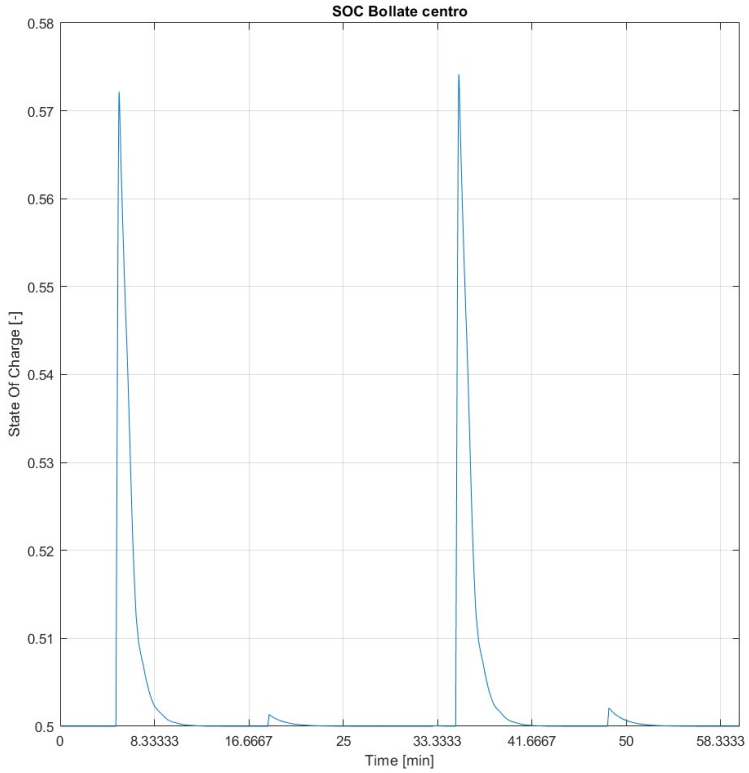

Figure 3.37 : Least loaded battery system.

As expected, the state of charge is higher than the corresponding case in the Off-peak hours without photovoltaic system.

3.4.2. Case 3 whole day

Case 3 consolidates all components of the DC Smart Grid. Because of this, simulations have been run for an entire day. The day simulated - June 19, 2022 – was selected because is the day with the higher availability of sunlight during the analyzed year: PV modules work at their highest capacity.

The trend of the electrical substations throughout the day is indicated on an hourly basis.

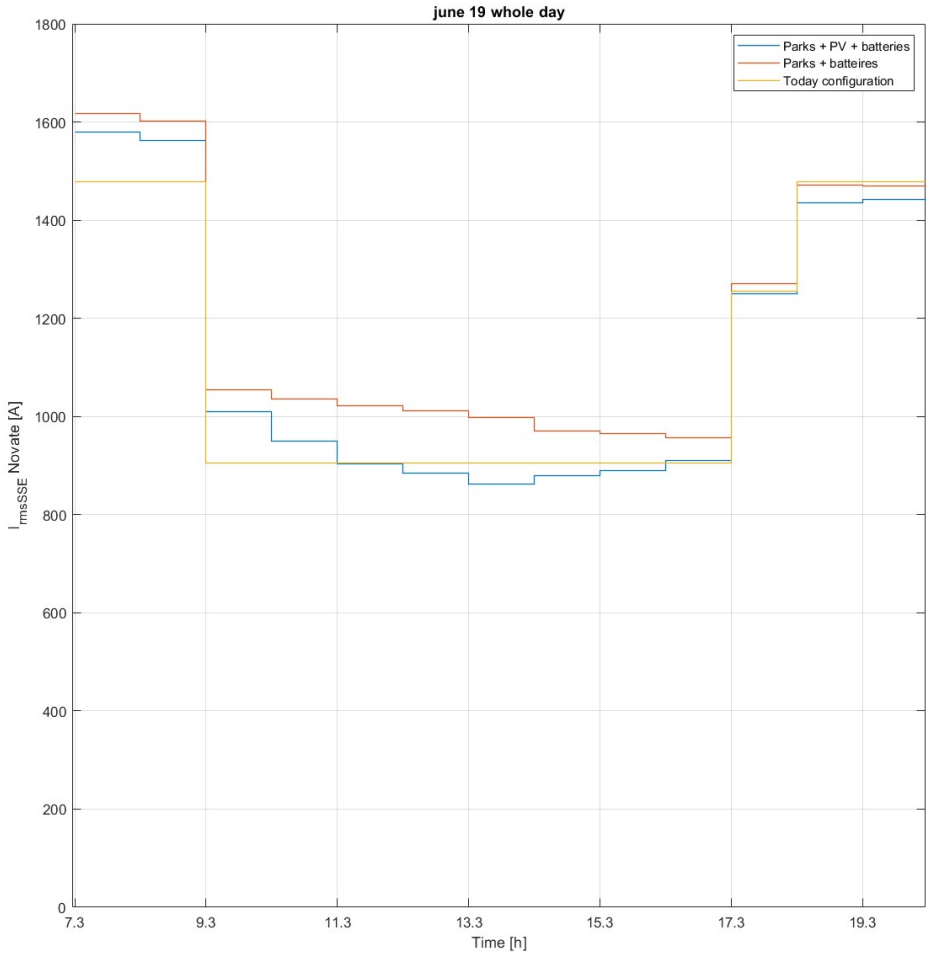

Figure 3.38 : Whole day current mean square, Novate.

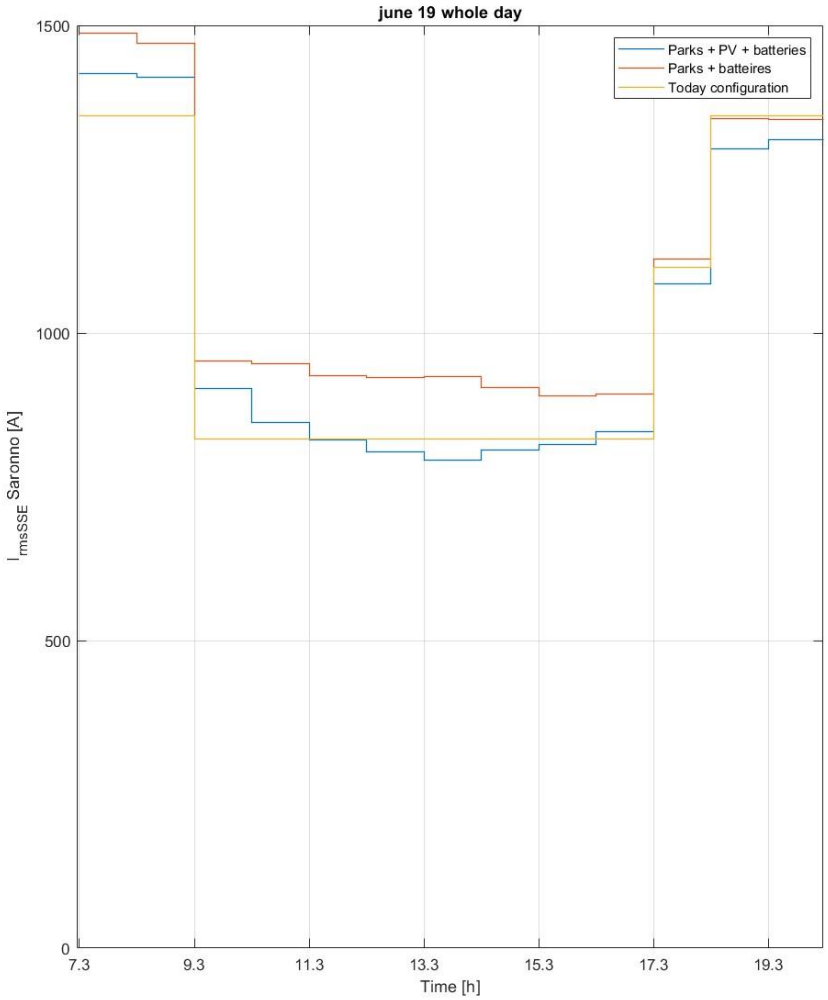

Figure 3.39 : Whole day current mean square, Saronno

Where:

1. The Yellow line represents current configuration of trains i.e. the Baseline network. It shows only two values as it is hour-periodic and the hours have been divided into Off-peak or Rush. To note an intermediate value between 17:30 and 18:30 as it was assumed that the Rush hours start again from 18:00 onwards and the calculation of the current in quadratic mean is on an hourly basis, as the regulations demand;
2. The Red line represents the configuration in which only photovoltaic generators are not present[7]. The two ESSs are more loaded in respect to the yellow line due

[7] It should also be noted that the configuration prior to this one (i.e. without stationary batteries) at the level of current in mean quadratic of the electrical substations, is very similar to this, and has therefore has not been shown.

to the electric car park, in the last hours of the day, a similar behavior of the two cases appear (due to the absence of charging electric cars in the last hours);

3. The Blue line represents the last configuration proposed, with all the proposed infrastructures.

The following observations can be made: firstly, it is clear that the addition of PV's allows during some specific time slots to make the system lighter (e.g. less load for the two ESS and smaller voltage drops in the line) despite the considerable load represented by the car parks. In addition, the gap between the configuration with or without photovoltaic (blue line and red line), increases towards 13:30 (when the power of the photovoltaic is maximum, due to solar time), and then decreases in the remaining hours of the day.

In the last hours of the day the parking lots are totally empty, or rather the cars parked have been recharged, so the trend between the colored lines of the last hours is different from that of the first hours of the day.

Last consideration, due to the solar time the minimum value of the current in square mean is not reached in the time slot shown in the description of the simulation above, but in the following hour (13:30 – 14:30), obtaining the value of 863 A for the first substation (Novate) and 795 A for the second (Saronno).

3.5. Summary of results

The following two tables summarize results contained in the previous paragraphs and highlight the relative errors determined through the following formulas:

$$Error_{\%} = \frac{X - Baseline\ value}{Baseline\ value} * 100\% \quad (3.1)$$

Rush Hour	**Vmax [V]**	**Vmin [V]**	**$I_{ESS,rms}$ Novate [A]**	**$I_{ESS,rms}$ Saronno [A]**	**Unrecovered Energy [MJ]**
Baseline Network	3289	2680	1499	1373	34.8
Electric car park (Case 1)	3281 (-0.24%)	2670 (-0.37%)	1630 (8.74%)	1471 (7.14%)	20.2 (-41.95%)
Stationary batteries (Case 2)	3260 (-0.88%)	2684 (0.15%)	1617 (7.87%)	1450 (5.61%)	16.5 (-52.59%)
PV generators (Case 3 – June 19)	3264 (-0.76%)	2687 (0.26%)	1580 (5.40%)	1420 (3.42%)	17.9 (-48.56%)

Table 3.26 : Rush hour results

Off-peak Hour	**Vmax [V]**	**Vmin [V]**	**$I_{ESS,rms}$ Novate [A]**	**$I_{ESS,rms}$ Saronno [A]**	**Unrecovered Energy [MJ]**
Baseline Network	3185	2810	914	836	22.4
Electric car park (Case 1)	3173 (-0.38%)	2805 (-0.18%)	1005 (9.96%)	904 (8.13%)	9.7 (-56.7%)
Stationary batteries (Case 2)	3164 (-0.66%)	2811 (0.03%)	998 (9.19%)	895 (7.06%)	8.1 (-63.84%)
PV generators (Case 3 – June 19)	3180 (-0.16%)	2818 (0.28%)	886 (-3.06%)	807 (-3.47%)	8.6 (-61.61%)

Table 3.27 : Off-peak hour results

4 Conclusion and future developments

This work analyzes an intense traffic railway line in a densely populated areas: a section of the Cadorna – Saronno railway line between its two electrical substations located at Novate and Saronno stations.

Railway stations of the selected sector are already organized with car parks to host a considerable number of daily commuters and may also represent a very suitable space for the installation of photovoltaic fields, increasing the share of power produced with renewable sources.

As a first part of the work, this railway sector is therefore modelled (the "baseline") to better assess the status of the railway electrical system, if technical and safety constraints are met and whether there is room to expand the network integrating it with new loads and/or generators: electric car parks, battery storage systems and photovoltaic modules.

Then this work considers (Case 1) the addition of electric car parks to the train network so to recover part of the energy that would otherwise be dissipated by the trains during braking. Case 1 simulations show that the ESS Quadratic Mean Currents increase of nearly 10% but Energy Recovery amounts to around 50% of the available energy. The additional load of the electrical car parks causes a few percents lower voltages.

The next case study (Case 2) introduces a storage system into the railway network for the sake of further stabilizing it but at the same time allowing additional recovery of energy when braking of trains generate a surplus of power within the system. Case 2 simulations show that the ESS Quadratic Mean Currents are slightly lower than Case 1 but Energy Recovery increases to around 60% of the available energy. Max Voltages are closer to the nominal value by more than 10% than the baseline, minimum voltages differences are negligible notwithstanding the additional load of the electrical car parks.

The last case study (Case 3), with the addition of the photovoltaic system. A source of generation is added in a location that can easily accommodate it, allowing to have all the benefits that a renewable source can add to the microgrid. Case 3 simulations show that in the sunny hours of a day the load on the ESSs is lower by slightly more than 3% in terms of Quadratic Mean Current. Voltages are close to those of the baseline.

With this last case the DC smart grid is complete.

Feasibility of the addition to the railway electrical system of such new infrastructures is confirmed: the simulations contained in this work demonstrate that there is room to expand/integrate an existing railway sector - sized to satisfy a high traffic demand and with a great potential to withstand additional loads during off-peak hours of the day - so to recover energy that would otherwise be lost (regenerative recovery of braking trains) and stabilize the railway electrical system voltage.

There is certainly room to improve the presented model by – for instance - implementing additional infrastructures and/or tuning some of the parameters such as selecting a less traffic intense railway sector (where the recoverable power is higher than the one taken as reference), and eventually implementing a vehicle-to-grid logic, which in this case should better be called “vehicle-to-train logic”.

Bibliography

[1] «Trasporti sicuri e sostenibili | Unione europea», *Unione Europea*, 2021. https://european-union.europa.eu/priorities-and-actions/actions-topic/transport_it.

[2] «Noi Italia 2022 - home», *Istat, Istituto nazionale di Statistica*, 2022. https://noi-italia.istat.it/pagina.php?id=3&categoria=13&action=show&L=0.

[3] «Cars, planes, trains: where do CO2 emissions from transport come from?», *Our World in Data*, 2022. https://ourworldindata.org/co2-emissions-from-transport (consultato 21 marzo 2023).

[4] F. Morulo, «Appunti di Sistemi di Trazione Elettrica». Istituto Tecnico Superiore Mobilità Sostenibile Trasporto Ferroviario, 2015.

[5] «15 kV AC railway electrification», *Wikipedia*. 18 febbraio 2023. Consultato: 21 marzo 2023. [Online]. Disponibile su: https://en.wikipedia.org/w/index.php?title=15_kV_AC_railway_electrification&oldid=1140088568

[6] M. Ahmadi, H. Jafari Kaleybar, B. Morris, F. Castelli-Dezza, e M. S. Carmeli, «Integration of Distributed Energy Resources and EV Fast-Charging Infrastructure in High-Speed Railway Systems», *Electronics*, vol. 10, fasc. 20, p. 2555, ott. 2021, doi: 10.3390/electronics10202555.

[7] M. Brenna, F. Foiadelli, e D. Zaninelli, «The Compatibility between DC and AC supply of the Italian railway system», in *2011 IEEE Power and Energy Society General Meeting*, San Diego, CA, lug. 2011, pp. 1–7. doi: 10.1109/PES.2011.6039536.

[8] EN 50163, «Railway applications — Supply voltages of traction systems». BRITISH STANDARD, 2020.

[9] EN 50388, «Railway Applications — Fixed installations and rolling stock — Technical criteria for the coordination between electric traction power supply systems and rolling stock to achieve interoperability». BRITISH STANDARD, 2020.

[10] RC1EA1R18RGTE0000001B, «PROGETTO FATTIBILITA' TECNICA ECONOMICA». RFI rete ferroviaria italiana, 2022.

[11] RFI rete ferroviaria italiana, «NORME PER LA CIRCOLAZIONE DEI ROTABILI». 2009.

[12] G. Fengyi, G. Xin, W. Zhiyong, W. Yuting, e W. Xili, «Simulation on Current Density Distribution of Current-Carrying Friction Pair Used in Pantograph-Catenary System», *IEEE Access*, vol. 8, pp. 25770–25776, 2020, doi: 10.1109/ACCESS.2020.2971314.

[13] A. Minoia, «Corso di Trazione elettrica, lezione 4», Università degli studi di Pavia, 2018. [Online]. Disponibile su: http://www-3.unipv.it/electric/cad/slide_TE/TE_Lezione_4.pdf

[14] A. Olivo e M. Olivari, «Tecnica ed economia dei trasporti ferroviari». 2012.

[15] EN 13674, «Railway applications - Track - Rail». BRITISH STANDARD, 2019.

[16] INTERNATIONAL ENERGY AGENCY, «World Energy Investment 2022», p. 11, 2022.

[17] «Trends in charging infrastructure – Global EV Outlook 2022 – Analysis», *IEA*, 2022. https://www.iea.org/reports/global-ev-outlook-2022/trends-in-charging-infrastructure.

[18] R. Strockl, «The future of E-charging infrastructure: Italy», *WFW*, 22 aprile 2020. https://www.wfw.com/articles/the-future-of-e-charging-infrastructure-italy/

[19] S. U. Jeon, J.-W. Park, B.-K. Kang, e H.-J. Lee, «Study on Battery Charging Strategy of Electric Vehicles Considering Battery Capacity», *IEEE Access*, vol. 9, pp. 89757–89767, 2021, doi: 10.1109/ACCESS.2021.3090763.

[20] L. A. Zadeh, «Fuzzy sets», *Inf. Control*, vol. 8, fasc. 3, pp. 338–353, 1965, doi: https://doi.org/10.1016/S0019-9958(65)90241-X.

[21] S. Nag e Kwang. Y. Lee, «Optimized Fuzzy Logic Controller for Responsive Charging of Electric Vehicles», *IFAC-Pap.*, vol. 52, fasc. 4, pp. 147–152, 2019, doi: 10.1016/j.ifacol.2019.08.170.

[22] M. Ahmadi, H. J. Kaleybar, M. Brenna, F. Castelli-Dezza, e M. S. Carmeli, «DC Railway Micro Grid Adopting Renewable Energy and EV Fast Charging Station», in *2021 IEEE International Conference on Environment and Electrical Engineering and 2021 IEEE Industrial and Commercial Power Systems Europe (EEEIC / I&CPS Europe)*, Bari, Italy, set. 2021, pp. 1–6. doi: 10.1109/EEEIC/ICPSEurope51590.2021.9584729.

[23] A. Cicek *et al.*, «Integrated Rail System and EV Parking Lot Operation With Regenerative Braking Energy, Energy Storage System and PV Availability», *IEEE Trans. Smart Grid*, vol. 13, fasc. 4, pp. 3049–3058, lug. 2022, doi: 10.1109/TSG.2022.3163343.

[24] S. D'Arco, L. Piegari, e P. Tricoli, «Comparative Analysis of Topologies to Integrate Photovoltaic Sources in the Feeder Stations of AC Railways», *IEEE Trans. Transp. Electrification*, vol. 4, fasc. 4, pp. 951–960, dic. 2018, doi: 10.1109/TTE.2018.2867279.

[25] M. Ceraolo, G. Lutzemberger, E. Meli, L. Pugi, A. Rindi, e G. Pancari, «Energy storage systems to exploit regenerative braking in DC railway systems: Different approaches to improve efficiency of modern high-speed trains», *J. Energy Storage*, vol. 16, pp. 269–279, apr. 2018, doi: 10.1016/j.est.2018.01.017.

[26] M. Brenna, F. Foiadelli, e H. J. Kaleybar, «The Evolution of Railway Power Supply Systems Toward Smart Microgrids: The concept of the energy hub and integration of distributed energy resources», *IEEE Electrification Mag.*, vol. 8, fasc. 1, pp. 12–23, mar. 2020, doi: 10.1109/MELE.2019.2962886.

[27] S. Nasr, M. Iordache, e M. Petit, «Smart micro-grid integration in DC railway systems», in *IEEE PES Innovative Smart Grid Technologies, Europe*, Istanbul, Turkey, ott. 2014, pp. 1–6. doi: 10.1109/ISGTEurope.2014.7028913.

[28] The MathWorks Inc., «MATLAB version 9.13.0 (R2022a)». Natick, Massachusetts, United States, 2022. [Online]. Disponibile su: https://www.mathworks.com

[29] Simulink, «Simulation and Model-Based Design». 2022. [Online]. Disponibile su: https://www.mathworks.com/products/simulink.html

[30] V. Cortese, «I treni», *Potenza Dei TSR*, vol. 300,301, pp. 16-21;12–17, gen. 2008.

[31] «Doppio Piano, parte 5: ALe.710-ALe.711 alias TSR (Treno Servizio Regionale)», *scalaeNNe - Note Sparse (Treni, Ferrovie e loro modellazione in Scala N)*, 24 ottobre 2020. https://scalaenne.wordpress.com/2020/10/24/doppio-piano-parte-5-tsr-treno-servizio-regionale/.

[32] G. Cassano, «Elementi dei tracciati ferroviari», 2009.

[33] RFI rete ferroviaria italiana, «Prospetto informativo rete 2021», p. 167, 2021.

[34] «Coals to Newcastle | Physics | Train Resistance». https://www.coalstonewcastle.com.au/physics/resistance/.

[35] C. F. D. Marshall, *The resistance of express trains.* London: The Railway engineer, 1925. Consultato: 24 marzo 2023. [Online]. Disponibile su: https://catalog.hathitrust.org/Record/001612412

[36] Infrastrutture Ferroviarie, «Meccanica della locomozione», *Mecc. Della Locomozione Parte 2*, p. 4, 2009.

[37] «Ferrovia Milano-Saronno», *Wikipedia*. 27 gennaio 2023. Consultato: 24 marzo 2023. [Online]. Disponibile su: https://it.wikipedia.org/w/index.php?title=Ferrovia_Milano-Saronno&oldid=131765221

[38] RFI rete ferroviaria italiana, «Wayback Machine», 31 ottobre 2008. https://web.archive.org/web/20081031101553/http:/www.fnmgroup.it/website/file/2423.pdf.

[39] «Orario grafico», *Wikipedia*. 4 febbraio 2019. Consultato: 24 marzo 2023. [Online]. Disponibile su: https://it.wikipedia.org/w/index.php?title=Orario_grafico&oldid=102555363

[40] UNI, «RAIL 60 E1 (UIC 60)», *VALENTE SPA*. https://www.valente1919.com/download/207/railway-rails/6447/60-e1-uic-60.pdf

[41] F. Fichera, A. Mariscotti, e A. Ogunsola, «Evaluating stray current from DC electrified transit systems with lumped parameter and multi-layer soil models», in *Eurocon 2013*, Zagreb, Croatia, lug. 2013, pp. 1187–1192. doi: 10.1109/EUROCON.2013.6625131.

[42] «Didattica della Chimica». https://www.bisceglia.eu/chimica/tabelle/resistivita.html.

[43] R. A. Jabr e I. Džafić, «Solution of DC Railway Traction Power Flow Systems Including Limited Network Receptivity», *IEEE Trans. Power Syst.*, vol. 33, fasc. 1, pp. 962–969, 2018, doi: 10.1109/TPWRS.2017.2688338.

[44] «An Algorithm for Modified Nodal Analysis». https://lpsa.swarthmore.edu/Systems/Electrical/mna/MNA3.html.

[45] «LU decomposition», *Wikipedia*. 24 marzo 2023. [Online]. Disponibile su: https://en.wikipedia.org/w/index.php?title=LU_decomposition&oldid=1146366204

[46] «Daily passeger mobility, 2021». https://www.stat.si/StatWeb/en/News/Index/10324.

[47] S. O. EV, «Worldwide Daily Driving Distance is 25-50km? What about AU, US, UK, EU, and...», *Solar On EV*, 20 ottobre 2021. https://www.solaronev.com/post/average-daily-driving-distance-for-passenger-vehicles.

[48] «EV Database», *EV Database*. https://ev-database.org/cheatsheet/energy-consumption-electric-car.

[49] A. D. Jadhav e S. Nair, «Battery Management using Fuzzy Logic Controller», *J. Phys. Conf. Ser.*, vol. 1172, p. 012093, mar. 2019, doi: 10.1088/1742-6596/1172/1/012093.

[50] A. M. A. Alshogeathri, «VEHICLE-TO-GRID (V2G) INTEGRATION WITH THE POWER GRID USING A FUZZY LOGIC CONTROLLER», 2012.

[51] M. Singh, P. Kumar, e I. Kar, «Implementation of Vehicle to Grid Infrastructure Using Fuzzy Logic Controller», *IEEE Trans. Smart Grid*, vol. 3, fasc. 1, pp. 565–577, mar. 2012, doi: 10.1109/TSG.2011.2172697.

[52] S. G. Li, S. M. Sharkh, F. C. Walsh, e C.-N. Zhang, «Energy and battery management of a plug-in series hybrid electric vehicle using fuzzy logic», *IEEE Trans. Veh. Technol.*, vol. 60, fasc. 8, pp. 3571–3585, 2011.

[53] «SoLink è Partner di Solar Tech Lab del Politecnico di Milano -», 17 gennaio 2018. https://solink.it/2018/01/17/solink-e-partner-di-solar-tech-lab-del-politecnico-di-milano/.

[54] ALEO SOLAR, «S18K250», *tettosolare*, 2018. https://www.tettosolare.it/imag/item/ALEO_SOLAR_S_18%20240-265W.pdf

[55] R. Tecnica, «Parcheggi? Progettarli non è facile. Ecco cosa devi sapere | Ediltecnico.it», *Ediltecnico*, 7 agosto 2019. https://www.ediltecnico.it/72078/progetto-parcheggi-come-si-fa/.

[56] «Google Maps», *Google Maps*. https://www.google.it/maps/

List of Figures

List if Tables